The nuclear chaperones NPM1 and Bag-1L in the regulation of androgen receptor action in prostate cancer cells

Zur Erlangung des akademischen Grades eines

DOKTORS DER NATURWISSENSCHAFTEN

(Dr. rer. nat.)

der KIT-Fakultät für Chemie und Biowissenschaften

des Karlsruher Instituts für Technologie (KIT)

genehmigte

DISSERTATION

von

Emmanuel Amankwah Ntim, (MPhil)

aus

Essikado, Ghana

1. Referent: Apl. Prof. Dr. Andrew C. B. Cato

2. Referent: Prof. Dr. Jörg Kämper

Tag der mündlichen Prüfung: 19th July, 2018

Zusammenfassung

Die Entstehung und Progression von Prostatakarzinomen sind in hohem Maß von Androgenen abhängig. Ihren Effekt entfalten die männlichen Geschlechtshormone durch die Bindung an den Androgen Rezeptor (AR), einen Liganden-gesteuerten Transkriptionsfaktor. In Abwesenheit von Hormonen befindet sich der inaktive AR in einem Komplex mit molekularen Chaperonen im Cytoplasma. Nach Bindung von Androgenen an den AR dissoziieren die Chaperone und der Rezeptor transloziert in den Nukleus, wo er die Expression von AR-regulierten Genen beeinflusst. Es wurde bisher angenommen, dass die Hauptfunktion der Chaperone darin liegt, die geeignete Konformation des AR zur Bindung von Androgenen zu gewährleisten. Es existieren jedoch auch Chaperone, die vorwiegend im Nukleus lokalisiert sind und die transkriptionelle Aktivität des AR beeinflussen. Die Wirkung, die diese Chaperone auf die AR Aktivität und auf die Krebsentwicklung haben, bleibt jedoch unklar. Zwei nukleare Chaperone, deren Beteiligung an der Regulation der transkriptionellen Aktivität des AR bereits gezeigt wurde, sind Bag-1L und NPM1. Der Mechanismus, der der Regulation durch die beiden Chaperone zu Grunde liegt, ist jedoch unbekannt. Das Ziel dieser Arbeit war die Charakterisierung der beiden nuklearen Chaperone (Bag-1L und NPM1) im Bezug auf die Regulation des AR Aktivität und das Wachstum von Prostatakrebszellen. Weiterhin sollte untersucht werden, ob die beiden Proteine ihren Effekt durch einen gemeinsamen oder zwei sich voneinander unterscheidenden Signalwege entfalten. In dieser Arbeit konnte zunächst nachgewiesen werden, dass die beiden Chaperone, neben der jeweiligen Interaktion mit dem AR, auch miteinander interagieren. Eine Herunterregulation von NPM1 führte weiterhin zu einem reduzierten Expressionslevel der Bag-1 Proteine (einschließlich Bag-1L). Darüber hinaus konnte gezeigt werden, dass der Knock-down von NPM1 die Translokationsgeschwindigkeit des AR von Cytoplasma in den Nukleus beeinträchtigt. Dieser Effekt war zum Teil reversibel, wenn in NPM1-Knock-down Zellen Bag-1L überexprimiert wurde. Dies lässt vermuten, dass der beobachtete Effekt teilweise durch reduzierte Bag-1L Level in den NPM1 knock-down Zellen hervorgerufen wurde. Der Knock-down von NPM1 beeinträchtigte ebenfalls die transkriptionelle Aktivität des AR, was bereits für den knock-out von Bag-1L gezeigt

werden konnte. Ein Vergleich von genomweiten Transkriptom-Datensätze der NPM1 knock-down Zellen mit denen der bereits veröffentlichten Bag-1L knock-out Zellen zeigte auffallend viele Überlappungen. Durch statistische Auswertung der Gene, die gemeinsam durch die beiden Chaperone reguliert werden, konnte ein Signalweg identifiziert werden, der zu der Bildung von oxidativen Stress in Prostatakrebszellen führt. Oxidativer Stress wurde lange, hauptsächlich mit einer schädlichen Wirkung auf die Zellvitalität in Verbindung gebracht. Neuere Studien zeigen jedoch, dass sich oxidativer Stress auch positiv auf das Überleben von Zellen und deren Proliferation auswirken kann. Da sowohl der knock-down von NPM1, als auch der knock-out von Bag-1L die Expression androgen-abhängiger Gene negativ beeinflusst, die für die Entstehung von oxidativen Stress wichtig sind, liegt die Schlussfolgerung nahe, dass Bag-1L und NPM1 in Prostatakrebszellen interagieren, um AR-vermittelte Signalwege zu aktivieren. Dies führt zur Entstehung von oxidativen Stress, was das Überleben der Tumorzellen begünstigt.

Abstract

The development and progression of prostate cancer (PCa) is mainly dependent on androgen signalling. The effects of androgens are mediated by the androgen receptor (AR). In the absence of androgens, the AR is localized in the cytoplasm of target cells in association with molecular chaperones. Upon hormone binding, the chaperones dissociate and the receptor translocates to the nucleus where it modulates the expression of AR responsive genes. It is thought that the main function of the chaperones is to work in a concerted manner to help the receptor bind to the hormone. However, there are chaperones that are equally important for the action of the receptor that mainly reside in the nucleus and whose contribution to AR action and prostate cancer progression remains unclear. Bag-1L and NPM1 are two such nuclear resident chaperones that have previously been reported to regulate the transcriptional activity of the AR and androgen-mediated prostate cancer cell proliferation but through unknown pathways. The object of this study was therefore to determine how these two nuclear resident chaperones control AR action and prostate cancer cell proliferation and to further determine whether they function through common or divergent pathways. First, it was shown in this work that these two chaperones interact with each other in addition to their known interaction with the AR. Second, it was shown that downregulation of NPM1 in the prostate cancer cells LNCaP and 22Rv.1 resulted in a concomitant downregulation of the expression level of Bag-1 proteins (including Bag-1L). Third, knockdown of NPM1 impaired AR nuclear translocation rate; an effect that can be partially rescued by overexpression of Bag-1L in the NPM1 knockdown cells, suggesting that the defects resulted from the decreased level of Bag-1L in the NPM1 knockdown cells. Fourth, knockdown of NPM1 also impaired the transcriptional activity of the AR as has previously been observed for the knockout of Bag-1L. Fifth, knockout of Bag-1L and knockdown of NPM both downregulated androgen-dependent cell proliferation. Comparison of the genome-wide AR-mediated transcriptomic datasets of the NPM1 knockdown cells with those of the corresponding published datasets of Bag-1L knockout cells revealed a striking degree of overlap. Data mining of the common genes regulated by the two chaperones identified a pathway leading to the generation of oxidative stress in the prostate cancer cells. Oxidative stress

once thought to be detrimental to cell viability has recently been shown to enhance cell survival and proliferation. As both the knockdown of NPM1 and knockout of Bag-1L impaired androgen dependent expression of genes concerned with the generation of oxidative stress in the prostate cancer cells, it was concluded that Bag-1L and NPM1 interact in prostate cancer cells to activate AR-mediated pathways that lead to the generation of oxidative stress and cell survival.

Contents

List of Figures

List of Tables

Abbreviations

AF-1	Activation function domain-1
Amp	amplitude
APS	Ammonium persulfate
AR	Androgen Receptor
ARE	Androgen responsive element
ATP	Adenosine triphosphate
ATPase	Adenosine triphosphatase
Bag	Bcl-2 associated athanogene
Bag-1	Bcl-2 associated athanogene 1
Bcl-2	B-cell leukemia/lymphoma 2
BLAST	Basic Local Alignment Search Tool
bp	base pairs
BSA	Bovine serum albumine
ºC	Degrees Celsius
cDNA	complementary DNA
CHIP	C-terminus of Hsc-70 interacting protein
CMV	cytomegalovirus
COOH-terminal	Carboxy- terminal
DBD	DNA binding domain
ddH_2O	Double distilled water
DMEM	Dulbecco's modified eagle's medium
DMSO	Dimethylsulfoxide
DNA	Deoxyribonucleic Acid
DNase	Deoxyribonuclease
dNTPs	deoxynucleosides triphosphate
DTT	Dithiothreitol
dUTP	2'-deoxyuridine 5'-triphosphate
ECL	Enhancer of chemioluminescence
EDTA	Ethylenediamine Tetraacetic Acid
e.g.	*Exempli gratia*, for example

ER	Estrogen receptor
et al.	*Et alii*, and others
FCS	Fetal calf serum
FKBP5	FK506 binding protein 5
g	gram
g	gravity (unit of relative centrifugal force)
GR	Glucocorticoid receptor
GST	Glutathion-S-transferase
h	hour
HCl	Hydrochloric acid
Hip	Hsp70 interacting protein
Hop	Hsp70/Hsp90 organizing protein
HRP	Horseradish peroxidase
Hsc70	Heat shock cognate protein 70 KDa
Hsp70	Heat shock protein 70KDa
IF	immunofluorescence
IRES	Internal ribosomal entry site
ITG	Institute of Toxicology and Genetics
JCV	John Cunningham Virus
KD	Knockdown
KCl	Potassium cloride
kDa	kilodalton
KO	Knockout
l	liter
LBD	Ligand binding domain
M	molar
µ	micro
m	milli
min	minute
mRNA	messenger RNA
n	nano

NaCl	Sodium chloride
NHR	Nuclear horomone receptor
NLS	Nuclear localisation signal
no	number
NP-40	Nonident P-40
NH_2-terminal	Amino- terminal
NPM1	Nucleophosmin 1
OD	optical density
O/N	overnight
PAGE	Polyacrylamide gel electrophoresis
PBS	Posphate buffer saline
PCD	programmed cell death
PCR	polymerase chain reaction
PFA	Paraformaldehyde
PMSF	phenylmethanesulphonylfluoride
PTB	polypyrimidine tract binding protein
PVDF	Polyvinylidene difluoride
RAR	Retinoic acid receptor
RNA	Ribonucleic acid
RNase A	Ribonuclease A
rpm	revolutions per minute
RPMI	Roswell Park Memorial Institute
RT	Room temperature
s	second
SD	standard deviation
SDS	Sodium dodecyl sulfate
SEM	standard error of the mean
SNT	supernatant
SV40	Simian Virus 40
TAE	Tri/acetate/EDTA elecrophoresis buffer
Tag	T antigen

TBS	Tris buffer saline
TEMED	tetramethylethylenediamine
Tris	Tris(hydroxymethyl)aminometane
TTBS	Tris buffer saline + Tween-20
U	units
ULD	Ubiquitin-like domain
UV	ultraviolet
V	volt
WB	Western blot
VDR	Vitamin D receptor
w/o	without
v/v	volume per volume
v/w	volume per weight

1.0 INTRODUCTION

1.1 Prostate Cancer

Prostate cancer (PCa) is the second leading cause of cancer related mortality in men worldwide (Torre et al., 2015; Siegel, 2017). The prostate gland exhibits profound dependence on the male hormone androgen for its development and functions (Huggins and Hodges, 1941). In normal prostate, androgens induce production of growth factors in the stromal cells that cause growth of the luminal secretory epithelial cells (Thompson, 1990). Androgens function via the androgen receptor (AR) (Evans, 1988), a ligand-activated transcription factor that is a member of the nuclear receptor superfamily (Evans, 1988). The AR controls gene expression programs in prostate epithelial cells, resulting in the expression of various proteins responsible for the functions of the gland (Chang et al., 1995). Due to the reliance of the prostate on androgens, when tumours develop from the prostatic epithelial cells, androgen deprivation therapy (ADT) is applied, either by reducing the levels of androgen or by blocking androgens at the level of the AR, which usually results in a favourable clinical response in over 80% of the patients due to a dramatic regression of prostate cancer through apoptotic cell death (Westin et al., 1995; Sprenger and Plymate, 2014). However, after an initial response to androgen ablation, the prostate cancers eventually become unresponsive, if endocrine therapy is continued long term (Lepor et al., 1982), and the tumour progresses to a disease state known as castration-resistant PCa (CRPC) which eventually kills the patients (Scher et al., 2004; Dutt and Gao, 2009; Knudsen and Scher, 2009). The recurrences almost always are associated with the reactivation of androgen receptor signaling (Shafi et al., 2013) but why the cancers do not respond to ADT from that stage is not currently understood. A need therefore exists to understand more about the factors that control the functions of the AR so that the mechanisms responsible for resistance to endocrine therapy can be revealed and eventually alleviated.

The human AR has 919 amino acids with a mass of 110 kilo Daltons, composed of four structurally and functionally distinct domains consisting of a NH_2-terminal domain (amino acids 1–537, also called activation function 1 or AF-1), a DNA-binding domain (amino acids 537–625), a hinge region (amino acids 625–669) and a ligand-binding COOH-

terminal domain (LBD, amino acids 669–919, also called activation function 2, AF-2) (Lonergan and Tindall, 2011). The unliganded AR resides in the cytoplasm of target cells but upon binding to androgen, the activated AR translocates into the nucleus. There it associates with coregulatory factors and binds to androgen response elements (ARE) of target genes leading to their expression or repression (Koochekpour, 2010). Previous clinical research showed that targeting AR is a valid therapeutic strategy for CRPC (Bishr and Saad, 2013) and indeed, recent clinical trials have shown that the AR antagonists enzalutamide (Scher et al., 2012) or abiraterone, an inhibitor of androgen synthetic pathways (Fizazi et al., 2012), are effective against CRPC. However, other recent studies have reported AR gene rearrangement leading to the expression of truncated AR splice variants (AR-Vs) in some prostate cancer tissues (Scher and Sawyers, 2005; Dutt and Gao, 2009; Sun et al., 2010). These AR-Vs lack the LBD and have constitutive activity and are resistant to anti-androgen therapy including enzalutamide and abiraterone (Mostaghel et al., 2011; Li et al., 2013; Antonarakis et al., 2014; Claessens et al., 2014; Francini et al., 2014; Sprenger and Plymate, 2014). Furthermore, AR inhibitors currently in clinical use all target the LBD, and there is therefore the need for new targets to overcome PCa resistance driven by both full-length AR (AR-FL) and constitutively active AR-Vs. The AR is a client protein to several molecular chaperones whose functions include maintenance of protein conformation to enable ligand binding, facilitating intracellular protein trafficking, preventing aggregation, aiding phosphorylation to enhance signalling complexes with other partners and mediating degradation of the receptor (Lindquist and Craig, 1988; Jäättelä, 1999; Jego et al., 2013; Cato et al., 2014). Obviously, the integral role of molecular chaperones in AR function speaks to their potential utility as therapeutic targets in the fight against prostate cancer resistance.

1.2 Molecular Chaperones of the Androgen Receptor and prostate cancer

Molecular chaperones and co-chaperones belong to a group of unrelated proteins that mediate the correct assembly of other proteins but are not themselves components of the final structure (Anfinsen, 1973). The AR is maintained in a ligand-binding competent state in the cytoplasm through its interaction with molecular chaperone system consisting of

the chaperones HSP40, HSP70 and HSP90 together with the co-chaperones HOP, p23, the immunophilins FKBP51/52 and Bag-1 (Querol et al., 2013). The initial steps in the formation of this complex is binding of HSP70 - HSP40 to the AR, which is followed by binding of HSP90 and co-chaperones and subsequent dissociation of HSP70 - HSP40 (Querol et al., 2013). HSP90 ensures that the AR retains a conformation with a high affinity for its primary ligand, dihydrotestosterone (DHT) (Fang et al., 1996). Binding of DHT leads to phosphorylation of the AR. This is followed by nuclear translocation, dimerization, and binding to androgen response elements (ARE) from which the receptor directs the transcription of androgen-regulated genes by the recruitment of coactivators (Mangelsdorf et al., 1995; Matsumoto et al., 2013). Owing to their integral role in AR function, it is not surprising that these proteins have been implicated in cancer of the prostate and have garnered considerable interest as novel treatment targets in metastatic CRPC (Ryan and Tindall, 2011). For example, AT13387, an inhibitor of HSP90 has been reported to decrease the expression of several HSP90 client proteins including wild-type AR and AR–V7 (an AR splice variant), and also disrupt nuclear localization of the AR (Azad et al., 2015). A phase I/II clinical trial of AT13387 alone or in combination with abiraterone acetate in patients with metastatic CRPC is in progress (Azad et al., 2015). Other HSP90 inhibitors such as NVP-HSP990 and PF-04929113 have been reported to be active against the AR in preclinical studies (Kim et al., 2009; Neckers and Workman, 2012). Another recent preclinical study has also reported that an inhibitor of the co-chaperone p23, AIL, can prevent AR's interaction with HSP90, resulting in the disruption of the AR-chaperone complex leading to ubiquitin / proteasome-mediated degradation of AR and consequential downregulation of the AR and the expression of its target genes in PCa cell lines and animal tumour models (He et al., 2016).

1.3 Nuclear Resident Chaperones of the AR

Aside chaperones that aid the action of the AR in the cytoplasm, others play various roles in the nuclear action of the receptor such as aiding DNA binding and transcriptional activity (Sabbah et al., 1996; Elbi et al., 2004; Mendillo et al., 2012; Jego et al., 2013). It is thought that some of the cytoplasmic chaperones such as Hsp70 or p23 also function

in the nucleus (Fang et al., 1996; Sabbah et al., 1996; Cato et al., 2014) but it is not clear how they get to the nucleus. There are however other chaperones that are exclusively nuclear which are reported to be involved in chromatin modification and gene transcription. Some examples include the Hsp70 co-chaperone Bag-1L (Froesch et al., 1998; Shatkina et al., 2003) and the histone chaperone NPM1 (Léotoing et al., 2008). Others include FACT (Belotserkovskaya et al., 2003), Vps75 (Berndsen et al., 2008), Nap1 (Avvakumov et al., 2011) etc. In contrast to the cytoplasmic chaperones that modulate AR action, less is known about how the nuclear chaperones regulate AR action.

Bag-1L (Knee et al., 2001; Shatkina et al., 2003; Jehle et al., 2014) and NPM1 (Léotoing et al., 2008; Stelloo et al., 2018) have individually been demonstrated to interact with the AR. Furthermore, a common feature reported about Bag-1L and NPM1 in AR regulation is that, in the absence of androgen both proteins bind the androgen response element on chromatin to which the AR binds for its transcriptional activity. Upon androgen treatment, both proteins make way for the AR to bind to its recognition site (Shatkina et al., 2003; Léotoing et al., 2008). It was therefore thought that these two proteins may play important role in the recruitment of the AR-co-activator complexes to their site of action for transcriptional activation. These reports together implicates Bag-1L and NPM1 in a common mechanistic regulation of AR action in prostate cancer. However, whether they function together in the regulation of the AR has not been investigated.

1.4 Nucleophosmin 1

Nucleophosmin 1 (also known as NPM1, B23, numatrin1 or NO38) was originally identified as a phosphoprotein in *Xenopus* egg extracts as a histone-binding factor that mediates nucleosome formation (Prestayko et al., 1974; Kang et al., 1975; Laskey et al., 1978). Three NPM family proteins, NPM1, NPM2 and NPM3, have been identified in mammals (MacArthur and Shackleford, 1997). NPM1 and NPM3 are expressed ubiquitously, whereas NPM2 (suggested to be required for proper decondensation and re-organization of male and female gametes) is expressed mainly in the ovary (Dalenc et al., 2002). NPM3 is also suggested to play a role in chromatin remodeling in fertilized eggs (McLay and Clarke, 2003).

The human NPM1 gene maps to chromosome 5q35 and contains 12 exons. Alternative splicing of the NPM1 transcript results into two isoforms, NPM1 and NPM1.2 (Wang et al., 1993). The full length protein contains 294 amino acid residues. The shorter NPM1.2 isoform consists of 259 amino acids and lacks 35 amino acids at the COOH-terminus. NPM1.2 is present in cells at low levels (Wang et al., 1993). While NPM1 is nearly exclusively nucleolar, NPM1.2 localizes in both the nucleoplasm and nucleoli (Wang et al., 1993; Colombo et al., 2006).

1.4.1 NPM1 interacts with both proteins and nucleic acids

NPM1 is a multifunctional protein involved in interactions with several partners in the regulation of various cellular activities, including but not limited to, transport of pre-ribosomal particles and ribosome biogenesis (Okuwaki et al., 2002), centrosome duplication (Okuda, 2002; Tarapore et al., 2002), response to stress-stimuli (Chan et al., 1985; Kurki et al., 2004), regulation of DNA transcription, maintenance of genomic stability and embryonic development (Grisendi et al., 2005). Through distinct molecular domains of NPM1, it is able to bind to many partners in distinct cellular compartments, including nucleolar factors (for example, nucleolin, fibrillarin and small nucleolar ribonucleoproteins) (Grisendi et al., 2006), transcription factors (for example, interferon regulatory factor 1 (IRF1), yin yang 1 (YY1) and Nuclear Factor kappa B (NF-κB) (Grisendi et al., 2006), steroid receptors (for example, androgen receptor, glucocorticoid receptor, estrogen receptor and progesterone receptor)(Léotoing et al., 2008), histones (for example, H1, H3, H4 and H2B) (Grisendi et al., 2006; Chen et al., 2014), proteins involved in cell proliferation (for example, DNA polymerase-α), mitosis (for example, never in mitosis gene A-related kinase 2 (NEK2A)) and the response to oncogenic stress (for example, Alternative reading frame (p14ARF) and p53)) (Grisendi et al., 2005, 2006; Okuwaki, 2008). NPM1 also associates with both DNA (Wang et al., 1994) and RNA (Dumbar et al., 1989; Wang et al., 1994; Hisaoka et al., 2010), and it has been reported to have endoribonuclease activity to ribosomal RNA (rRNA) (Savkur and Olson, 1998). NPM1 also forms complexes with the second messenger phosphatidylinositol (3,4,5)-trisphosphate (PIP_3) in the nucleus in response to anti-apoptotic factors (Ahn et al., 2005).

These plethora of interactions that NPM1 is involved in depends on distinct molecular and biochemical domains unique to this protein. **Figure 1.1** shows the functional domains of NPM1 which account for its diverse biochemical interactions (Grisendi et al., 2005; Okuwaki, 2008).

1.4.2 Functional domains of NPM1

NPM1 polypeptide chain has a modular structure containing distinct sequence motifs. The NH_2-terminal domain of the Nucleoplasmin / Nucleophosmin family is highly conserved from *Xenopus* to *Homo sapiens* and represents the core domain in the Nucleoplasmin / Nucleophosmin family of proteins (Hingorani et al., 2000; Okuwaki, 2008). This part of the protein contains one hydrophobic segment that is involved in oligomerization as well as chaperone activity. It is this domain that is required for the suppression of misfolding and aggregation of target proteins (Dingwall et al., 1987; Hingorani et al., 2000). In addition to the oligomerization properties, the NH_2-terminal domain contains two leucine rich nuclear export signals (NES) that are targeted by the nuclear export receptor CRM1 for nuclear-cytoplasmic shuttling (Dingwall et al., 1987; Wang et al., 2005; Yu et al., 2006).

The central domain appears unstructured and is marked by the presence of highly acidic regions composed of strings of aspartic and glutamic acids (A2 and A3). These two acidic stretches are important for binding to histones (Dingwall et al., 1987; Arnan et al., 2003). The central portion between the two acidic domains is required for ribonuclease activity, together with the C-terminal domain, which contains basic regions involved in nucleic acid binding (Hingorani et al., 2000). This domain also hosts a classic bipartite nuclear localization signals (NLS) with the consensus sequence KRN10KKK, where N accounts for any amino acid (Yu et al., 2006). The C-terminal domain contains basic clusters for interaction with nucleic acids. This is followed by an aromatic stretch, which contains two tryptophan residues (288 and 290) that are required for nucleolar localization of the protein (Nishimura et al., 2002).

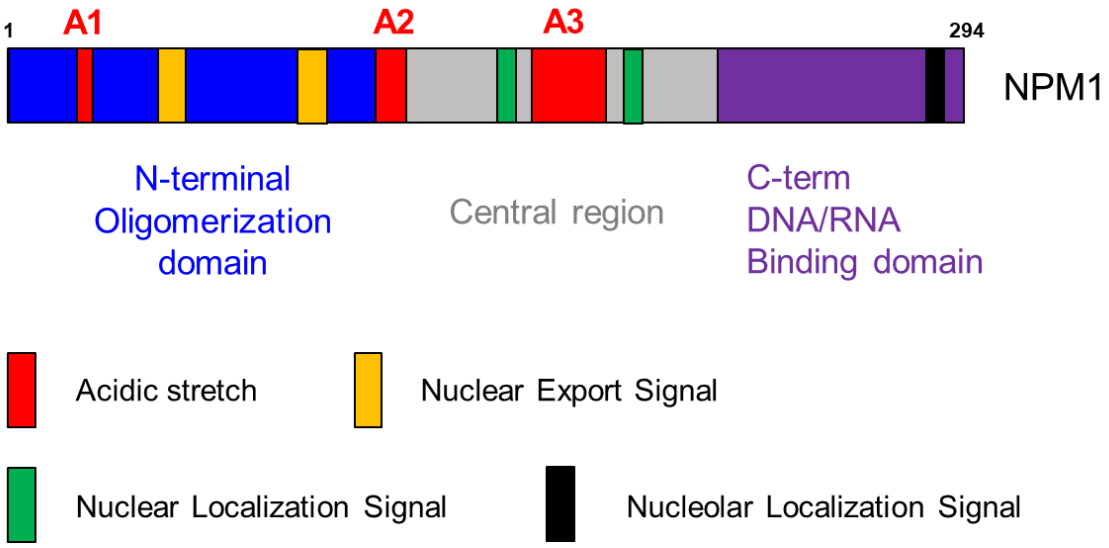

Figure 1.0: Nucleophosmin 1 protein

The figure is a schematic representation of the structure of human Nucleophosmin 1 protein. Blue represents the NH_2-terminal oligomerization domain, gray is the central domain and the violet COOH-terminal DNA/RNA binding domain. The red represents acidic stretches and the yellow represents a nuclear export signal (NES). The green represents a bipartite nuclear localization signal (NLS) and the black represents a nucleolar localization signal (NoLS). Adopted from Mitrea and colleagues' work (Mitrea et al., 2014).

1.4.3 Functions of Nucleophosmin 1

NPM1 has been documented to perform several cellular functions. Below are some of the cellular processes that the protein is involved in.

***NPM1 is a nuclear chaperone*:** Chromatin of all eukaryotic chromosomes is a highly compacted structure consisting mainly of genomic DNA in association with the four histone proteins. Due to chromatin's occluded nature, significant chromatin remodeling is required to allow transcription factors to gain access to their DNA cognate sites. Thus, chromatin remodeling is capable of acting as a specific controlling mechanism, playing a role in a number of important biological events, including transcription, replication, cell development, stress response, and cell cycle progression (Burgess and Zhang, 2013).

NPM1 is biochemically defined as a member of the nucleoplasmin / nucleophosmin family of nuclear chaperones (Schmidt-Zachmann et al., 1987; Hingorani et al., 2000; Okuwaki et al., 2001; Frehlick et al., 2007; Prinos et al., 2011). As a nuclear chaperone, NPM1 can bind to histones and assemble nucleosomes *in vitro* (Laskey et al., 1978) and *in vivo* (Okuwaki et al., 2001). NPM1 binds to core histones and transfer DNA to them in a reaction that requires ATP. NPM1 also functions as chromatin decondensation factor (Grisendi et al., 2006). NPM1's histone chaperone activity is enhanced by p300 mediated acetylation on the COOH-terminal domain of the protein, which is required to modulate *in vitro* transcription from chromatin templates by RNA Pol II (Swaminathan et al., 2005).

NPM1 is involved in multiple transcriptional Regulation: NPM1 proteins can regulate transcription either by directly functioning as transcription factors, or indirectly by influencing the activity of other transcription factors.

- Directly, it has been reported that acetylated NPM1 has an enhanced ability to interact with acetylated core histones and activate transcription from chromatin template (Swaminathan et al., 2005)**.** Interestingly, NPM1 was found to be enriched on a number of human gene promoters, such as those for interleukins (IL) - encoding genes, the tumor necrosis factor alpha (TNF-α) encoding gene, and Homeobox-encoding genes. However, no global enrichment of NPM1 on all gene promoters was detected, indicating that NPM1 is directly involved in the transcriptional regulation of specific genes (Shandilya et al., 2009).
- Indirectly, NPM1 has been reported to regulate a plethora of transcription factors such as Forkhead box protein M1 (FoxM1) (Bhat et al., 2011), c-Myc, the tumour suppressors p53, retinoblastoma protein (Rb) and p14ARF (Grisendi et al., 2006).

1.4.4 NPM1 regulates androgen receptors action

NPM1 specifically influences the activities of the androgen receptor (Léotoing et al., 2008). The Androgen receptor (AR) interacts with NPM1 *in vitro* (Léotoing et al., 2008) and *in vivo* (Léotoing et al., 2008; Stelloo et al., 2018) and their domain of interactions have been mapped out (Léotoing et al., 2008). NPM1 uses its NH_2- and COOH-termini to bind to the AR. This consists of its oligomerization domain at its NH_2-terminus and the

nucleic acid binding domain at its COOH-terminus. On the side of the AR, it has been demonstrated that the DNA binding domain and the Hinge region of the AR are implicated in the interaction with NPM1 (Léotoing et al., 2008). The presence of NPM1 increased several folds in AR binding to its response element, as well as, enhancement in AR transcriptional activity (Léotoing et al., 2008). Conversely, downregulation of NPM1 levels by siRNA technology downregulated androgen response (Léotoing et al., 2008).

1.4.5 Role of NPM1 in cell proliferation, survival and apoptosis

NPM1 expression levels have been implicated in controlling the cellular apoptotic response and cell survival. In a variety of cell based models, it has been demonstrated that down-regulation of NPM1 sensitizes cells to apoptosis, while increased levels of the protein protects against apoptosis and increases proliferation (Wu et al., 2002b, 2002a; Ahn et al., 2005). Below are few examples:

1. In a disease setting, the balance between NPM1 expression and cell fate is demonstrated in hypoxia-driven cancers. For example, suppression of hypoxia-induced NPM1 expression promotes apoptosis whereas overexpression protects from hypoxia-mediated cell death (Li et al., 2004).
2. NPM1 has been reported to bind Protein kinase B / AKT in order to modulate cell survival. AKT binds NPM1 in the nucleus in response to growth factor stimulation to protect NPM1 against caspase-3-mediated proteolytic degradation and promote cell survival (Lee et al., 2008).
3. Similarly, NPM1 stability is enhanced by interacting with erythroid differentiation-associated gene (EDAG), promoting acute myeloid leukemia (AML) cell survival (Zhang et al., 2012).
4. In another instance, the interaction of G-Antigen (GAGE) with NPM1 also enables NPM1 stability to promote resistance to interferon-γ-induced apoptosis (Kular et al., 2009).
5. NPM1 has also been portrayed as regulating cell fate by modulating both the intrinsic and extrinsic apoptosis pathways. During the intrinsic apoptotic response, p53 is required in the mitochondria to enable cytochrome C release.

Overexpression of NPM1 prevents the translocation of p53 from the nucleus to the mitochondria (Dhar and St. Clair, 2009), suggesting that NPM1 may protect cells from apoptosis by reducing the mitochondrial level of p53.

6. Similarly, cytoplasmic localized NPM1 has been indicated to impede apoptosis by directly inhibiting the proteolytic function of caspase-6 and -8 in the cytoplasm (Leong et al., 2010).

These reports suggest that NPM1 may be required in the regulation of the apoptotic pathways.

1.4.6 NPM1 is altered in human cancers

The diversity of the cellular activities that NPM1 is involved in obviously makes it both a potential oncogene and a potential tumour suppressor, depending on the circumstances. It is therefore not surprising that NPM1 has been directly implicated in human tumorigenesis (Grisendi et al., 2006). NPM1 is one of the most frequent targets of genetic alterations in haematopoietic tumours (Raimondi et al., 1989; Morris et al., 1994; Redner et al., 1996; Yoneda-Kato et al., 1996; Grisendi et al., 2006; Okuwaki, 2008). NPM1 protein is overexpressed in various solid tumours and it has been proposed as a marker for gastric (Tanaka et al., 1992), colon (Nozawa et al., 1996), ovarian (Shields et al., 1997) and prostate (Subong et al., 1999) carcinomas. In some cases, the expression levels of NPM1 have been correlated with the stage of tumour progression (Grisendi et al., 2006). For instance, overexpression of NPM1 mRNA is independently associated with the recurrence of bladder carcinoma and progression to a more advanced stage of the disease (Tsui et al., 2004). Although there have been controversial reports on NPM1 level in prostate cancer in the past (Bocker et al., 1995; Subong et al., 1999), current studies show that NPM1 is overexpressed in prostate cancer (Léotoing et al., 2008; Loubeau et al., 2014). Immunohistochemistry studies conducted using prostate cancer tumours at various stages of the disease demonstrated a strong and extensive staining for NPM1 in neoplastic prostate tissues while it was present at lower levels in the basal and luminal epithelial non-tumour cells (Grisendi et al., 2005; Léotoing et al., 2008; Loubeau et al., 2014; Destouches et al., 2016).

1.5 Bcl-2 associated athanogene 1 (Bag-1) Protein

Bag-1L is a member of Bag-1 family of proteins which consist of an evolutionary conserved group of proteins present in several species in Eukaryotes (Sondermann et al., 2001, 2002; Doukhanina et al., 2006). The first gene of the Bag-1 family was identified in a screen for interaction partners of the anti-apoptotic protein Bcl-2 (Takayama et al., 1995). This led to the identification of a gene that increased synergistically the anti-apoptotic action of Bcl-2 and was therefore named BAG-1 or Bag-1: Bcl-2 associated athanogene (from the Greek: a-, anti- and thanaton, death) member 1. The Bag-1 proteins are believed to function as adaptors for the dynamic organization of complexes involved in several pathways such as apoptosis (Takayama et al., 1995), cell proliferation (Wang et al., 1996b) and cellular stress response (Froesch et al., 1998). The Bag-1 proteins also play crucial roles in development (Götz et al., 2005; Greenhough et al., 2016), neurodegenerative diseases (Da Costa et al., 2010) and cancers (Froesch et al., 1998). Such a broad range of functions is covered by the presence of different domains of the protein family.

1.5.1 Bag-1 Proteins and their Functional Domains

It has been shown that at least four isoforms of Bag-1 proteins can arise from alternative initiation of translation within a common mRNA: Bag-1S, Bag-1, Bag-1M (RAP46/HAP46), and Bag-1L (**Figure 1.2**) (Packham et al., 1997; Takayama et al., 1998). The translation initiation site of the largest isoform, Bag-1L, consists of a non-canonical CUG, while three in-frame AUG downstream forms the start codons for the other isoforms (Yang et al., 1998). These isoforms all contain the Hsp/Hsc70-binding BAG domain near the COOH-terminus (Takayama et al., 1997; Briknarová et al., 2001). Through this domain, the Bag-1 family members interact with Hsp70/Hsc70 and a wide variety of other proteins including Bcl-2 (Takayama et al., 1995), the E3 ubiquitin ligase CHIP (Carboxyl-terminus of Hsc70-interacting protein) (Arndt et al., 2005) and nuclear receptors (Froesch et al., 1998; Shatkina et al., 2003; Cato et al., 2017).

All the four Bag-1 isoforms also contain ubiquitin-like domain (ULD) present in the central part of the proteins (Manchen and Hubberstey, 2001). Ubiquitin is a 76 residues

polypeptide binding covalently as a tag to proteins that are directed to the proteasome for degradation (Hershko et al., 1979). The ULD links the chaperone activity of Hsp70 to the degradation of unfolded substrates (Lüders et al., 2000). It interacts with the 20S core and 19S subunit of the proteasome in a complex involving Hsp70 and the E3 ubiquitin ligase CHIP where it facilitates the release of unfolded substrates to the proteasomal machinery (Demand et al., 2001).

However, all the four Bag-1 proteins differ in the lengths of their NH_2-terminal regions. Bag-1L, the longest isoform, contains both an SV40-LargeT-like and nucleoplasmin-like candidate NLS preceded by a unique 50 amino acid-domain. This Bag-1 isoform is predominantly nuclear (Froesch et al., 1998; Knee et al., 2001; Lange et al., 2007). Bag-1M contains only a portion of the candidate NLS and has been shown to reside in the cytoplasm unless stimulated to traffic into the nucleus by associating with other proteins, such as the glucocorticoid receptor (Schneikert et al., 2000). Bag-1 and the shorter and rarer isoform, Bag-1S, are predominantly found in the cytoplasm (Froesch et al., 1998; Lange et al., 2007).

An additional motif, the TXSEEX repeat sequence, has been recognized within the NH_2-terminal segments of the Bag-1 proteins (Froesch et al., 1998; Lange et al., 2007). It is present in eight copies in Bag-1L and –M and two in Bag-1 and 1 in Bag-1S (Cutress et al., 2003). The predicted structure of the repeats is an alpha helix with the acidic residues oriented toward one side. This structure represents the site of phosphorylation for some kinases (e.g. creatine kinase) (Takayama et al., 1998) and it has indeed been found to be phosphorylated (Schneikert et al., 2000) but its function is not known yet.

In general, the expression levels and the cellular localization of the different Bag-1 isoforms can vary considerably for different pathological conditions (Takayama et al., 1998).

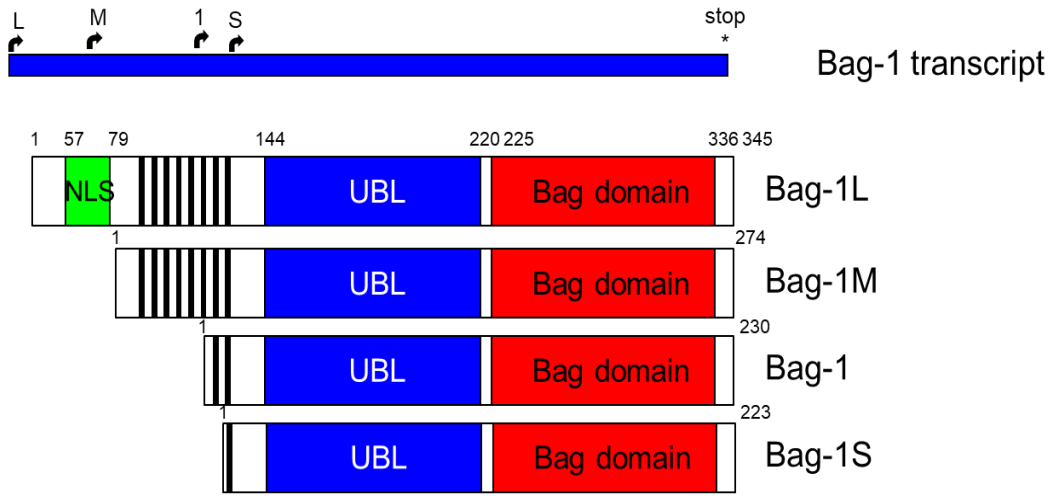

Figure 1.1: The Bag-1 family of proteins

The figure shows a schematic representation of the structure of human BAG-1 family of proteins. Red represents the BAG domain, blue is the ubiquitin-like domain and the light green represents the nuclear localization signal (NLS). The vertical bars represent the TXSEEX repeats (adapted from Takayama and Reed, 2001).

1.5.2 Regulation of proliferation and apoptosis

Several mechanisms have been proposed to explain the action of Bag-1 in cell proliferation and apoptosis.

First, Bag-1 is reputed to regulate cell proliferation and cell growth through its interaction with the serine / threonine kinase Raf-1 (Wang et al., 1996b). Raf-1 phosphorylates and activates the mitogen-activated protein (MAP) kinase cascade leading to enhanced cell proliferation (Huang et al., 1993). It is therefore thought that Bag-1 increases cell growth through its interaction with this protein. In addition, it has been shown that Bag-1 concentrates Raf-1 at the proximity of the mitochondrial membrane where it interacts with Bcl-2. In this situation, Raf-1 can phosphorylate proteins to which it is otherwise inaccessible such as the pro-apoptotic protein Bcl-2-associated death promoter (BAD) which is then dissociated from B-cell lymphoma-extra-large (Bcl-X_L) leading to cell survival (Wang et al., 1996a). Bag-1 proteins also interact with B-Raf in a complex with

AKT and Hsp70 which leads to the phosphorylation of BAD at serine 136 and the inhibition of apoptosis. Disruption of this complex results in early lethality in hematopoietic and neuronal cells in a Bag-1 knock-out mouse model (Götz et al., 2005).

Second, Bag-1 is reputed to bind to the membrane form of the heparin binding EGF-like growth factor (pro-HB-EGF) (Lin et al., 2001) to decrease etoposide-induced apoptosis in LNCaP and PC3 metastasis-derived prostate cancer cells. The interaction of the two proteins occurs through the cytoplasmic tail of pro-HB-EGF and a region on Bag-1 including the ULD but lacking the Bag domain (Lin et al., 2001).

1.5.3 Bag-1 in transcription regulation

Similar to NPM1, Bag-1 proteins can either regulate transcription directly by functioning as transcription factors or indirectly by influencing the activity of other transcription factors like the nuclear hormone receptors (NHR) (Wang et al., 1996b; Froesch et al., 1998; Shatkina et al., 2003; Krajewska et al., 2006).

The genes that are activated directly by the Bag-1 proteins are mainly from viral origin. For instance, Bag-1M, but not Bag-1L and Bag-1S, can induce the transcriptional activity of the Cytomegalovirus (CMV) early region promoter requiring both the NH_2- and the COOH-terminal regions of Bag-1M (Takahashi et al., 2001). Moreover Bag-1S can function as transcription factor stimulating the transcription of the John Cunningham Virus (JCV) early promoter (Devireddy et al., 2000). The mechanism by which the Bag-1 proteins regulate viral gene expression is not understood but it is likely through discrete binding sites of the protein to DNA. It has been reported that Bag-1L and Bag-1M are able to bind DNA through certain amino acid sequences found at their NH_2-terminal region (Zeiner et al., 1999; Shatkina et al., 2003). It has been determined that this sequence consists of two clusters of three lysine (from 2 to 4) and three arginine (from 6 to 8) included in the nuclear localization sequence present partially in isoform Bag-1M and fully in Bag-1L (Zeiner et al., 1999).

1.5.4 Bag-1 proteins and the nuclear hormone receptors

Bag-1 proteins have also been reported to bind nuclear receptors and influence their transcriptional activity (Takayama et al., 1995; Froesch et al., 1998; Briknarová et al., 2001). Nuclear hormone receptors are transcription factors structurally organized in distinct domains: a highly variable NH_2-terminal domain (NTD) containing a ligand-independent transcription activation function 1 (AF1) followed by a well conserved DNA-binding domain (DBD), crucial for recognition of specific DNA sequences; a hinge region which is important for nuclear translocation of the receptor and a COOH-terminal region containing a ligand-binding domain(LBD) which is important for hormone binding, protein - protein interactions, and additional transactivation activity (AF-2) (Kumar and Thompson, 1999; Robinson-Rechavi et al., 2003).

In all the cases analyzed, it was found that the COOH-terminal region of the Bag-1 proteins bind nuclear receptors (Froesch et al., 1998; Kullmann et al., 1998; Liu et al., 1998; Guzey et al., 2000). Since this region also binds Hsp70 (Froesch et al., 1998), it suggests that the mediation of Hsp70 in the regulation of nuclear receptor action requires Bag-1 proteins. The table below shows examples of some of the reported specific interactions and modulation of nuclear receptor actions by Bag-1 proteins.

Table 1.0: Bag-1 proteins regulation of nuclear receptors

Isoform	**Interaction partner**	**Action**	**Reference**
Bag-1L / M	GR	Reduction of DNA binding	(Kullmann et al., 1998)
Bag-1L	ER	Increases transcriptional activity	(Cutress et al., 2003)
Bag-1	RAR	Inhibition of transcriptional activity	(Liu et al., 1998)
Bag-1L	AR	Increases transcriptional activity	(Froesch et al., 1998; Knee et al., 2001; Shatkina et al., 2003)

Bag-1L	VDR	Increases transcription, overexpression Inhibits transcription	(Guzey et al., 2000; Witcher et al., 2001; Lee et al., 2007)

GR = Glucocorticoid receptor; RAR = Retinoic acid receptor; AR = Androgen receptor; VDR = Vitamin D receptor

1.5.5 Bag-1L regulates AR action

Within the Bag-1 family of proteins, it has been shown that Bag-1L is the only isoform of Bag-1 capable of enhancing the transcriptional activity of the AR (Froesch et al., 1998; Knee et al., 2001). Thus, despite evidence that Bag-1M and Bag-1 can interact with the AR *in vitro*, only Bag-1L interacts with AR in cells (Froesch et al., 1998) and alters its transactivation function (Knee et al., 2001). Recent study has further indicated that Bag-1L enhances AR binding to chromatin and that Bag-1L knockout in prostate cancer cell (LNCaP) reduced drastically the ability of AR to function (Cato et al., 2017).

Interaction and functional studies have also shown that Bag-1L action on AR function is mediated through the direct interaction between two regions of each protein. Bag-1L binds via its COOH-terminal BAG domain to the AR NH_2-terminal domain (NTD) (Shatkina et al., 2003) and recently, it has been shown that Bag-1L uses a NH_2-terminal duplicated GARRPR motif to bind to a pocket near the AR LBD, termed binding function-3 (BF-3) (Jehle et al., 2014).

Multiple studies have also indicated that the COOH-terminal Hsc70-binding domain of Bag-1 family members (Höhfeld and Jentsch, 1997; Takayama et al., 1997; Zeiner et al., 1997) is required for interactions with AR *in vitro* and for co-immunoprecipitation of Bag-1L with AR from cell lysates (Froesch et al., 1998; Shatkina et al., 2003). Furthermore, it has been reported that the BAG domain of Bag-1 is sufficient for association with the AR *in vitro* (Knee et al., 2001). However, whether this interaction requires HSP70 is not currently clear.

1.5.6 Bag-1 in cancer

In addition to its role in transcription, studies of overexpression of Bag-1 proteins *in vivo* led to the suggestion that Bag-1 levels could be used as prognostic marker for patient outcome (Krajewski et al., 1999; Tang, 2002). The overexpression of Bag-1 proteins in cancer is directly correlated with the anti-apoptotic action of these proteins resulting in a survival advantage for the cancer cells (Reed, 1994). The isoforms of the Bag-1 family have distinct anti-apoptotic function in tumour cells (Knee et al., 2001). For example Bag-1L and Bag-1M are shown to be the only members of the family that increase resistance to anti-cancer drug treatment in cervical carcinoma cells (Chen et al., 2002) and in breast cancer cell line MCF-7 (Liu et al., 2009). Overexpression of Bag-1 has been detected in patient specimen of colorectal tumour (Clemo et al., 2008), laryngeal cancer (Yamauchi et al., 2001), cervical tumour (Yang et al., 1999) and follicular thyroid carcinoma (Ito et al., 2003). In breast cancer, nuclear expression of Bag-1 has been associated with poor prognosis (Tang et al., 1999) while reduced nuclear and increased cytoplasmic levels have been related to invasive tumours (Krajewski et al., 1999). Intense staining for nuclear Bag-1 proteins associated with more aggressive tumours was also detected in prostate tumour biopsies in patient with metastatic CRPC (Cato et al., 2017). In addition, it has been shown that Bag-1 gene is amplified and overexpressed in hormone refractory prostate cancers (Maki et al., 2007; Cato et al., 2017).

1.6 Study Aim

Earlier studies reported that Bag-1L and NPM1 bind to chromatin in the absence of hormone and the two proteins are displaced when the liganded AR binds its cognate binding sites (Shatkina et al., 2003; Léotoing et al., 2008). Since the two proteins modulate AR action, it was postulated that they possibly influence each other´s activity or work together in the regulation of AR activity in prostate cancer. However, recent studies (Jehle et al., 2014; Cato et al., 2017) have shown that Bag-1L is not bound to chromatin in the absence of hormone but it is most likely recruited by the liganded AR. Currently, no such findings on NPM1 have been made and it is unclear whether Bag-1L and NPM1

proteins work together in the modulation of the AR action. The aim of the study is therefore to investigate:

1. How NPM1 influences the action of the androgen receptor
2. Whether Bag-1L and NPM1 function together in regulating AR action in prostate cancer cell proliferation.

2.0 MATERIALS AND METHODS

2.1. Materials

2.1.1 Chemicals and consumables

Table 2.0: Chemicals used for the project

Description	Supplier
Acrylamide Mix	Roth, Karlsruhe
Agarose	Peqlab, Erlangen
Ampicillin	Roth, Karlsruhe
Ammonium Persulfate (APS)	Roth, Karlsruhe
Bovine Serum Albumin (BSA)	PAA Laboratories GmbH, Pasching
Bacto-Agar	Otto Nordwald GmbH, Hamburg
Bacto-petri dishes	Greiner Labortechnik, Nürtingen
Bacto-Trypton	Roth, Karlsruhe
Bacto-yeast extract	Roth, Karlsruhe
Bromophenol-blue	Sigma–Aldrich Chemie, Steinheim
Chloroform	Merck, Darmstadt
Crystal violet	Lighting Powder Company, INC.
Dimethyl sulfoxide (DMSO)	Fluka, Neu Ulm
Dithiothreitol (DTT)	Gibco, Invitrogen, Karlsruhe
DNA Marker 1 Kb	PeqLab, Erlangen
DNA Marker 100 bp	PeqLab, Erlangen
DRAQ5	Biostatus Limited, United Kingdom
ECL™ Western Blot Detection Reagents	Amersham Pharmacia Biotech, Freiburg
Ethylenediamine Tetraacetic Acid (EDTA)	Roth, Karlsruhe
Ethanol (EtOH)	Roth, Karlsruhe
Ethidium Bromide	Roth, Karlsruhe
Glycine	Roth, Karlsruhe
Glycerol	Roth, Karlsruhe

Glucose	Roth, Karlsruhe
HEPES	Roth, Karlsruhe
Isopropyl β-D-1-thiogalactopyranoside	PeqLab Biotechnologie GmbH, Erlangen
Isopropanol	Roth, Karlsruhe
Kanamycin	Sigma-Aldrich, St. Louis/ USA
Magnesium Chloride	Roth, Karlsruhe
Methanol (MeOH)	Roth, Karlsruhe
β-mercaptoethanol	Roth, Karlsruhe
Milk powder	Saliter, Obergünzburg
Nonident P - 40 (NP-40)	Boehringer, Mannheim
Protease Inhibitor cocktail (PIC)	Sigma Aldrich, Taufkirchen
Phosphate Buffered Saline w/o $CaCl_2$ and $MgCl_2$	1X and 10X Gibco, Invitrogen, Karlsruhe
Phenol	Roth, Karlsruhe
PMSF (phenylmethane sulphonyl fluoride)	Sigma Aldrich, Taufkirchen
Potassium Chloride	Merck, Darmstadt
Poly-L-lysine	Sigma Aldrich, Taufkirchen
PVDF (polyvinylidene fluoride) membranes	Merck Millipore, Darmstadt, Germany
Protein Marker	PeqLab Erlangen
Rotiphorese® Gel30: Acrylamide/ bisacrylamide (30% / 0.8%)	Roth, Karlsruhe
Sodium Acetate	Roth, Karlsruhe
Sodium Chloride	Roth, Karlsruhe
Sodium Dodecyl Sulphate (SDS)	Roth, Karlsruhe
Sodium Hydroxide	Roth, Karlsruhe
Sodium N-lauryl sarcosinate (Sarkosyl)	Sigma Aldrich, Taufkirchen
SYBR Green	Promega, Karlsruhe
Tetramethylethylenediamine (TEMED)	Roth, Karlsruhe
Tris-base	Roth, Karlsruhe
Tris-HCl	Roth, Karlsruhe

Triton-X-100	Sigma Aldrich, Taufkirchen
Tryptone / Peptone ex Casein	Roth, Karlsruhe
Tween-20	Roth, Karlsruhe
Yeast extract	Roth, Karlsruhe

2.1.2 Consumables

Table 2.1: Summary of consumables used for the project.

Description	**Supplier**
Cell culture flasks (T-25, T-75, T-175)	Greiner Bio-one GmbH, Frickenhausen
Cryogenic vials, 2.0 ml round-botton	Corning, Inc., New York/ USA
Immobilon-P Membrane (PVDF)	Millipore GmbH, Schwalbach
PeqGold Gel Extraction kit	PeqLab Biotechnologie GmbH, Erlangen
Qiagen Plasmid Midi and Maxi kit	Qiagen GmbH, Hilden
innuPREP RNA purification Kit	analytikjena, Jena,Germany

2.1.3 Bacteria and eukaryotic cell lines

Bacteria

Table 2.2: Bacteria used in the project

Strain	**Description (Supplier)**
E. coli DH5 α	Chemically competent strains for plasmid amplification
E. coli BL21 (DE3)	Chemically competent strains for protein expression

Eukaryotic cell lines

All the cells grew adherently in monolayers at 37 °C with 5% CO_2 on Cellstar® Petri dishes or Cell culture flasks (T-25, T-75, T-175) (Greiner Bio-one, Frickenhausen, Germany).

Table 2.3: Eukaryotic cell lines used in the project

Name	Source and description
LNCaP	Human cancer cell line derived from a needle aspiration biopsy of the left supraclavicular lymph node of a 50-year-old Caucasian male with confirmed diagnosis of metastatic prostate carcinoma (Horoszewicz et al., 1983).
22Rv1	Human prostate carcinoma cell line derived from a human prostate carcinoma (Sramkoski et al., 1999)
HeLa	Human cervical cancer cell line taken from Henrietta Lacks, a patient who died of cancer (Scherer, 1953)
HEK293T	The 293T cell line is a derivative of human embryonic kidney 293 cells, and contains the SV40 T-antigen. This cell line is competent to replicate vectors carrying the SV40 region of replication. It gives high titers when used to produce retroviruses. (Ref: www.atcc.org/products/all/CRL-3216.aspx#characteristics)

2.1.4 Cell culture media and materials

Table 2.4: Cell culture media and materials used in the project

Name	Source
1X Dulbecco's Phosphate Buffered Saline (PBS)	Gibco®, Thermo Fisher Scientific, USA
Cell culture Dishes, flasks and multi-well plates	Greiner Bio-one GmbH, Frickenhausen
Dulbecco's Modified Eagle Medium (DMEM)	Gibco®, Thermo Fisher Scientific, USA
FBS (South American Origin)	Gibco®, Thermo Fisher Scientific, USA
L-glutamine	Gibco®, Thermo Fisher Scientific, USA
Penicillin/Streptomycin 10000 U/ml	Gibco®, Thermo Fisher Scientific, USA
RPMI medium 1640	Gibco®, Thermo Fisher Scientific, USA

Trypsin 0,025%	Difco, Detroit
Trypsin 0,025% with EDTA	Gibco, Invitrogen, Karlsruhe
Fibronectin	Sigma Aldrich, Taufkirchen
G418 (Geneticin®)	Sigma Aldrich, Taufkirchen

2.1.5 Antibodies

Primary Antibodies

Table 2.5.0: Primary antibodies used in the project

Name	**Description**	**Experimental condition**	**Producer**	**Appli-cation**
Anti-B23	Mouse monoclonal antibody	1:1000 (10% Milk in 1X PBST) O/N, 4ºC	Santa Cruz Biotech	WB
Anti-B23 (c-19)	Rabbit polyclonal antibody	1:1000 (10% Milk in 1X PBST) O/N, 4ºC	Santa Cruz Biotech	WB
		1:250 in blocking buffer (10% FCS in 1X PBS), O/N, 4ºC		IF
Anti-Beta Actin (C4)	Mouse monoclonal antibody	1:1000 (10% Milk in 1X PBST) O/N, 4ºC	Santa Cruz Biotech	WB
Anti-HA	Mouse monoclonal antibody	1:1000 (10% Milk in 1X PBST) O/N, 4ºC		WB
Anti-Histone H2A ab18255	Rabbit monoclonal antibody	1:10000 (10% Milk in 1X PBST) O/N, 4 ºC	Abcam	WB
Anti-AR (N-20)	Rabbit polyclonal	1:1000 (10% Milk in 1X PBST) O/N, 4ºC	Santa Cruz Biotech	WB

Anti-Bag1 (CC9E8)	Mouse monoclonal antibody	1:1000 (10% Milk in 1X PBST) O/N, 4ºC	Santa Cruz Biotech	WB
		1:250 in blocking buffer (10% FCS in 1X PBS), O/N, 4 ºC		IF
Anti-HSP70/ HSC70	Mouse monoclonal antibody	1:5000 (10% Milk in 1X PBST) O/N, 4ºC	Santa Cruz Biotech	WB
Anti-IgG (Rabbit)	Polyclonal rabbit antibody		Santa Cruz Biotech	WB

Secondary Antibodies

All secondary antibodies used were Horseradish peroxidase (HRP)-conjugated and were purchased from Advansta, USA. All secondary fluorescently-labelled antibodies were purchased from Jackson Immuno Research (USA).

Table 2.5.1: Secondary antibodies used in the project

Description	Supplier	Use
Goat anti-rabbit-IgG HRP	Advansta, USA	1 : 10000 dilution (in 10% milk in PBST), 1 h at RT
Goat anti-mouse-IgG HRP	Advansta, USA	1 : 10000 dilution (in 10% milk in PBST), 1 h at RT
Rabbit anti-goat-IgG HRP	Advansta, USA	1 : 10000 dilution (in 10% milk in PBST), 1 h at RT
All fluorescently-labelled secondary antibodies	Jackson Immuno Research (USA)	1:10000 in blocking buffer (10% FCS in 1X PBS), 1 h at RT

2.1.6 Enzymes and Buffers used for cloning

All restriction enzymes were purchased from New England BioLabs (Beverly, USA), Promega (Mannheim, Germany) and Invitrogen GmbH (Karlsruhe, Germany).

Table 2.6: Restriction enzymes used in the project

Description	**Supplier**
Digestion	
Enzyme: EcoRI-HF	New England BioLabs, Inc, Ipswich/ USA
Enzyme: XhO1	New England BioLabs, Inc, Ipswich/ USA
Buffer: 10x CutSmart buffer	New England BioLabs, Inc, Ipswich/ USA
Ligation	
Enzyme: T4 DNA Ligase	New England BioLabs, Inc, Ipswich/ USA
Buffer: 10x T4 DNA Ligase buffer	New England BioLabs, Inc, Ipswich/ USA

2.1.7 Plasmids

Table below shows pcDNA based plasmids (Invitrogen, Karlsruhe, Germany) used for stable or transient transfections of mammalian cells in the project.

Table 2.7: pcDNA used in the project

Name	**Description**
pcDNA3.1-Bag-1L	Bag1-L expression plasmid with the starting codon CTG mutated to ATG
pcDNA3.1-HA-NPM1	Nucleophosmin 1 expression plasmid with an HA-tag
pcDNA3.1-AR-mEOS2	Androgen receptor expression plasmid with an EOS fluorophore
pcDNA3.1-CFP-AR-YFP	Androgen receptor expression plasmid which expresses both Cyanide and Yellow fluorescent proteins
pcDNA3.1-AR-GFP	Androgen receptor expression plasmid with a Green fluorescent fluorophore

2.1.8 Lentiviral Assembling Plasmids

Table below shows plasmids used for the production of Lentiviral particles for gene delivery into mammalian cells (Invitrogen, Karlsruhe, Germany).

Table 2.8: Lentiviral assembling vectors used in the project

Plasmid	**Characterization**
Gag-Pol	Lentivirus packaging plasmid
VSV-G	Lentivirus envelope plasmid
pOZN-Flag-HA-NPM1	NPM1 lentivirus transfer plasmid
pOZN	Lentivirus transfer vector (empty vector)
pOZN-Flag-HA-Bag-1L	Bag-1L lentivirus transfer plasmid

2.1.9 Real-Time PCR Primers

Primers used for Real-time quantitative PCR (qRT-PCR) for relative gene expression analysis in this project are listed in the Table below:

Table 2.9: Real-time PCR primers pairs used in the project

Primers for qRT-PCR	**Sequences (5´ – 3´)**
Androgen Receptor primer	**Forward** AGCGACTTCACCGCACCT
	Reverse GTTTCCCCTTCAGCGGCTCTTTT
Bag-1 primer	**Forward** AGGGTTTTCTGGCCAAGGATTT
	Reverse AGCCTTTTTCTGCTACACCTCAC
Beta-Actin primer	**Forward** CATGTACGTTGCTATCCAGGC
	Reverse CTCCTTATTGTCACGCACGAT
DUOX1 primer	**Forward** GTGCTCCCTCTGTTGTTCGT
	Reverse GCTTCTCAGACACGATGCTGCTCT
NPM1 primer	**Forward** GGAGGTGGTAGCAAGGTTCC
	Reverse TTCACTGGCGCTTTTTCTTCA
RND3 primer	**Forward** GCCGCGTTTCAGAGAGAAAAT
	Reverse CATGGAGCAGCGCAGTTTTT

PMEPA1 primer	**Forward** CTGCAAACGCTCTTTGTTCCA
	Reverse GATGAAGGACCGTGCAGACA
TSC22D1 primer	**Forward** GTTGAAGGTGCTACCGCTGA
	Reverse TACCACACTTGCACCAGAGGA
TMEFF2 primer	**Forward** GAGCCATCTTGCAGGTGTGA
	Reverse GGGGCATTTCCTTGTGATGC
CAMK2N1 primer	**Forward** CTGCAAGCTATCTGCCCAAG
	Reverse CAGGCTGCTCACACAACAGA
SAT1 primer	**Forward** GCCGACTGGTGTTTATCCGT
	Reverse TTTCTTCCCTTTGCGGACCA
RUNX1 primer	**Forward** ACTTCCTCTGCTCCGTGCT
	Reverse GCGGTAGCATTTCTCAGCTC
Actin primers (**Quality control**)	**Forward** TTCCTTCCTGGGCATGGAGT
	Reverse TGTGTTGGCGTACAGGTCTTTG

2.1.10 Equipments

All the Equipments that were used to carry out this project are listed in the table below:

Table 2.10: Equipments used in the project

Description	**Supplier**
Controlled Environment Incubator	Diagenode, Inc., Sparta/ USA
Minus 80 ^{o}C Freezer	Labotect Labor-Technik Gottingen GmbH, Gottingen
Minus 20 ^{o}C Freezer	Liebherr GmbH, Germany
Spectrophotometer BioPhotometer	Epppendorf AG, Hamburg
Vortex 70	Bruker Optik GmbH, Ettlingen
Eppendorf Microcentrifuge 5417R	Eppendorf AG, Hamburg
Eppendorf Centrifuge 5810R	Eppendorf AG, Hamburg

Eppendorf Centrifuge 5804	Eppendorf AG, Hamburg
Hermle ZK 401 Centrifuge	HERMLE Labortechnik GmbH, Wehingen
Incubator Binder KB720 for bacteria	Binder GmbH, Tuttlingen-Mohrigen
Incubator for mammalian cells	Forma Scientific Labortech GmbH, Göttinghen, Germany
NanoDrop Lite Spectrophotometer	Thermo Fisher Scienctific, Inc., Rockford/ USA

2.1.11 Software for Data processing

Software used for the analyses of Data in this project are listed in the table below:

Table 2.11: Software programs used in the project

Description	Supplier
ImageJ for Windows	National Institute of Health, Bethesda/ USA; http://rsbweb.hih.gov/ij
Primsm 6 for Windows	GraphPad Software, Inc., La Jolle / USA

2.2 Methods

2.2.1 Cloning of DNA constructs

The DNA of interest were first of all amplified from a template using PCR. The target fragments were digested with bacterial restriction enzymes to obtain the desired fragments with sticky ends. With the use of Agarose gel, the DNA fragments of interest were separated by electrophoresis and afterwards, extracted from the gel. Finally, the DNA fragments of interest obtained were ligated with a backbone plasmid to confer resistance to selectable marker(s).

2.2.1.1 Polymerase Chain Reaction (PCR)

All Polymerase chain reactions were carried out in a Thermal Cycler machine (GeneAmp® PCR System 2700, Applied Biosystem). The reaction volume was usually of 20 µl containing 10 ng of plasmid template or 500 ng of genomic cDNA template. The PCR reaction solution also contained 100 - 200 µM deoxynucleosides triphosphate (dNTPs), 10 pmol of forward and reverse primers, reaction buffer (containing a final concentration of 20 mM Tris-HCl pH 8.8, 10 mM $(NH_4)_2SO_4$, 10 mM KCl, 0.1% Triton X-100 and 0.1 mg/ml bovine serum albumine) and 0.25 - 1 unit (U) of Pfu proofreading DNA polymerase (from the archaeon *Pyrococcus furiosius*). The Pfu was stored in storage buffer (20 mM Tris-HCl, pH 8.2, 1 mM DTT, 0.1% Tween 20 and 50% glycerol) at -20 ºC. Cycle number and reaction conditions were determined empirically for each fragment of DNA amplified. For amplifying the NPM1 DNA template, the following programme was used:

Table 2.12: PCR programme used for template amplifications in the project

Step	Temperature	Time	Number of cycles
1	94ºC	1	
2	94ºC	1	35x
3	65ºC	1	35x
4	72ºC	1	35x
5	4ºC	Hold	

The steps 2 - 4 were repeated for 35 cycles.

2.2.1.2 Ethanol Precipitation of PCR Products

At least, 3 PCR tubes containing reaction mixture of 20 µl each were pooled together for the ethanol precipitation (ppt) of the PCR products. Distilled water and 5 M NaCl were added to the 3 pooled PCR products (60 µl) to obtain a final volume of 100µl at 0.3 M NaCl. 200 µl of 99% Ethanol was then added to the mixture. Thereafter 5 µl of a carrier (glycogen) was added to enhance the ppt of the DNA. This mixture was kept at -20ºC O/N. Thereafter, the mixture was then centrifuged at 14000 rpm for 15 minutes at 4ºC. The impure pellet was resuspended in 70% ethanol and centrifuged at 10000 rpm to

obtain a relatively pure pellet of DNA. The pellet was air dried and resuspended in distilled water.

2.2.1.3 Double Digestion

The pOZN-Flag-HA-NPM1 plasmid was cloned by double digestion of PCR product containing the sequence for NPM1 and lentiviral donor pOZN plasmid empty vector with 1 unit (U) bacterial restriction enzymes each (New England BioLab, Inc., Ipswich / USA). The enzymes used were Not1-HF and XhO1. These enzymes were used with CutSmart buffer (New England BioLab, Inc., Ipswich / USA) and adjusted the reaction volume to 20 µl each. The mixture was then incubated O/N at 37ºC.

2.2.1.4 Separation of nucleic acids by agarose gel electrophoresis

DNA fragments were separated in an agarose gel according to size in an electric field. Negatively charged DNA migrates towards the positive charged terminal. DNA separation was performed on a horizontal agarose gel ranging from 1 to 2% concentration according to the size of the fragments to be separated. The desired amount of agarose was dissolved in TAE buffer 1X (0.04 M Tris pH 7.2, 0.02 sodium acetate, 1mM EDTA). To dissolve the agarose the solution, the solution was boiled and then cooled down to an approximate temperature of 60 ºC. Thereafter Ethidium bromide was added to the solution to have a final concentration of 0.4 mg/ml. The solution was then poured into a horizontal gel chamber and a comb was placed over the chamber to allow the formation of wells where the samples could be loaded. For the electrophoretic separation, the chamber was filled with TAE buffer 1X and the samples mixed with DNA sample buffer (5mM EDTA, 50% glycerol, 0,01g Bromophenol blue) and loaded onto the gel gently. The standard ladder used was either the peqGOLD 1 kb DNA-Leiter (0.5 mg DNA/ml, for fragments ranging from 250 to 10000 bp) or the peqGOLD 100 bp DNA-Leiter (for fragments from 80 to 1031 bp). The electrophoresis was carried at 120 volts and the separation was visualized under a UV light source. Since agarose gel contains ethidium

bromide double nitril-based gloves were used for the handling to prevent causing harm to self.

2.2.1.5 DNA fragment extraction from agarose gel

For extracting distinct DNA fragments from agarose gel, the peqGOLD gel extraction kit (PeqLab Biotechnologie GmbH, Erlangen, Germany) was used. When the run was completed, the distinct bands stained with ethidium bromide were visualized under a source of UV light of mild intensity and removed with a scalpel into 1.5 ml Eppendorf tubes. The pieces of gel bands were weighed and dissolved in equivalent volume of XP2 Binding Buffer at 65 ºC. The solution turns yellow when the agarose is optimally dissolved and at a pH lower than 7.5. The pH was controlled by the addition of few microliters of 3 M Na-Acetate until colour changed to light-yellow, if the solution was not initially yellow. Thereafter the solution was added to a HiBind® DNA spin column and centrifuged at 12000 rpm (Eppendorf centrifuge 5417R) 1 min. The column was washed once with XP2 Binding Buffer and twice with SPW Wash Buffer (completed with ethanol 80% final concentration) by centrifugation at 10000 rpm (Eppendorf centrifuge 5417R), 1 min at 4 ºC. Residual ethanol was remove from the column by one additional centrifugation at 12000 rpm (Eppendorf centrifuge 5417R) for 1 min. 30 µl of elution buffer was then added in the centre of the column and collected into an Eppendorf tube by centrifugation at 8000 rpm (Eppendorf centrifuge 5417R) for 1 min. The presence of the DNA fragment was confirmed by separating 2 µl using Agarose gel electrophoresis as already described.

2.2.1.6 Quantification of DNA

The DNA quantification was determined using the NanoDrop Lite Spectrophotometer (Thermo Fisher Scientific, Inc., Rockford / USA). The light absorbance at 260 nm was used since nucleic acids absorb light at wave-length of 260 nm. Protein absorption wavelength is at 280. Therefore a ratio OD_{260} / OD_{280} = 1.8 indicates a nucleic acid preparation relatively free from protein contamination. Also, a ratio OD_{260} / OD_{230} above 1.6 indicates a preparation free of organic chemicals and solvents.

2.2.1.7 Ligation of DNA fragments

All ligations were performed using 1 U of the enzyme T4 DNA ligase (Fermentas, St Leon-Rot - Germany). For insertion of a specific DNA fragment into a vector the ratio insert to vector was of or 1 : 6.5. The reaction was carried out in T4 DNA ligase buffer (containing a final concentration of 50 mM Tris-HCl, pH 7.5, 10 mM $MgCl_2$, 10 mM DTT, 1 mM ATP, 25 µg/ml BSA) in a final volume of 20 µl O/N at 4 ºC. Every ligation experiment was performed incubating the empty vector digested with the same restriction enzymes as control. The reaction was stopped by inactivation of the enzyme at 65 ºC for 10 min.

2.2.1.8 Transformation of plasmid DNA into bacteria

For transformation, typically 50 µl of chemically competent bacteria *E.coli* DH5α (for plasmid amplification) or BL21 (protein expression) was incubated with 10 µl of the ligation mix or 500 ng of the purified plasmid DNA for 20 min on ice. Thereafter the cells were thermally shocked at 42 ºC for 2 min and then incubated on ice for 2 min. The transformed bacteria were then allowed to grow in a final volume of 500 µl of SOC medium without ampicillin for 30 min at 37 ºC on a shaker. In the meantime LB 1X agarose plates with selection antibiotics were pre-warmed at RT. Finally, 100 µl of SOC medium containing bacteria was plated and incubated O/N at 37 ºC.

Table 2.13: Media and buffers for plasmid preparation

Description	Components
SOC medium	2% (w/v) bacto tryptone, 0.5% (w/v) yeast extract, 10 mM NaCl, 2.5 mM KCl, 10 mM MgCl2, 10 mM $MgSO_4$, 20 mM Glucose
LB_{Amp} agar plates	1% (w/v) tryptone, 0.5 (w/v) yeast extract, 1% (w/v) NaCl, 1.5% (w/v) bacto agar (pulv.), 100 µg/ml ampicillin
LB_{Kan} agar plates	1% (w/v) tryptone, 0.5 (w/v) yeast extract, 1% (w/v) NaCl, 1.5% (w/v) bacto agar (pulv.), 100 µg/ml kanamycin
LB_{Amp} medium	1% (w/v) tryptone, 0.5% (w/v) yeast extract, 1% (w/v) NaCl, 100 µg/ml Ampicillin

LB_{Amp} medium	1% (w/v) tryptone, 0.5% (w/v) yeast extract, 1% (w/v) NaCl, 100 µg/ml Kanamycin
P1 resuspension buffer	50 nM tris-HCl, pH 8.0, 10 nm EDTA, 100 µg/ml RNase A
P2 Lysis buffer	200 nM NaOH, 1.0% (w/v) SDS
P3 neutralization buffer	3 M potassium acetate, pH 5.5
QBT equilibration buffer	750 mM NaCl, 50 mM MOPS, pH 7.0 , 15% (v/v) isopropyl alcohol, 0.15% (v/V) Triton X-100
QC wash buffer	1 M NaCl, 50 mM MOPS, pH 7.0, 15% (v/v) isopropyl alcohol
QF elution buffer	1.25 M NaCl, 50 mM tris-HCl, pH 8.5, 15% (v/V) isopropyl alcohol

2.2.2 Small-scale purification of plasmid DNA

For mini-preparation of DNA, single colonies of transformed bacteria picked from the agar plates were incubated in 3 ml LB 1X with ampicillin or kanamycin O/N at 37 ºC on a shaker at 220 rpm. Thereafter 1 ml of the bacteria culture was transferred into an Eppendorf tube and centrifuged at 12000 rpm for 1 min at 4 ºC (centrifuge Eppendorf 5417 R). The purification was performed using the solutions P1, P2 and P3 from the Qiagen Plasmid Maxi Kit® (Qiagen, Hilden - Germany). The SNT was removed, the pellet was re-suspended in 100 µl of solution P1 with RNase A and incubated 5 min at RT. Alkaline lysis was performed by adding 200 µl of solution P2 (200mM NaOH, 1% SDS) and incubating for 5 min on ice. Thereafter addition of 200 µl of buffer P3 (3 M Na Acetate, pH 4.8) followed by vortexing and incubation again for 5 min on ice neutralized the pH. To separate the lysate from cells debris the solution was then centrifuged at 12000 rpm for 15 min at 4 ºC (Eppendorf centrifuge 5417R). The SNT was transferred into a new Eppendorf tube and the DNA was precipitated by adding 1 ml of isopropanol to 400 µl of aqueous solution. The reaction was incubated at -20 ºC for 30 min. The DNA was collected by centrifugation at 12000 rpm at 4 ºC for 15 min (Eppendorf centrifuge 5417R).

After discarding the SNT the DNA pellet was washed from residual salts with 200 µl of 70% Ethanol. After centrifugation at 12000 rpm for 2 min at 4 ºC (Eppendorf centrifuge 5417R) the SNT was discarded and the residual ethanol allowed to evaporate. The DNA was resuspended in 30 µl of double-distilled water and dissolved by incubation at 50 ºC for 10 min and thereafter stored in -20 ºC.

2.2.3 High-scale purification of plasmid DNA

For high-scale purification of plasmid DNA, the Qiagen Plasmid Midi or Maxi kit was used. Bacteria was cultured the day before the purification in 200 – 500 ml of LB 1X depending on whether the plasmid has a low or high copy number yield with either ampicillin or kanamycin at 37 ºC with shaking at 220 rpm O/N. The next day, the bacteria was collected by centrifugation at 4000 xg for 25 min at 4 ºC in a fixed angle rotor (centrifuge Hermle ZK 401) and resuspended in 10 ml of buffer P1 containing RNase A. After incubation for 10 min at RT, alkaline lysis was performed by adding 10 ml of buffer P2 and vortexing. The reaction was allowed to proceed for 10 min on ice which convert the mixture to blue. Thereafter the pH was neutralized by 10 ml of buffer P3 and the mixture was mixed thoroughly until colour changed from blue to colourless. To separate the soluble part from the insoluble cell wall and membrane debris, the suspension was centrifuged at 6000 xg, 30 min at 4 ºC (centrifuge Hermle ZK 401). After centrifugation the supernatant (SNT) was poured into a Qiagen Tip 500 column which has been pre-equilibrated with 15 ml of buffer QBT (700 mM NaCl, 50 mM MOPS pH 7.0, 15% isopropanol (v/v), 0.15% Triton X-100 (v/v)). The column contained a resin able to bind DNA and to purify it from the lysate. Thereafter the column was washed twice with 30 ml of buffer QC (1 M NaCl, 50 mM MOPS pH 7.0, 15% isopropanol (v/v)). The DNA was eluted from the resin by addition of 15 ml of buffer QF (125 mM NaCl, 50 mM Tris-HCl pH 8.5, 15% isopropanol (v/v)) and collected in a Falcon tube. To precipitate the DNA, 11 ml of isopropanol was added to the eluted solution and the mixture obtained was thoroughly mixed and incubated on ice for 15 min. To collect the precipitated DNA the solution was then centrifuged at 5000 xg for 30 min at 4 ºC (centrifuge Beckman Coulter). The SNT was discarded and the pellet was resuspended in 1 ml of 70% ethanol and transferred into a 1.5 ml Eppendorf tube. After

centrifugation at 12000 rpm for 2 min at 4 ºC (Eppendorf centrifuge 5417R) the SNT was removed and the pellet air-dried. The DNA was dissolved in 200 - 300 µl of TE buffer (10 mM Tris pH 8.0, 1 mM EDTA, ddH_2O) and stored at -20 ºC.

2.2.4 Cell culture and transfection methods

2.2.4.1 Cell culture

All mammalian cells were cultured in standard conditions of 37 ºC, 5% of CO_2 and 95% of humidity in an incubator (Forma Scientific Labortech GmbH, Göttinghen, Germany). All cell lines were grown in sterile Cellstar® Petri dishes or Flasks (Greiner Bio-One, Frickenhausen, Germany) of different formats depending on the experimental conditions. Cells were grown to a confluence of 80 - 90%, then the culture medium was removed, washed once with PBS 1X pre-warmed at 37 ºC and incubated with trypsin for approximately 3 minutes at room temperature. Thereafter, fresh medium containing 10% FCS was used to stop the action of trypsin and the cells spinned down at 1000 rpm for 3 minutes at room temperature using new Falcon tubes. The supernatant was aspirated off and the cells re-suspended in fresh medium. The human prostate cancer cell line Lymph Node metastasis Carcinoma of the Prostate (LNCaP) cell and 22Rv.1 cells were cultured in Roswell Park Memorial Institute (RPMI) 1640 enriched with 10% FBS and L-Glutamine (Invitrogen, Karlsruhe, Germany). LNCaP95 cell line was cultured in phenol red free RPMI supplemented with 10% CCS (charcoal stripped serum) and 1% L-Glutamine (Invitrogen, Karlsruhe, Germany). HeLa cells and HEK293T cells were cultured in DMEM medium supplemented with 10% FCS and 1% L-Glutamine.

2.2.4.2 Generation of Stable NPM1 knockdown clones

Wild-type LNCaP cells were cultured in RPMI 1640 medium with phenol red as pH indicator (GIBCO®, Thermo Fisher Scientific, USA) supplemented with 10% heat-inactivated fetal bovine serum (FBS). For depletion of NPM1, NPM1 shRNA lentiviral particles recommended for the inhibition of NPM1 expression in human cells were used to infect LNCaP and HeLa cells according to the manufactures protocol (Sigma Aldrich

Missions). Lentiviral particles were a pool of concentrated transduction-ready viral particles containing five target-specific constructs that encoded 58 nucleotides shRNA (SHCLNV-NM_002520, Sigma Aldrich) and another lentiviral particles containing non-target scrambled shRNA nucleotide sequence (SHC016V-1EA, Sigma Aldrich). Exactly 24 h after infecting the cells, the media containing the excess viruses were aspirated off and fresh media added to the cells to allow transduced genes to be expressed. After 48 h of growth, monoclonal selection was performed by trypsinizing the cells and seeding them in a much diluted cell suspension in medium containing 1 µg/ml of Puromycin to select stably transduced cells. Selected clones were assessed for the level of NPM1 silencing by using Western blotting with anti-NPM1 antibody (Santa Cruz Biotechnology). The table below contains the list of all the 5 target specific shRNA pool and the non-target specific pLKO.1-puro shRNA sequences used.

Table 2.14: Nucleotide sequences of shRNAs and siRNAs used in the project

ID	**shRNA NPM1**	**Nucleotide Sequence**
Clone ID:**NM_002520.4-169s1c1**	Target shRNA	CCGGGCCGACAAAGATTATCACTTTCTCGAGAAAGTGATAATCTTTGTCGGCTTTTTG
Clone ID:**NM_002520.4-1120s1c1**	Target shRNA	CCGGGCCAAGAATGTGTTGTCCAAACTCGAGTTTGGACAACACATTCTTGGCTTTTTG
Clone ID:**NM_002520.4-664s1c1**	Target shRNA	CCGGGCGCCAGTGAAGAAATCTATACTCGAGTATAGATTTCTTCACTGGCGCTTTTTG
Clone ID:**NM_002520.4-817s1c1**	Target shRNA	CCGGCCTAGTTCTGTAGAAGACATTCTCGAGAATGTCTTCTACAGAACTAGGTTTTTG
Clone ID:**NM_002520.4-253s1c1**	Target shRNA	CCGGGCAAAGGATGAGTTGCACATTCTCGAGAATGTGCAACTCATCCTTTGCTTTTTG

Clone ID:**NM_002520.5-876s21c1**	Target shRNA	CCGGCCTAGTTCTGTAGAAGACATTCTCGAGA ATGTCTTCTACAGAACTAGGTTTTTG
Non-Target shRNA Control **SHC016V**	Non-target shRNA	CCGGGCGCGATAGCGCTAATAATTTCTCGAGA AATTATTAGCGCTATCGCGCTTTTT

2.2.4.3 Transient NPM1 knockdown using siNPM1

10^5 cells were seeded and allowed 1 h to settle in the 6-well plates used. At the same time, transfection complex made up 100 nM of target specific siRNA or non-target specific siRNA (scrambled) and HiPerFect transfection reagent (Qiagen) diluted in Optimem was being incubated at room temperature for 10 min. Afterwards, the complexes were added to the cells in dropwise manner. The plates were thereafter swirled gently to ensure uniform distribution of complexes. The transfection was repeated 24 h after the first. 48 h after the second transfection, cells were harvested and divided into pairs. One part was lysed in 2X Laemmli sample buffer for SDS-PAGE and Western blotting with anti-NPM1 (section 2.2.6). The second part were used for total RNA extraction, cDNA synthesis and quantitative RT-PCR analysis with target specific primer pairs (section 2.2.5). The NPM1 siRNA (sc-29771, Santa Cruz Biotechnology) used contained a pool of 3 target-specific 19 - 25 nucleotide for the silencing of NPM1. The control siRNA-A (sc-27007) also contained a pool similar to that of the target specific siRNA according to the manufacturer (Santa Cruz Biotechnology)

2.2.4.3 Generation of Bag-1L stable clones

The stable retroviral transduction of Bag-1L was carried out in 2 stages. The first stage included the production of the retroviruses carrying the target gene: Bag-1L. This was carried out as followed:

HEK 293T cells were seeded to 80% confluent in DMEM culture medium supplemented with 10% FBS. After 6 h, the cells were transfected with a mixture made up of retroviral packaging vector pCG-gagpol (5 µg), envelope vector pCG-VSV-G (5 µg) and the transfer vector pOZN-Bag1L (10 µg) or pOZN empty vector (as control) plasmids using Lipofectamine 2000® (Qiagen) according to the manufacturer's protocol. Exactly 24 h after transfection, the medium was aspirated off and fresh medium added to the cells for O/N incubation. After 24 h, the medium was collected and stored at 4 ^{o}C and fresh medium was added to the cells and incubated for another 24 h. The second medium was collected after 24 h and pooled together with the previous medium collected. The harvested media contained viruses, cells and cell debris. The cells and cell debris were gently filtered through a 0.2 µm cellulose acetate filter (Sigma Aldrich) and aliquoted for use in the next stage of infecting the cells of interest. However, some of the aliquots were frozen at -80^{o}C for future use.

Infection: The infection was carried out by seeding 10^6 cells of interest (NPM1 knockdown cells and Bag-1L knockout cells) in 6-well plates in RPMI supplemented with 10% FCS and 1% L-glutamine and incubated for 24 h. Thereafter, the media were replaced with 2 ml each from either Bag-1L virus containing medium or pOZN empty vector virus containing medium. Thereafter the cells were incubated for 24 h and the media replaced with fresh media and incubated for further 48 h for the infected cells to express the selectable marker.

While the cells were being incubated with the viral media, magnetic beads (M-450 Dynabeads, Invitrogen) were prepared to be used for selection. This was carried out as followed: 0.1% IgG-free BSA (Jackson Immunoresearch VWR) in PBS 1X was prepared and sterilized by filtering through 0.2µm filter. 1 ml of magnetic bead slurry was then washed in BSA/PBS solution 3 times. After the 3rd wash, anti-IL-2 Receptor alpha (Millipore / Upstate Biotech, Cat No 05-170) antibody diluted in BSA/PBS (1: 40 dilution) was added to the beads and incubated on a rotor overnight at 4 ^{o}C. The next morning, beads were collected by putting tubes in magnetic apparatus (BioMag, PolySciences, Cat No 84102S) to cause the beads to cling to the tubes' walls and the solutions which contained unbound antibodies were removed by gently pipetting it off; as strong forces could dislodge beads from magnet. Tubes were removed from magnet and beads

resuspended in 1 ml of BSA / PBS solution. The process of using the magnet to separate the beads with bound IL-2 from unbound IL-2 was repeated 3 times as washing steps and bound beads were finally resuspended in volume of 1 ml of the washing buffer. The beads coupled to anti-IL-2 alpha antibody was then stored at 4 ^{o}C to be used for selection.

Selection of the infected cells was carried out as followed: cells were trypsinized gently at room temperature for 2 minutes after which medium containing 10% FCS was used to stop the action of trypsin. The cells were spinned down and resuspended in 1 ml of medium in 1.5 ml Eppendorf tubes. Thereafter 200 µl of the prepared magnetic Dynabeads (M-450 Dynabeads, Invitrogen) coupled with IL-2-antibody (Millipore) was added to the cells and incubated at room temperature for 1 h, with constant turn of the tubes every 10 minutes to allow the beads to evenly mix with the cells. After 1 h, cells bound to the beads were separated by placing the tubes in the magnet and removing the media gently by pipetting. The separated cells were resuspended in fresh medium gently and re-separated using the magnet. This cycle of selection with the magnet was carried out 3 times to ensure maximum selection of only bead coupled cells. The infected cells that were separated had beads decorating their cell membranes. These cells were further expanded and Western blotting carried out to check the expression of Flag-HA-Bag-1L using anti-Bag-1 antibody (CC9E8, Santa Cruz Biotechnology).

2.2.4.4 Cell Proliferation Assay

Cell proliferation assay was performed by direct cell counting of the number of cells over a period of 7 days and normalized against the starting number (day 0 cell count). 10^5 cells from both shNPM1 and Control cells were seeded in 6-well plates in triplicates in multiple plates of 5 in RPMI medium supplemented with 10% FCS and 1% L-Glutamine. After 24 h, when the cells had fully adhered to the plates, the culture media was changed to starvation medium [(Phenol-red free RPMI 1640 medium (Invitrogen) supplemented with 3% Charcoal stripped serum, and 1% L-Glutamine)] after washing 2 times with PBS 1X. After 72 h in starvation media, the first plates from each clone was counted and used as the day 0 count. The rest of the cells were either treated with solvent or DHT (10^{-8} M) and this treatment was repeated every 48 h. After 24 h post treatment, a batch was counted.

The next batches were counted after 3, 5 and 7 days of growth. The cell counts were normalized against day 0 count to determine the fold increase in cell number.

2.2.4.5 Immunofluorescent Experiments

Cover slips were placed in 24 well plates and sterilized using 80% ethanol for 15 min. Thereafter, the ethanol was aspirated off and the remnant allowed to air-dry under cell culture biosafety hood. Afterwards, the wells containing the cover-glasses were washed three times with PBS 1X. Thereafter cells were trypsinized, washed twice with PBS 1X and $1x10^4$ cells seeded in each well containing a cover slip. After 48 h, the medium was removed, the cells washed with PBS 1X once and fixed with ice-cold 4% paraformaldehyde (PFA) in PBS 1X for 5 min. Thereafter, the PFA was aspirated and cells washed twice with PBS 1X and incubated with permeabilization solution (0.1% Triton X-100 in PBS 1X) for 5 min at room temperature. The permeabilization solution was removed and the cells washed twice with PBS 1X and incubated with blocking buffer (10% Fetal Bovine serum in PBS 1X) for 60 min at room temperature and subsequently incubated with primary antibodies and DRAQ5® (nuclear stain, 1:1000 dilution) diluted in blocking buffer O/N at 4 ^oC. Cells were then washed three times with cold PBS 1X and incubated with secondary antibody (1:10000 dilution) diluted in blocking buffer for 60 min at room temperature. Finally cells were washed four times, 10 minutes each with ice-cold PBS 1X. The cells were finally washed for the fifth time for 30 min (this is very important for the removal of all background stains from the secondary antibodies). Finally, the coverslips with the cells were dipped once in distilled water to remove salts and semidried by the edge with tissue paper whiles preventing contact with surface with the cells. The coverslips with the fixed cells were mounted onto a microscope slide (Erie Scientific, Portsmouth, US) with 10 µl volume of mounting medium (polyvinilalcohol (PVA)). Samples were air-dried in dark place for about 2 h at room temperature to enable the mounting medium to stabilize the coverslip at a fixed position, because any form of movement of the coverslip whiles mounting medium has not fully dried damaged the sample quality. Signals were visualized using confocal laser scanning microscope (LSM510, Zeiss) and analyzed with LSM510 software.

2.2.4.6 Live Cell Fluorescent Imaging Experiments

Cells were always passaged 24 h before using for transfection studies. After 24 h of growing, cells were trypsinized and washed once with PBS 1X. Thereafter, $5x10^4$ cells were seeded in each well of a 4-well glass Lab-Tek® II Chamber Slide™ System (VWR International, Bruchsal, Germany) in phenol red free RPMI 1640 medium supplemented with 3% CCS (charcoal stripped serum) and 1% L-Glutamine (Invitrogen). The cells were at this moment transiently transfected with 500 ng plasmids / well for the expression of fluorescently tagged androgen receptor (e.g. yellow fluorescent protein-androgen receptor-cyani fluorescent protein (YFP-AR-CFP) or Eos-androgen receptor (mEos2-AR)) using Lipofectamine 2000® transfection reagent (Thermo Fischer Scientific) in the following steps. After 1 h of seeding the cells in the 4-well chambers, plasmids and transfection reagents which have been diluted in Optimem® (cell culture medium without serum or antibiotics) and incubated for 20 min at room temperature to enable complex formation between the transfection reagent and DNA, was dropwise delivered onto the cells and swirled gently for even distribution of the complexes. The cells were maintained in the same medium for 12 h after which the medium was replaced with fresh starvation medium for additional 36 h.

2.2.4.6.1 Kinetics of Androgen receptor (AR) nuclear translocation

Live cell imaging was carried out (in collaboration with the group of Prof. Dr. G. Ulrich Nienhaus, KIT) by using an Andor Revolution® XD spinning disk laser scanning microscope (BFi OPTiLAS, München, Germany) (Yang et al., 2013). YFP was excited at 488 nm (187 µW, 80 ms). The emission was passed through a bandpass filter (560 / 55 nm center wavelength / width, AHF, Tübingen, Germany). Data collection was started immediately after adding 10 nM dihydrotestosterone (DHT), using customized time intervals for different time-lapse experiments.

Image quantification: Images were analyzed using ImageJ (Abràmoff et al., 2004). For the control cells, shNPM1 cells, shNPM1-Bag-1L rescue cells and shNPM1-vector cells, the time-dependent fluorescence intensities in the nuclei, $I_{Nucleus}(t)$, were calculated as

$$I_{Nucleus}(t) = \frac{F_{Nucleus}(t)}{F_{Nucleus}(t=0)} \times 100\%,$$

where F represents the fluorescence intensity after background subtraction. The background intensity (I_B) was determined in a 4.4 × 4.4 μm^2 region of interest without any YFP fluorescence signal. I_B was calculated for each frame. $F_{Nucleus}(t)$ was obtained by calculating the integrated intensity in the nuclear region. All intensities were normalized by the initial intensity in the nucleus, $F_{Nucleus}(t=0)$.

For comparing the data from the Bag-1L control cells (B3a), Bag-1L knockout (E5) cells, Bag-1L KO-Bag-1L rescue cells and Bag-1LKO-vector cells, the relative fluorescence intensities in the nucleus, $I_{rel}(t)$, were determined by scaling the intensities to those of the whole cell:

$$I_{rel}(t) = \frac{I_{Nucleus}(t)}{I_{Cell}(t)} \times 100\% = \frac{F_{Nucleus}(t)}{F_{Cell}(t) \cdot I_{rel}(t=0)} \times 100\%,$$

where F denotes the fluorescence intensity after background subtraction. $F_{Cell}(t)$ was obtained by calculating the integrated intensity of the whole cell. And the intensities were normalized by the initial $I_{rel}(t=0)$, with $I_{rel}(t=0) = \frac{F_{Nucleus}(t=0)}{F_{Cell}(t=0)}$.

2.2.5 RNA Analysis

2.2.5.1 RNA Extraction

Total cellular RNAs were extracted using InnuiPrep® RNA extraction kit (analytikjena Innuscreen GmbH, Germany) as prescribed by the manufacturer. This kit was used because, it prevented very large variation in the RNA quality and the mRNA levels of housekeeping genes. Briefly, 400 µl Lysis Solution RL was added to cells cultured in 6-well plates directly after washing cells with PBS 1X and incubated for 2 minutes at room temperature. The cells were re-suspend completely by pipetting up and down and Incubated for further 3 minutes at room temperature. Spin Filters D were placed into Receiver Tubes and the lysed sample were transferred into the Spin Filter D and centrifuged at 12,000 rpm for 2 minutes. The Spin Filters D were discarded; it contained

proteins and DNA. Another spin filter which traps RNA (spin filter R) was then employed. Spin Filters R were placed into a new Receiver Tubes and equal volume (approx. 400 µl) of 70% ethanol was added to the filtrate from step 2 and mixed the sample thoroughly by pipetting several times up and down. The samples were transferred into Spin Filters R and centrifuged at 11,000 rpm for 2 minutes. The Spin Filters R with the bound RNA were placed into new Receiver Tubes whiles the Receiver Tubes with filtrates were discarded. The Spin Filters R were washed first with 500 µl Washing Solution HS by adding 500 µl HS solution and centrifuging at 12,000 rpm for 1 minute. The Spin Filters R were washed next with 700 µl Washing Solution LS and centrifuged at 12,000 rpm for 1 minute. The Spin Filters R were placed into new Receiver Tubes and centrifuged at 12,000 rpm for 3 minutes to remove all traces of ethanol. The Spin Filters R were then placed into Elution Tubes, 80 µl RNase-free water added to the Spin Filters R and incubated at room temperature for 1 minute. After the incubation, the Spin Filters R were centrifuged at 8,000 rpm for 1 min to elute the RNA into the Elution tubes.

2.2.5.2 Quantification of RNA Concentration

The concentrations of RNA were determined by measuring the optical density (OD) of RNA samples at 230, 260 and 280 nm using NanoDrop® ND-1000 spectrophotometer (PeqLab Biotechnologie GmbH, Germany). A ratio of OD_{260}/OD_{280} within 1.8 - 2.0 indicates a sample of acceptable purity, relatively free of proteins, while OD_{260}/OD_{230} 1.6 and above shows a preparation relatively free of organic chemicals and solvents.

2.2.5.3 Complementary DNA (cDNA) Synthesis

To synthesize cDNA from RNA, first, 1 µg of RNA was incubated with 1 unit of DNAse1, in a total reaction volume of 10 µl in PCR tube, at 37 °C for 30 min, in a thermocycler (GeneAmp® PCR System 2700, Applied Biosystem), to digest genomic DNA contaminants, if there were any. After incubation with DNase1, 1 µl of RQ1 DNase Stop Solution® (Promega, Mannheim) was added and incubated at 65 °C for 10 min in thermocycler to inactivate DNase1. Thereafter, 1 µl Random primer (200 ng/µl) was

added to each tube and incubated for 5 minutes at 70 ^{o}C in the thermocycler for random primers to anneal to RNA. Afterwards, a master mix containing the following reagents were prepared depending on the number of RNA samples to be reverse transcribed into cDNA. For one sample, the following master mix was utilized:

Table 2.15: Reagents and enzymes used for reverse transcription

Reagent	**+ reverse transcriptase**	**- reverse transcriptase**
5x buffer	4 µl	4 µl
dNTPs (10mM)	2 µl	2 µl
Reverse transcriptase (M-MLV RT [H-])	1 µl	0 µl
RNAse free water	3 µl	4 µl

10 µl each from the master mix with either (+) reverse transcriptase or (-) reverse transcriptase was transferred into the separate PCR reaction tubes from above labeled +RT and -RT respectively. The tubes were incubated in parallel in the thermocycler using the following cDNA synthesis protocol:

Table 2.16: PCR conditions used for cDNA synthesis in the project

Step	**Temperature**	**Time**
1	25°C	10 min
2	42°C	60 min
3	70°C	10 min
4	4°C	Hold

After cDNA synthesis, the content of +RT and -RT PCR were diluted with 100 µl sterile RNAse-free water. Samples were used immediately or stored in -20^{o}C for future use. The +RT tube contains reverse transcriptase for normal cDNA synthesis, whereas the –RT contains no reverse transcriptase and therefore, serves as quality control (quality control PCR) check for detecting genomic DNA contamination. The QC-PCR was performed as shown below.

2.2.5.4 Quality Control PCR (QC-PCR)

To check for genomic DNA contaminants which might have occurred during RNA extraction, 4 µl of the +RT and -RT PCR products (Section 2.2.5.3) were taken into separate tubes and 16 µl QC-PCR master mix containing Actin gene primer pairs (4 µl GoTag Polymerase 5X buffer, 0.5 µl of 100 nM dNTPs, 1 µl forward primer, 1 µl reverse primer, 0.25 µl of Go Tag Polymerase and 9.25 µl water) added to each tube. The samples were incubated in a themocycler (GeneAmp® PCR System 2700, Applied Biosystem) using the QC-PCR protocol below.

Table 2.17: Quality control PCR conditions used in the project

Step	**Temperature**	**Time**	cycles
1	95°C	2 min	1
2	95°C	2 min	34x
3	55°C	40 s	34x
4	72°C	45 s	34x
5	4°C	Hold	

The steps 2-4 were repeated for 34 cycles.

The resultant PCR products were run on agarose gel and visualized (section 2.2.1.4). The presence of DNA fragments in the -RT PCR product indicates genomic DNA contamination.

2.2.5.5 Quantitative Real-Time PCR (qRT-PCR)

To carry out gene expression analysis using qRT-PCR, 4 µl of cDNA (+RT PCR product, obtained from Section 2.2.5.3) was pipetted into qRT-PCR plates (Steinbrenner Laborsysteme, Wiessenbach). Next, 16 µl of qRT-PCR master mix containing gene specific primers (10 µl SYBR Green qPCR-Mix (Promega), 1 µl forward primer, 1 µl reverse primer, 4 µl RNase-free water) was added to the cDNA. The qRT-PCR was ran in StepOnePlus Real-Time PCR system (Life Technologie, Carlsbad, California), with an initial denaturation stage carried out at 95 °C for 15 min. This was followed by 40 cycles

of a two-step stage of 95 °C for 15 s, and 60 °C for 30 s, for hybridization and amplification, and finally, a melting curve with a starting temperature of 60 °C, with stepwise increase of 0.5 °C to 95 °C that was maintained for 15 s. The relative mRNA expression of a target gene was calculated as 2^-(CT $_{(target\ gene)}$ - CT $_{(reference\ gene)}$).

2.2.5.6 RNA-Sequencing And Analysis

To determine the genome-wide androgen mediated gene expression, LNCaP cells were seeded in triplicates in starvation medium for 72 h. After starvation, cells were eitherr treated with DHT or solvent for 16 h as indicated below:

1. Solvent treated cells (basal),
2. DHT treated cells (hormone induced),

Thereafter, the cells were washed with ice-cold PBS 1X three times and scraped into 2 ml Eppendort tubes in PBS 1X. The cells were then spinned down, the supernatants pipetted off and frozen rapidly at -80 ^{o}C. The cell pellets were then transported to our collaborating partners (Jaice Rottenberg, Laura Cato, Irene Lee I. and Myles Brown) at the Department of Medical Oncology, Dana-Farber Cancer Institute, Harvard Medical School, Boston, United States, for RNA extraction, library preparation, RNA-Sequencing and Bioinformatic analysis to be carried out.

The RNA-Sequencing was carried out and the data processed through a Visualization Pipeline for RNA-seq (also known as VIPER: https://bitbucket.org/cfce/viper). The data were also analysed using Limma (a package for differential expression analysis of data arising from microarray experiments) and DESEQ2 Bioconductor tools (Love et al., 2014) to obtain the differential gene expression analysis.

2.2.6 PROTEIN ANALYSIS

2.2.6.1 Preparation of Whole Cell Lysate

Protein extraction from cells was carried out by first, washing the cells with PBS 1X and either trypsinized or scraped into specified volume of PBS 1X. The resuspended cells

were counted using Improved Neubauer cell counting chamber. Equal number of cells were counted and lysed with 2X Laemmli (65.8 mM Tris-HCl pH 6.8, 4% SDS, 20% glycerol, 12.5% mM EDTA pH 8.0, 2% β-mercaptoethanol, 0.02% bromophenol blue, 37.5% ddH_2O) buffer in the ratio of 10^6 cells per 200µl 2X Laemmli sample buffer plus protease inhibitor cocktail (1:100 ratio). The samples were then incubated at 95 °C on a heating block (Eppendorf Thermomixer 5436, Eppendorf-Netheler-Hinz GmbH, Hamburg) for 5 min. After heating, the lysate was spinned down at 5000 rpm for 1 min and sonicated at an amplitude of 50, 5 pulses [(Branson Sonifier Cell disrupter B 15 (G.Heinemann Ultraschall- und Labortechnik, Schwäbisch Gmünd)]. The sonicated sample was then spinned down at 5000 rpm at 4 °C for 1 min. Typically, volumes of 60 µl the whole lysates were resolved in SDS-Polyacrylamide gel electrophoresis.

2.2.6.2 Separation of proteins by Sodium Dodecyl Sulfate PolyAcrylamide Gel Electrophoresis (SDS-PAGE)

The Penguin Doppelgelsystem P9DS apparatus (PeqLab, Erlangen, Germany) was used to cast the polyacrylamide gel. Typically 10% polyacrylamide gel was used (for 30 ml of final volume, 11.9 ml of ddH_2O, 10 ml of 30% Acrylamide mix, 7.5 ml of Tris 1.5 M pH 8.8, 300 µl of 10% SDS, 300 µl of APS, 12 µl of TEMED). The resolving gel was poured and overlaid with Isopropanol. After polymerization the isopropanol was washed away with distilled water and the separating gel was covered with stacking gel (for 10 ml of solution 6.8 ml of double distilled water, 1.7 ml of 30% Acrylamide mix, 1.25 ml of Tris 1 M pH 6.8, 100 µl of 10% SDS, 100 µl of APS, 10 µl of TEMED). A comb of appropriate number was placed over to allow the formation of wells where the samples would be loaded. The gel was then fixed in the running chamber and 1X Laemmli buffer (for 1L of 10X solution: 30.26 g of Tris base, 144.13 g of Glycin, 50 ml of SDS 20% in 1 L ddH_2O) was poured over. Equal volume of cell lysate representing equal number of cell were then loaded onto the SDS gel. Samples were run at 90 V in the stacking gel and 140 V in the separating gel for 3 - 4 hours.

2.2.6.3 Transfer of Proteins onto Membranes

The proteins resolved by SDS-PAGE were transferred onto PVDF (polyvinylidene fluoride) membranes (Merck Millipore, Darmstadt, Germany) in an electrophoretic wet-transfer chamber (Bio-Rad, Heidelberg). To do this, the membrane was activated by soaking it in methanol for 10 s, and placed above the gel, which was already laid on three layers of wet filter paper, in a cassette. The membrane was thereafter covered with another three layers of filter paper. The cassette was placed in a transfer chamber filled with Western blot transfer buffer (25 mM Tris-base, 192 mM glycine, 10% methanol). The transfer was carried out at 35 V at 4 °C overnight.

2.2.6.4 Western blotting

After the proteins were transferred onto the membrane, Western blotting analysis was carried out as followed. First of all, to reduce unspecific binding of the antibody, the membrane was incubated with blocking buffer (10% milk powder dissolved in PBST) for 1 h at RT with gentle shaking on a shaker (Heidolph Instuments, Polymax 1040). For detecting the protein of interest, the membrane was thereafter incubated with specific primary antibody diluted in blocking buffer O/N at 4 ºC (see table of antibodies for detailed information). Thereafter the membrane was washed three times with PBST 1X (3.2 mM Na_2HPO_4, 0.5 mM KH_2PO_4, 1.3 mM KCl, 135 mM NaCl, in deionized water, 0.02% Tween-20®, pH 7.4) for 10 min each. After washing, the membrane was incubated with the secondary antibody also diluted in blocking buffer for 1 h at RT and washed 3 times with PBST 1X, 10 minutes each. Detection of proteins was finally performed using the enhancer of chemioluminescence (ECL) western blot detection reagent (Biorad, Heidelberg) and signals detected with ChemDoc Touch imager (BioRad, Heidelberg) according to manufacturer instructions.

2.2.6.5 Membrane stripping

To use the membranes more than once for Western blot analysis, the filters were incubated with stripping buffer (3.125 ml of Tris-HCl 1 M pH 6.8, 5 ml of 20% SDS, 400

µl of β-mercaptoethanol in a final volume of 50 ml) at 55ºC for 14 min with shaking to remove the previous antibodies bound to the membranes. The membranes were then washed 10 min each 3 times with PBST 1X and reused.

2.2.6.6 Cell Fractionation into Cytoplasmic and Nuclear Fractions

Cells were washed off media with ice cold 1X PBS twice and scrapped into 1 ml cold PBS 1X with Protease Inhibitor cocktail (1:100 dilution). The cells were pelleted at 2000 rpm for 4 minutes. The supernatant was discarded and cells resuspended in ice-cold fractionation buffer (10 nM HEPES pH 7.5, 10 mM KCl, mM EGTA, mM EDTA, mM DTT, 1X Protease Inhibitor) and re-centrifuged to remove remnant of PBS. The pellets were re-suspended in 400 µl of ice-cold fractionation buffer containing PIC and incubated on ice for 15 minutes. 25 µl of 10% NP-40 was added and vortexed vigorously for 10 sec 3 times. The solutions were centrifuged at 13000 rpm at 4 ^{o}C for 15 min. The supernatant was separated into new Eppendorf tubes as the cytoplasmic fraction. The nuclear pellets were then washed 4 times with 1 ml fractionation buffer to remove remnants of cytoplasmic fraction around nuclear pellets. The nuclear pellets were reweighed and the initial weight of empty Eppendorf tube subtracted to obtain the weight of the nuclear pellet. The nuclear pellets were resuspended in 2X Laemmli sample buffer depending on the weight after normalizing with the weight of the minimum pellet. Thereafter, the samples were heated at 95 ^{o}C for 15 min while shaking rigorously. After boiling, nuclear fractions were subjected to 2 times 15 min high frequency sonication to render the nuclear pellet soluble. Typically, 30 µl was used for SDS-PAGE and Western blotting.

The cytoplasmic fractions were also subjected to 15 min of sonication and centrifuged at 14000 rpm for 15 min at 4 ^{o}C. The supernatants were transferred into new Eppendorf tubes and the concentrations of the cytoplasmic fractions determined using Bradford method of protein quantification. Typically, 50 µg each was boiled in 50 µl 2X SDS Laemmli sample buffer for 10 min. Thereafter 50 µl of each sample was taken through SDS-PAGE and Western Blotting.

2.2.6.7 Quantification of Eukaryotic protein extracts

Extracted proteins were quantified using Bradford assay. Typically 5 µl of protein extract was diluted in 500 µl of 1x Bradford reagent (Bio-rad, Munich, Germany). 200 µl of the solution was pipetted into a 96 well plate and the intensity of the signal was defined by reading at wave length of 595 nm using ELX 808 UI Ultra Microplate Reader (software KC4 v 3.01) for measurement of optical absorbance. The signal background was determined by diluting 5 µl of lysis buffer in 500 µl of 1x Bradford solution. A standard curve using defined amount of BSA was used to calculate the final protein content using the formula:

y= ax+b,

y= amount of protein (µg)

a= slope of the curve

x= absorbance (at 595 nm)

b= origin on y axis

2.2.6.8 GST-pull down experiments

2.2.6.8.1 Preparation of GST-fused proteins

For preparation and purification of GST-fused proteins, *E. coli* BL21 bacteria was transformed with the plasmid encoding for the desired GST-fused protein and incubated O/N in 20 ml LB 1X + ampicillin. The following day the bacteria culture was expanded to 1 L of LB 1X and allowed to grow at 37 ºC till OD_{600} = 0.5 - 0.8, measured with a spectrophotometer / Biophotometer (Eppendorf, Wesseling-Berzdorf, Germany). Thereafter, the bacterial culture was cooled to room temperature and isopropilthiogalactoside (IPTG) added to make a final concentration of 1 mM to induce the production of the recombinant protein at room temperature for 3 hours on a shaker. At the end of the induction, the bacteria was pelleted by centrifugation at 4000 xg, 25 min at 4 ºC in a fixed angle rotor (centrifuge Hermle ZK 401). The bacterial pellets were resuspended in resuspension buffer (2 mM EDTA, 2 mM PMSF in PBS 1X). Thereafter

to ensure cell lysis, 1 mg/ml of lysozyme (Sigma Aldrich, Taufkirchen, Germany) was added to the mixture and incubated for 10 min on ice. To have a complete protein extraction, 1% Triton-X-100 was added to the solution and incubated at 4 ºC on a rotor. In order to effectively extract proteins, even in inclusion bodies, 1% of sodium N-Laurylsarcosinate (or Sarkosyl) was added and incubated for 30 min at 4 ºC on a rotor. Thereafter the solution was sonicated at Amplitude of 60 and 20 pulse per second and centrifuged at 8000 xg, 30 min at 4 ºC (centrifuge Beckman Coulter). In the meantime approximately 1 ml of Amintra glutathione-affinity resin (Expedeon Protein solutions, UK) was washed twice with PBS 1X. The GST-fused proteins present in the supernatants were then added to the washed glutathione resin and incubated O/N at 4 ºC on a rotor. Thereafter they were washed with ice-cold PBS 1x by centrifugation at 2000 rpm, 2 min, RT (Eppendorf centrifuge 5417R) three times to remove all the unbound proteins. The recombinant proteins bound to the beads were then resuspended in a solution of PBS 1X containing 1 mM DTT and protease inhibitor cocktail (dilution 1:100) and kept at 4 ºC for short term storage (maximum 48 hours). For longer storage (about 2 to 4 weeks), 30% glycerol was added to the solution of DTT, protease inhibitor cocktail and the bead-bound fusion proteins and stored at -80 ºC. Before using the GST-fusion proteins for experiments, the protein amount was quantified by SDS-PAGE and subsequent staining with Coomassie® blue. Defined amount of BSA (Promega, Mannheim, Germany) were used as standard to estimate the concentration of proteins present in each GST-fusion proteins.

2.2.6.8.2 Incubation of GST-fusion proteins with cell lysate

For GST-pull down, wild type LNCaP cells were cultured about 90% confluence. The day of the experiment the medium was aspirated and cells were scraped in approximately 5 ml of ice cold PBS 1X. After centrifugation at 1000 rpm, 3 min at 4 ºC (centrifuge Beckman Coulter), the cell pellet was resuspended in 500 µl of lysis buffer (10 mM Na_2HPO_4 pH 7.4, 1 mM EDTA, 150 mM KCl, glycerol 15% in ddH_2O). The resuspended cells were subjected to 3 - 5 cycles of freeze-thaw by immersion in liquid nitrogen followed by incubation at 37 ºC. Thereafter the lysate was sonicated at Amp 50, 10 pulses and

centrifuged at 12000 rpm, 15 min at 4 ºC (centrifuge Beckman Coulter). The supernatant was collected in a new Eppendorf tubes and protein concentration quantified using the Bradford assay. In parallel GST-fused proteins bound to glutathione resin were quantified by loading onto a polyacrylamide gel together with defined amounts of BSA as described above. Approximately 400 µg of cell extract was incubated with 10 µg of GST-fused protein in binding buffer (20 mM Hepes. KOH pH 7.9, 100 mM NaCl, 2.5 mM $MgCl_2$, 0.1 mM EDTA, 1 mM DTT, protease inhibitors 1:100, 0.05% NP40, 1.5% Triton-X-100) in a final volume of 200 µl, O/N at 4 ºC on a rotor. The next day the sample were washed 4 times with binding buffer and centrifuging at 2000 rpm, 2 min at 4 ºC (Eppendorf centrifuge 5417R). The beads were resuspended in 50 µl of 2X Laemmli sample buffer and boiled at 95 ºC with rigorous shaking, for 5 min to destroy the interaction between the beads and the proteins. Afterwards the samples were centrifuged at 12000 rpm for 5 min (Eppendorf centrifuge 5417R) to get the beads at the bottom and the proteins in the supernatant. Thereafter, 20 µl of each sample was taken through SDS-PAGE and Western blotting. To check for equal loading of recombinant protein, at the end of the Western blotting, the membrane was stained with Coomassie® blue.

2.2.6.8.3 Staining with Coomassie® brilliant blue

For staining with Coomassie® blue the polyacrylamide gel was washed twice with distilled water for 10 minutes at room temperature on a shaker to remove the salts that could interfere with the staining. Thereafter the gel was incubated 3 h at RT on a shaker with SimplyBlue™ Safe stain (Invitrogen, Karlsruhe, Germany). Finally the gel was washed several times with distilled water to remove the excess staining and stored at 4 ºC. To stain a membrane with Coomassie, after Western blotting, the membrane was incubated in Coomassie as described in this paragraph. The membrane was washed 3 times with methanol to destain unbound coomassie and washed in distilled water. The membrane was finally air-dried.

2.2.6.8.4 Ponseau Staining

Mostly, Ponseau staining of PVDF membrane was carried out to check whether the transfer worked properly before going further through the Western blotting steps. This staining was carried out as followed: Membranes were incubated in Ponseau staining solution (1g Ponceau S, 50 ml acetic acid made up to 1L with ddH_2O) for 1 h with gentle agitation. The membrane was washed gently in distilled water until the background was clean. Thereafter, the membrane was taken through blocking and primary antibody incubation as already mention.

3.0 Results

3.1 The Bag-1L protein interacts with NPM1

Bag-1L enhances the action of the AR through a direct interaction between the two proteins (Froesch et al., 1998; Knee et al., 2001; Shatkina et al., 2003; Jehle et al., 2014). The ability of Bag-1L to enhance AR action, most likely, depends on the contribution of its interacting partners. NPM1 was identified as one of Bag-1L interacting partners from a tandem affinity purification followed by Mass spectrometric protein identification carried out by Laura Cato (a member of our collaborating partners in the Department of Medical Oncology, Dana-Farber Cancer Institute and Harvard Medical School, Boston, USA). To validate this interaction, Bag-1L was expressed as fusion proteins of glutathione-S-transferase (GST) to generate recombinant GST fusion proteins for pull-down assay. As a control, the other three members of Bag-1 protein family were also expressed and used in the pull-down assay. These GST fusion proteins were expressed in *E. coli* BL21, harvested, lysed and isolated by affinity chromatography. An amount of 5 µg of each fusion protein was used with LNCaP cell lysate in the pull-down assay. It could be confirmed from the Western blotting that only Bag-1L interacts with NPM1 (**Figure. 3a**) (This result was generously provided by Dr. Antje Neeb, a former Lab member). Furthermore, this study sought to investigate whether the 2 proteins also co-localize in the cell which might suggest an *in vivo* interaction of the 2 proteins.

LNCaP cells were seeded on coverslips, fixed and immuno-stained with anti-NPM1 (Red) and anti-Bag-1 (Green) antibodies. The nuclei were stained with Draq5® and imaged with the aid of a confocal microscope. From the immunofluorescence images shown in **Figure. 3b**, it could be seen that, the 2 proteins strikingly co-localized in the nuclei as indicated by the yellow stain in the nuclei. However, the anti-Bag-1 antibody used recognizes all the Bag-1 isoforms and therefore recognized cytoplasmic Bag-1 isoforms which did not show any interaction with NPM1 and therefore did not co-localize with NPM1 in the immunofluorescence image. Altogether, what this results suggest is that, Bag-1L does not only interact with NPM1 *in vitro* but also *in vivo*.

A

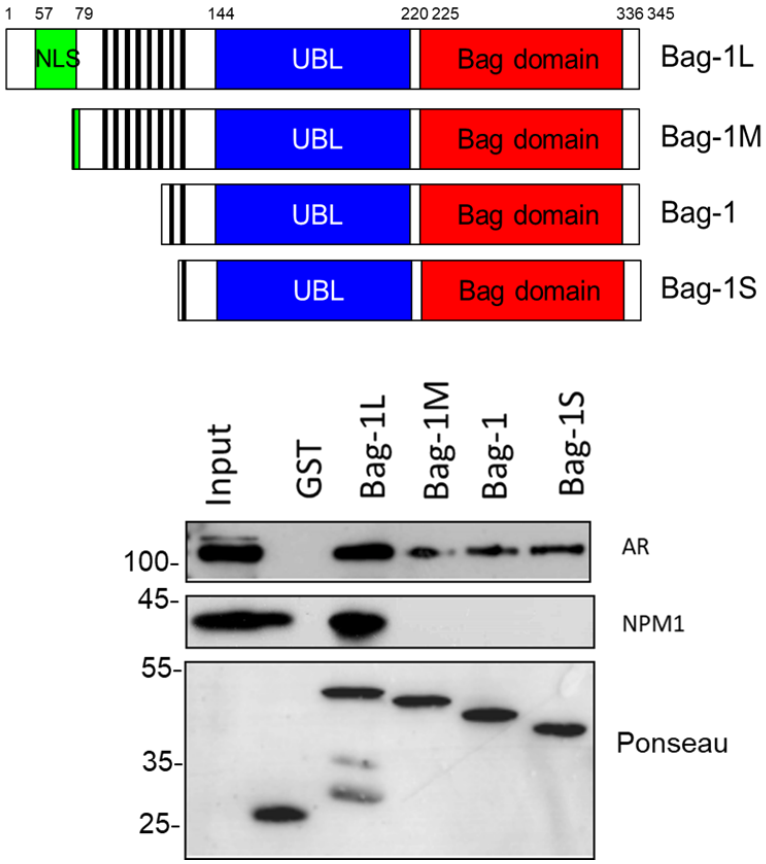
1 57 79 144 220 225 336 345
NLS
UBL
Bag domain
Bag-1L
Bag-1M
Bag-1
Bag-1S
Input
GST
Bag-1L
Bag-1M
Bag-1
Bag-1S
100-
45-
55-
35-
25-
AR
NPM1
Ponseau

B

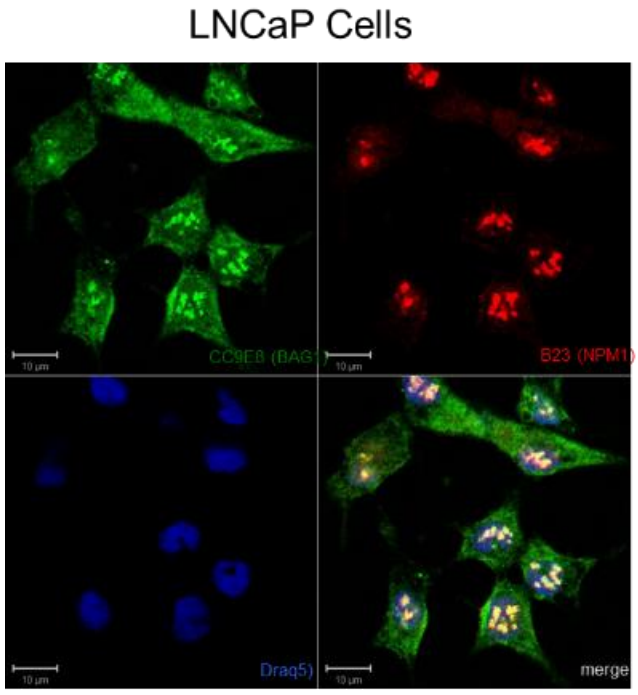
LNCaP Cells
B23 (NPM1)
Draq5)
merge

Figure 3.1: Bag-1L interacts with NPM1.

(A) Only Bag-1L in the Bag-1 protein family interacts with NPM1. The figure shows a Western blotting of different GST fusion proteins of the Bag-1 isoforms (represented in the figure schematically) in a pull-down experiment with LNCaP cell lysate. Fusion proteins' interaction with NPM1 and AR proteins were visualized by Western blotting using anti-NPM1 and anti-AR antibodies. Equal protein loading was confirmed with Ponceau staining. (**B)** Nuclear Bag-1 (Bag-1L) and NPM1 co-localized in the nuclei in LNCaP cells. Equal number of cells (10^4) were seeded on coverslips in 24 well-plates and incubated for 48 h. The cells were then fixed and incubated with anti-NPM1 (1:250 dilution) and anti-Bag-1 (1:250 dilution) primary antibodies and Draq5 (1:1000 dilution) to determine the distribution of NPM1 and Bag-1 proteins. The images were acquired using confocal laser microscope (LSM510, Zeiss) with a 64× 1.6 numerical aperture oil objective lens and processed using the LSM510 software for cellular distribution of NPM1 and Bag-1. NPM1 was stained red, Bag-1 was stained green and the nuclei were stained blue. The co-localization pattern (Merged, yellow) was derived from the merge of nuclear Bag-1 and NPM1 in the nuclei. The figure is composed of representative pictures taken from one of three independent experiments. (Scale bar: ~10 µm).

3.1.1 The N-terminus of Bag-1L protein interacts with NPM1

As only Bag-1L within the 4 members interacted with NPM1 (**Figure 3.1 A**), it was hypothesized that the NH_2-terminus of Bag-1L was, most likely, the domain of the protein involved in the interaction with NPM1. Therefore a further interaction investigation was carried out using the 3 main domains of Bag-1L as GST-fusion proteins in a pull-down experiments with LNCaP cell lysate to ascertain which of them is involved in the interaction. In **figure 3.2**, it was shown that the NH_2-terminus (amino acids 1-128) of Bag-1L was indeed the only domain that interacted with NPM1 (This result is from Katja Jehle, a former Lab member). The N-terminal 1-128 amino acids of Bag-1L contain a duplication of the motif GARRPR shown to bind the AR LBD (Jehle et al., 2014) and a nuclear localization sequence that mediates the nuclear localization of Bag-1L (Knee et al., 2001). As NPM1 is reported to have a strong affinity for NLS of proteins (Szebeni et al., 1995), and aids in the intracellular transport of proteins (Borer et al., 1989), it was reasoned that NPM1 possibly might play a role in the nuclear transport of Bag-1L.

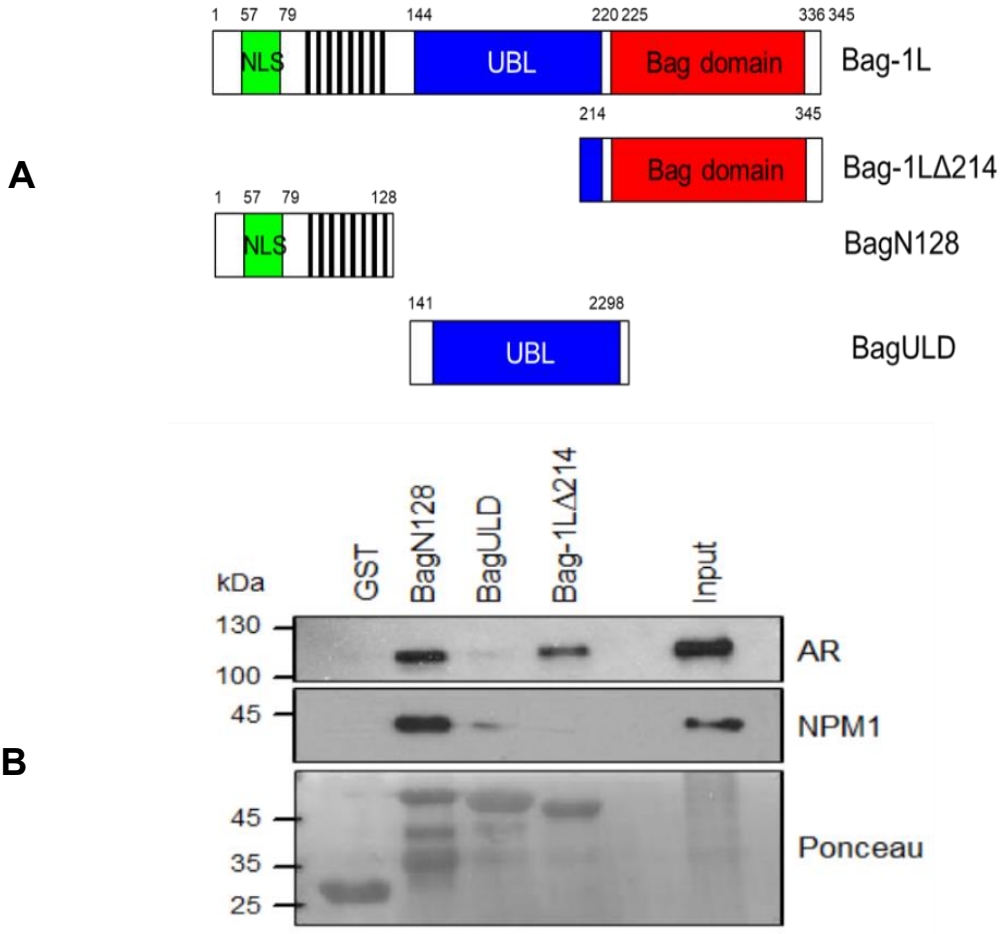

Figure 3.2: N-terminus of Bag1L (amino acid 1-128) interacts with NPM1.

(**A**) The figure shows a schematic representations of the different truncations of Bag-1L as GST fusion proteins. The truncations used were; Bag-1L (N-terminus amino acid 1 – 128), Bag-1L ubiquitin-like domain (blue) and BAG domain (red). (**B)** The figure shows a Western blot carried out using 5 µg each of the fusion GST proteins in a pull-down experiments with LNCaP cell lysate. Protein interactions were visualized by Western blotting using anti-NPM1 (1:1000 dilution) and anti-AR (1:1000 dilution) antibodies. Equal protein loading were confirmed by Ponceau staining.

Immunofluorescence experiments were therefore designed to study the cellular localization of Bag-1L under condition of a decreased NPM1 level. Therefore stable knockdown of NPM1 clones were generated in LNCaP cells by transduction with lentiviral particles containing different short hairpin RNA (shRNA) targeted against NPM1 mRNA

and scramble shRNA sequence (sequence designed such that it does not target any known genes in the target cell). The cells were then selected in puromycin, grown to high confluence and Western blotting carried out to determine the degree of knockdown of NPM1. Three NPM1 knockdown clones (A, D and H) with different degrees of NPM1 knockdown were selected. Quantification of the knockdown by scanning the bands in the Western blots of 3 independent experiments revealed the following degrees of knockdown: clone A (64 ± 5 %), clone D (85 ± 9%) and clone H (89 ± 4%); all compared to the control (**Figure. 3.3**). As clone H showed the most knockdown, it was used in most of the subsequent studies.

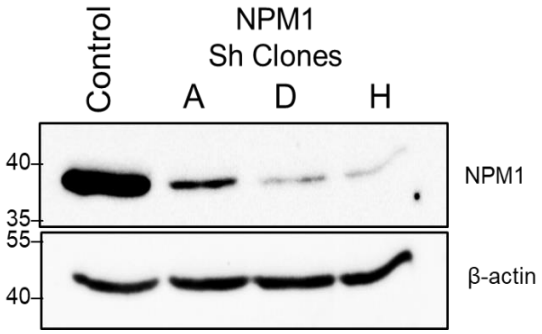

Figure 3.3: NPM1 knockdown clones in LNCaP cells.

The figure shows a Western blot of 4 clones with different levels of knockdown of NPM1 in LNCaP cell: A, D, H and control clones. These were generated using lentiviral particles containing either target-specific constructs (shNPM1) or non-target sequences (control) to infect LNCaP cells for 24 h. The cells were trypsinized and diluted into single cells and plated in selection medium containing 1 µg/ml puromycin. Colonies were selected, expanded and Western blotting carried out by resolving 60 µl of whole protein lysates on 10% SDS-PAGE. Proteins were detected with anti-NPM1 and normalized with anti-β-Actin antibodies. The contribution of Dr. Mohammed Salama in the generation of these knockdown clones is greatly appreciated.

3.2 NPM1 knockdown decreases Bag-1 protein in LNCaP Cells

To determine the cellular localization of Bag-1L, immunofluorescence experiments were carried out as described in section 3.1. The control and NPM1 knockdown clone H cells were used for these studies and stained with anti-NPM1 (Red) and anti-Bag-1(Green) antibodies. From the images in **Figure 3.4**, it could be shown that the knockdown of NPM1 evident by a diminution of the red nucleolar signal in the H clone also showed a strong reduction of the nucleolar green staining attributed to Bag-1L in **Figure 3.1B.** On the contrary, the cytoplasmic green stain attributed to the other Bag-1 isoforms was still present when the NPM1 knockdown clone H was compared to the control clone, albeit to a lesser degree. In the absence of any commercially available Bag-1L specific antibody, a clear conclusion cannot be made about the cellular localization of Bag-1L in this experiment except that the level of the Bag-1 protein (in particular Bag-1L) was significantly reduced in the NPM1 knockdown clone compared to the control (**Figure 3.4)**.

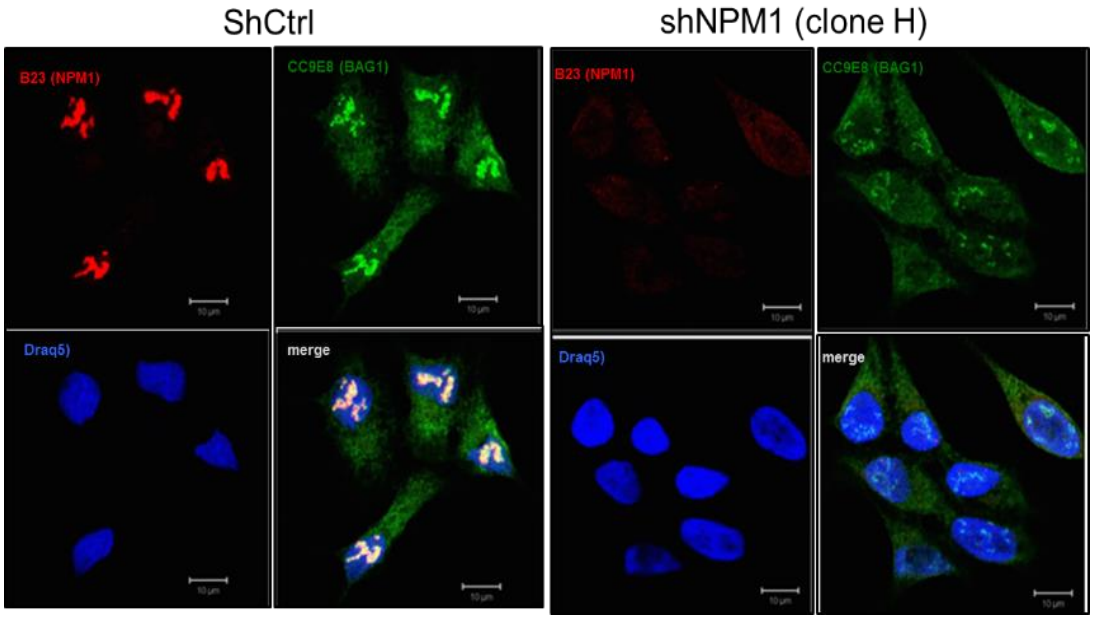

A

Figure 3.4: NPM1 knockdown reduces Bag-1 signal

The figures show immunofluorescence images of Control shRNA (Ctrl sh) and shNPM1 knockdown cells (clone H). Cells were seeded on coverslips as described previously. The coverslips with the fixed, permeabilized and immunostained cells were mounted and images acquired using confocal laser microscopy (LSM510, Zeiss) to determine the cellular distribution of NPM1 and Bag-1. Images were taken

with a 64 × 1.6 numerical aperture oil objective lens and processed using the LSM510 software. NPM1 was stained red, Bag-1 was stained green and the nuclei were stained blue. The figure is composed of representative pictures taken from one of three independent experiments. (Scale bar: ~10 μm).

3.3 NPM1 knockdown decreased Bag-1 proteins in LNCaP, 22Rv.1 and HeLa cells

The observation that Bag-1 protein signal in the immunofluorescence images were reduced in the shNPM1 (NPM1 knockdown) cells compared to the control was further investigated using Western blotting analysis. All 3 LNCaP NPM1 knockdown clones (A, D and H) were analyzed along with siNPM1 knockdown in 22Rv.1 cells and shNPM1 knockdown in the human cervical carcinoma cell line, HeLa, for the expression of NPM1 and Bag-1. Housekeeping control proteins (β-actin or β-tubulin) were blotted to show equal protein loadings. The reduced expression of NPM1 in all three cell lines was associated with a concomitant reduction in expression of all the Bag-1 isoforms (**Figure 3.5 A - C**). Note that 22Rv.1 cells showed 2 distinct bands corresponding to NPM1, which most likely, are full-length NPM1 (upper band) and a spliced form (lower band) (Grisendi et al., 2006). Together these results show that downregulation of expression of NPM1 results in reduced expression of all the Bag-1 proteins.

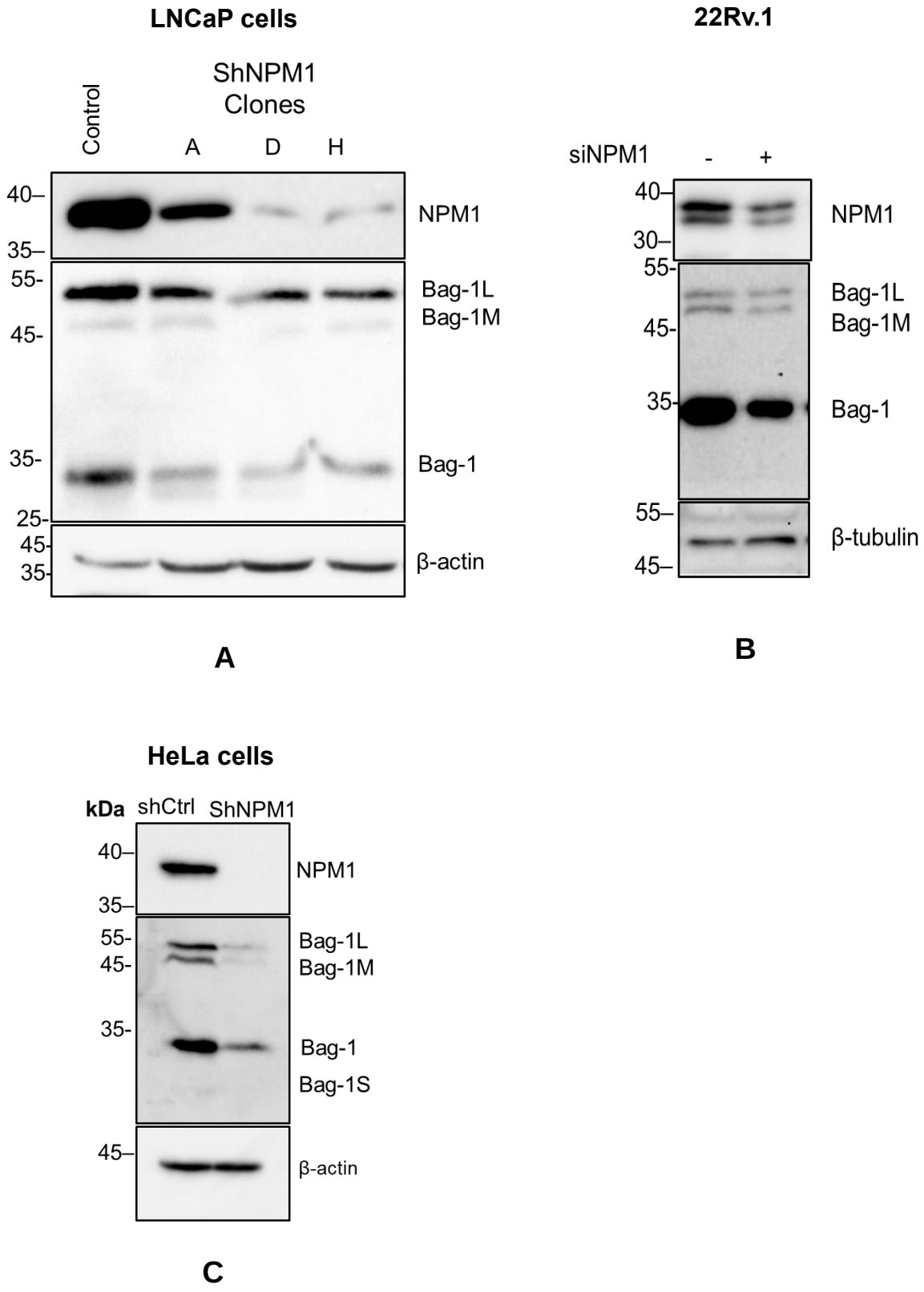

Figure 3.5: NPM1 knockdown reduces protein levels of Bag-1.

(**A**) Western blots showing NPM1 and Bag-1 protein expression in shNPM1 LNCaP knockdown clones and control (**B**), control and siNPM1 in 22Rv.1 cells and **(C**) control and shNPM1 in HeLa cells. Western blotting experiments were carried out as already described under **figure 3.3** using anti-NPM1 (1:1000 dilution) or anti-Bag-1 (1:1000 dilution) antibodies and either β-Actin or β-tubulin as loading control.

3.4 NPM1 knockdown is correlated with decreased Bag-1 mRNA levels

To investigate whether the decrease in Bag-1 protein levels in the NPM1 knockdown cells is a result of reduced mRNA, Bag-1 mRNA expression in the control and NPM1 knockdown cells was therefore investigated by reverse transcribing mRNAs and qRT-PCR studies carried out. Beta-actin expression was measured and used as internal reference gene for normalizations. **Figures 3.6 A - C** show that, knockdown of NPM1 decreased the relative mRNA level of Bag-1 in all the three cell lines.

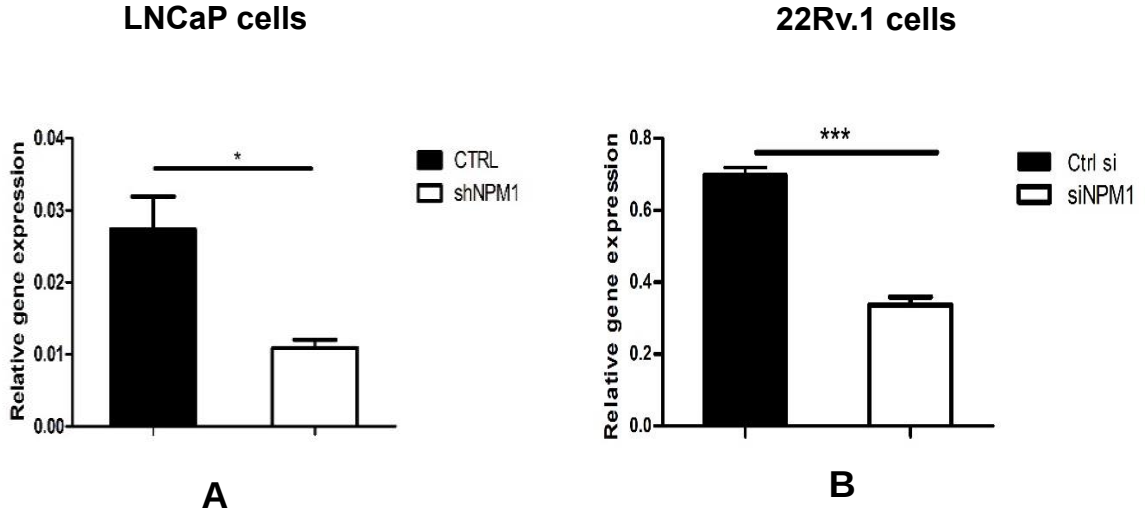

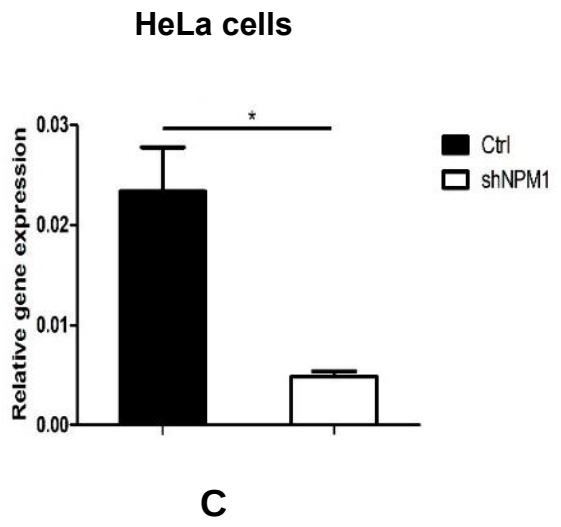

Figure 3.6: NPM1 knockdown reduces Bag1 mRNA levels.

A, B, C, The figures show the relative gene expression of Bag-1 in LNCaP cells (Ctrl sh and shNPM1), 22Rv.1 (Ctrl si and siNPM1) and HeLa cells (Ctrl sh and shNPM1). Total RNAs were extracted from these cells, 1 µg each was reverse transcribed and relative expression determined using qRT-PCR. The data represents the mean of three independent experiments, each in duplicate ± standard error of mean (error bars). *p* values were calculated using a standard t test,* $p \leq 0.05$.

3.5 NPM1 knockdown decreases Bag-1 mRNA stability in LNCaP cells

To determine the cause of the reduced steady-state Bag-1 mRNA level in the NPM1 knockdown cells, the stability of the Bag-1 mRNA was analyzed in the control and NPM1 knockdown LNCaP cells. The seeded cells were treated for 0, 1, 3, 5 and 7 h with 5 µg/ml Actinomycin D (an inhibitor of mRNA Polymerase II) in the culture medium to inhibit transcription so that the rate of decay of already synthesized mRNA could be determined. Total RNA were extracted from the cells and 1 µg each reverse transcribed into cDNA and qRT-PCR carried out to determine the relative Bag-1 mRNA at each time point. It could be seen that mRNA from the control cells showed an increase over 3 h following Actinomycin D treatment before showing a decrease. In contrast, Bag-1 mRNA showed a continuous steady decrease over the period of the Actinomycin D treatment (**Figure 3.7)**. Thus, Bag-1 mRNA decayed faster in the NPM1 knockdown cells compared to the

control, which might be a cause of the decreased relative Bag-1 transcripts at steady state.

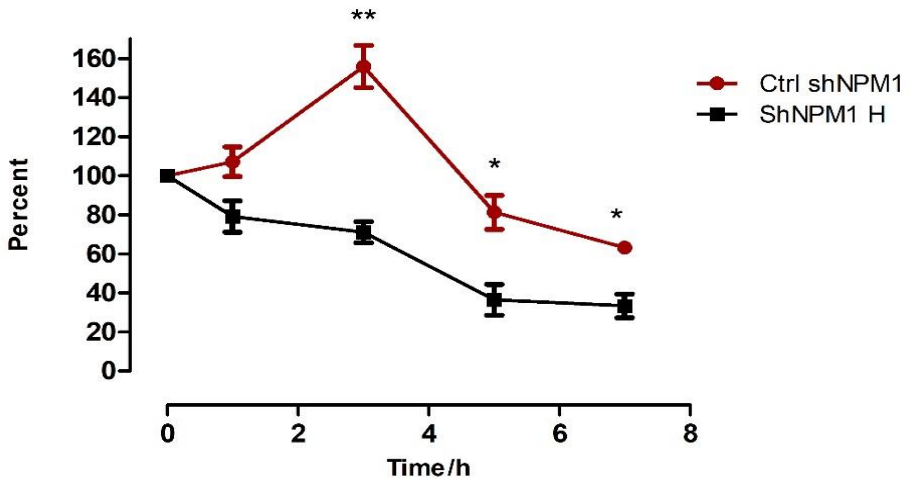

Figure 3.7: NPM1 knockdown decreases Bag-1 mRNA stability

The figure shows Bag-1 mRNA stability curve assayed using quantitative RT-PCR to assess Bag-1 mRNA decay. Cells from control and shNPM1 clones were treated with 5 µg/ml Actinomycin D containing medium and harvested at time points 0, 1, 3, 5 and 7 h. Thereafter, total RNA were extracted and 1 µg RNA each was reverse transcribed into cDNA and relative expression of Bag-1 mRNA determined using quantitative RT-PCR. β-Actin expression was measured as a reference transcript for the normalization. Each time point represents the mean of three independent experiments, ± standard error of mean (SEM). *p* values were calculated using a standard t test, *$p \leq 0.05$. Legend: Red curve – Control sh and Black curve – shNPM1 cells.

3.6 Bag-1L knockout has no effect on NPM1 protein level in LNCaP cells

As the knockdown of NPM1 decreases the level of the Bag-1 protein, including the level of Bag-1L with which NPM1 interacts, the question was asked whether the converse situation applies, where a decreased level of Bag-1L impacts NPM1 level. Therefore LNCaP cells with a TALEN (transcription activator-like effector nuclease)-specific knockout of Bag-1L expression (Cato et al., 2017) was used for further investigation. As the Bag-1 proteins are produced by a leaky scanning mechanism of translation from the

same mRNA, a knockout of the first codon that leads to the production of Bag-1L resulted in increased expression of the other isoforms (**Figure 3.8**). However, a knockout of Bag-1L has no effect on the expression of NPM1 as determined by Western blot analysis in **Figure 3.8**.

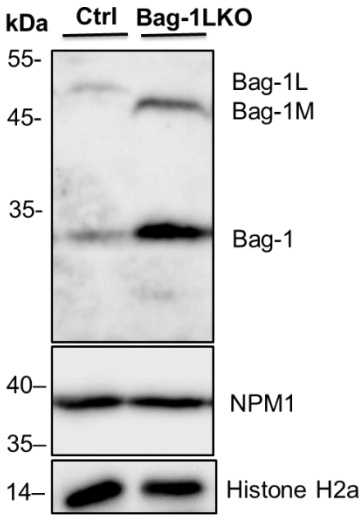

Figure 3.8: Bag-1L knockout has no effect on NPM1 protein levels

Western blot analysis was carried out with control and Bag-1L knockout LNCaP cells as previously described using anti-Bag-1 and anti-NPM1 antibodies. Histone H2A expression was used as an internal reference protein for equal protein loading by blotting with an anti-histone H2A antibody.

3.7 Regulation of androgen receptor action

3.7.1 NPM1 knockdown impairs androgen receptor cytoplasmic-nuclear translocation

Having established that Bag-1L interacts with NPM1 and the knockdown of NPM1 reduces the expression of Bag-1 proteins, further studies were carried out to investigate the effect of knockdown of NPM1 on AR action, i.e. the cytoplasmic-nuclear translocation of the AR and the transactivation function of the AR.

To investigate AR nuclear translocation which is the first step in the action of the AR, lysates from NPM1 knockdown and control cells treated to different time points with DHT

were fractionated into nuclear and cytoplasmic proteins and subjected to Western blot analysis to determine the levels of the AR in the different fractions. Cytoplasmic marker, β-actin and nuclear marker, Histone H2A were used to show the purity of the fractions and for estimation of equal protein loading. The kinetics of disappearance of the AR band in the cytoplasm following DHT treatment was reduced in the NPM1 knockdown cells compared to the control. Similarly, the kinetics of increased AR signal in the nucleus was significantly more in the control compared with that of the knockout cells (**Figure 3.9**). Thus, there is a delayed translocation of the AR into the nucleus in the NMP1 knockdown cells compared to the control.

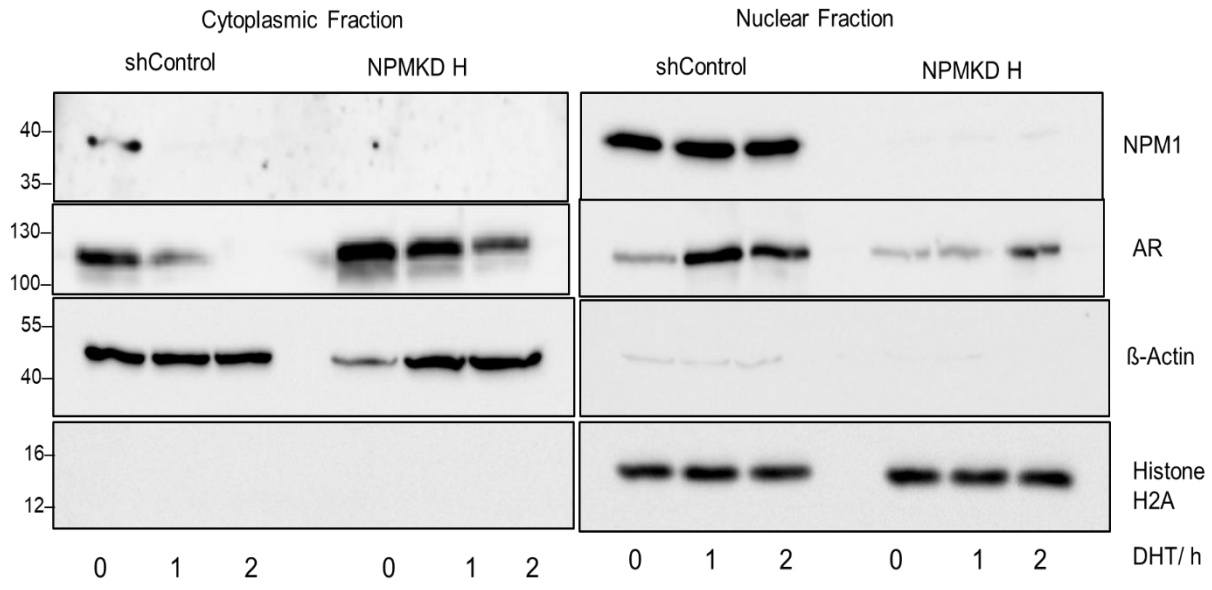

Figure 3.9: Nuclear translocation of the AR is impaired in NPM1 knockdown compared to control LNCaP cells.

Control and shNPM1 LNCaP cells were cultured in starvation medium (phenol-red free RPMI medium supplemented with 3% charcoal stripped serum (CCS)) for 72 h. Thereafter, the cells were treated with DHT (10^{-8} M) for 0, 1 and 2 h. Afterwards, cells were fractionated into cytoplasmic and nuclear fractions and assessed for relative levels of AR, NPM1, β-actin, and Histone H2A using anti-AR, anti-NPM1, anti-β-actin and anti-histone H2A antibodies respectively. Total protein loaded were assessed by the abundance of β-Actin and histone H2A in cytoplasmic and nuclear fractions respectively.

The NPM1 knockdown effect on AR nuclear translocation was further studied using live cell fluorescent imaging technique to track the rate of AR translocation from the cytoplasm into the nucleus. This was carried out by transiently transfecting NPM1 knockdown and control cells with fluorescently labelled AR; Cyani Fluorescent Protein-Androgen Receptor-Yellow Fluorescent Protein (CFP-AR-YFP) plasmid. Thereafter, DHT was administered and the translocation of the receptor tracked using a Andor Revolution® XD spinning disk laser scanning microscope (BFi OPTiLAS, München, Germany) (Yang et al., 2013). At time *t=0* there was a clear cytoplasmic localization of the AR in both the control and NPM1 knockdown cells. However, at *t=85* min, most of the AR had translocated into the nuclei in the control cells, but not in the NPM1 knockdown cells (**Figure 3.10A**). The live cell images additionally revealed that NPM1 knockdown leads to AR aggregation in the presence of DHT, an observation consistent with earlier report that NPM1 is an anti-aggregation protein and that silencing of this protein leads to aggregation of protein to which it binds (Szebeni and Olson, 1999). **Figure 3.10B** shows the quantification of the AR cytoplasmic - nuclear translocation rate from multiple experiments indicating an impaired AR nuclear translocation rate in the NPM1 knockdown cells.

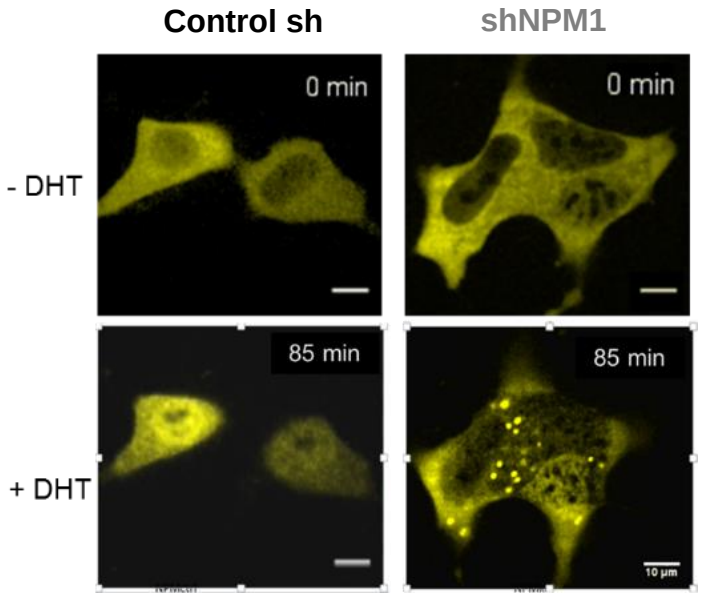

A

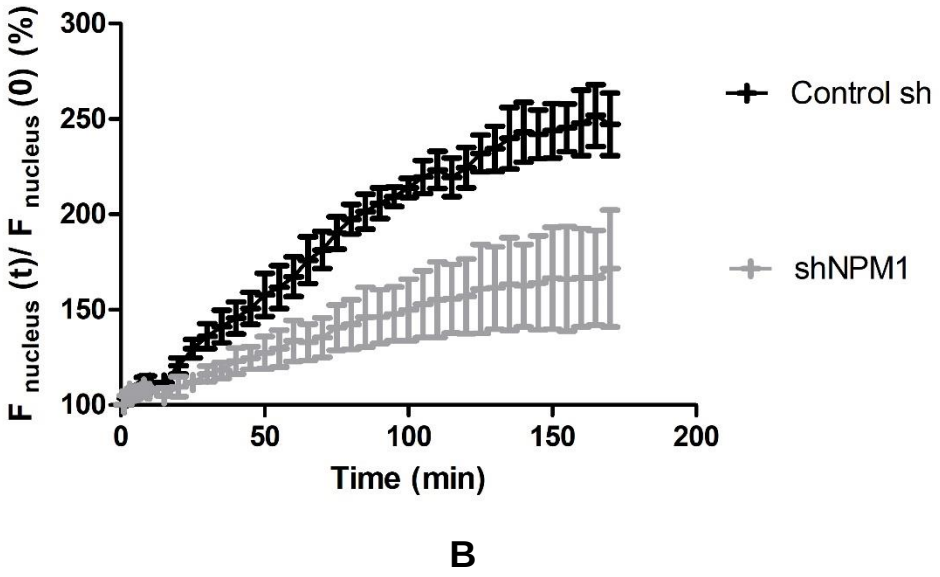

Figure 3.10: NPM1 knockdown impairs AR cytoplasmic-nuclear translocation kinetics.

NPM1 knockdown impaired AR cytoplasmic-nuclear translocation rate. **(A)** Control and NPM1 knockdown cells were transiently transfected with 500 ng of CFP-AR-YFP plasmids in starvation medium using Lipofectamin 2000. The medium was replaced with fresh starvation medium after 24 h and starvation was continued for the next 48 h. Cells were then treated with DHT (10^{-8} M) and the translocation of the AR into the nucleus tracked using an Andor Revolution® XD spinning disk laser scanning microscope.
(B) shows the quantification of the AR cytoplasmic-nuclear translocation rate from multiple experiments using ImageJ (Abràmoff et al., 2004). The microscopy studies were carried out with the help of Linxiao Yang in the group of Prof. Dr. Gerd Ulrich Nienhaus.

3.7.2 Bag-1L knockout impairs androgen receptor cytoplasmic-nuclear translocation

Having established that NPM1 knockdown leads to an impairment of AR cytoplasmic-nuclear translocation rate in the presence of DHT, this study investigated whether a similar phenomenon can be observed in cells lacking Bag-1L to which NPM1 binds. Similar to the studies described earlier, live cell fluorescent imaging experiment was carried out by transiently transfecting Bag-1L knockout and control cells with CFP-AR-YFP plasmids. The cells were then treated with DHT and the translocation of AR into the nucleus tracked as previously described in section 3.7.1 (Yang et al., 2013). To demonstrate the authenticity of the cells, lysates of the cells were subjected to Western blot analysis with anti-Bag-1 antibody and vinculin antibody as a loading control. In the

fluorescence experiment, at time *t=0*, a clear cytoplasmic localization of the AR in both the control and Bag-1L knockout cells was seen. However, at *t =70* min, most of the AR had translocated into the nuclei in the control cells but not in the knockout cells (**Figure 3.11B**). The quantified AR translocation rate from 3 independent experiments confirms the delayed nuclear translocation in the Bag-1L knockout cells (**Figure 3.11C**)**.** However unlike the situation in the NPM1 knockdown cells, there were no AR aggregates detected in the Bag-1L knockout cells. To determine whether the impaired AR translocation was a direct effect of the loss of Bag-1L, Bag-1L was expressed in the Bag-1L KO cells and the AR translocation studies were repeated. As shown in **figure 3.11D**, the expression of Bag-1L in the Bag-1L KO rescued the AR translocation defect indicating that Bag-1L directly plays a role in this process.

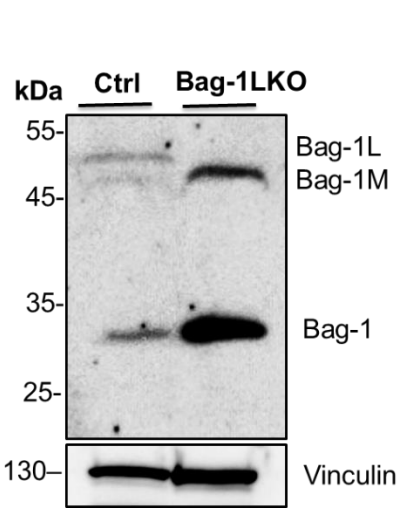

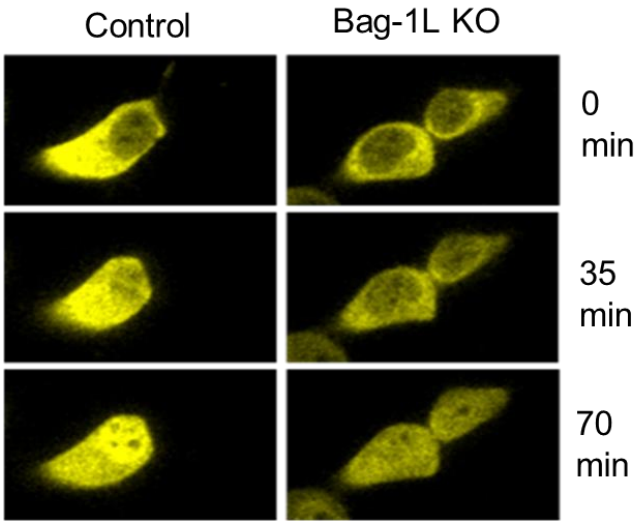

A **B**

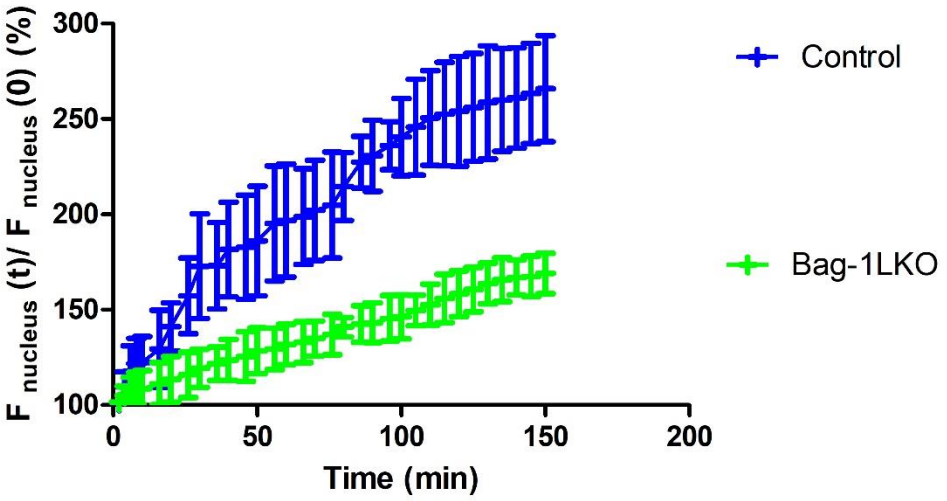

C

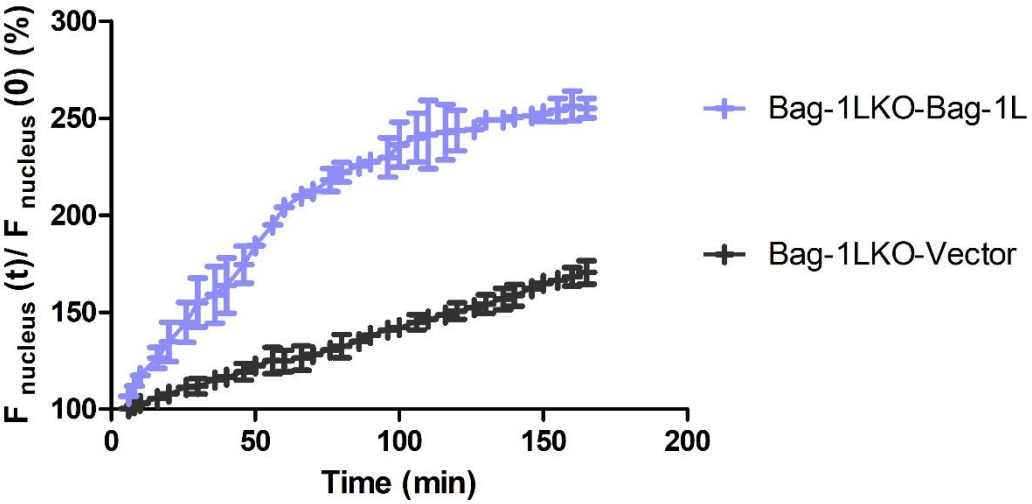

D

Figure 3.11: Bag-1L knockout impairs AR cytoplasmic-nuclear translocation kinetics and Bag-1L expression in the Bag-1L knockout cells rescues AR nuclear translocation defect

(A) Western blot analysis showing control and Bag-1L knockout LNCaP cells using anti-Bag-1 and anti-NPM1 antibodies. Vinculin expression was used as an internal reference protein for equal protein loading by blotting with an anti-vinculin antibody. (**B)** Control and Bag-1L knockout cells were transiently transfected

with 500 ng of CFP-AR-YFP plasmid and cultured for 48 h in starvation medium similar to previously described experiments. Cells were then treated with DHT (10^{-8} M) for at least 150 min. Translocation of the AR into the nucleus was tracked using an Andor Revolution® XD spinning disk laser scanning microscope. (**C)** Quantification of the AR cytoplasmic-nuclear translocation rate determined from three independent experiments. Legend; blue curve – control cells, Green curve - Bag-1L knockout cells. (**D)** A figure showing the quantified AR translocation rate in Bag-1L KO cells rescued with either Bag-1L or empty vector as control. Legend; grayish-blue curve – Bag-1L knockout+Bag-1L cells, Black curve - Bag-1L knockout + empty vector cells (n = 3). These microscopy experiments were carried out with the help of Linxiao Yang.

3.7.3 Bag-1L overexpression in NPM1 knockdown cells partially rescues androgen receptor nuclear translocation in LNCaP cells

As the expression of Bag-1L recues the nuclear translocation defect of the AR in the Bag-1L knockout cells, this study investigated whether Bag-1L overexpression in NPM1 KD cells could also rescue the AR translocation defect in these cells. This is particularly important as the NPM1 knockdown downregulates the expression of all the Bag-1 proteins including Bag-1L (**Figure 3.5**). The NPM1 knockdown cells were therefore stably transduced with lentiviral particles controlling either the expression of Bag-1L or an empty vector as a control and subjected to Western blot analysis. **Figure 3.12A** shows a very strong expression of Bag-1L in the NPM1 KD cells. These cells were then used in translocation experiment to determine the effect of Bag-1L overexpression on the AR nuclear translocation rate in the NPM1 knockdown cells. CFP-AR-YFP plasmid construct was transfected into the NPM1 KD-Bag-1L and NPM1 KD-vector cells. Following treatment of the cells with DHT, translocation of the AR into the nucleus was tracked as previously described and the signals quantified. From the quantified data, it could be seen that from time *t=0* min to *t= 90* min, there was no rescued effect on the cytoplasmic-nuclear translocation rate and the AR translocation kinetics in the two cell lines were nearly identical. Thereafter (between *t=90* and *t=150*) the kinetics of nuclear translocation of the AR was faster in the Bag-1L overexpressing cells compared to the control (**Figure 3.12B**) suggesting that regulation of AR action by Bag-1L may overlap to some degree with that of NPM1.

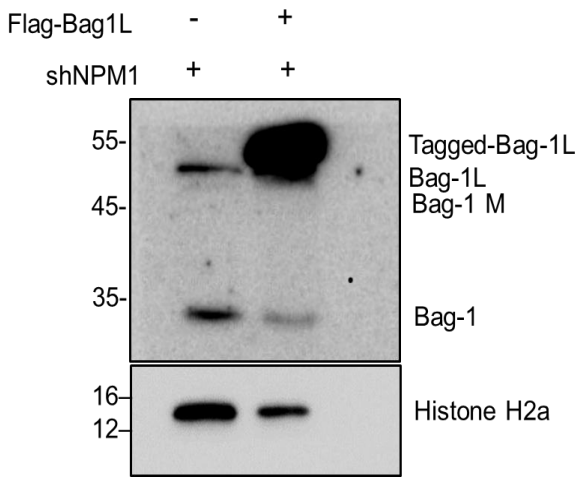

A

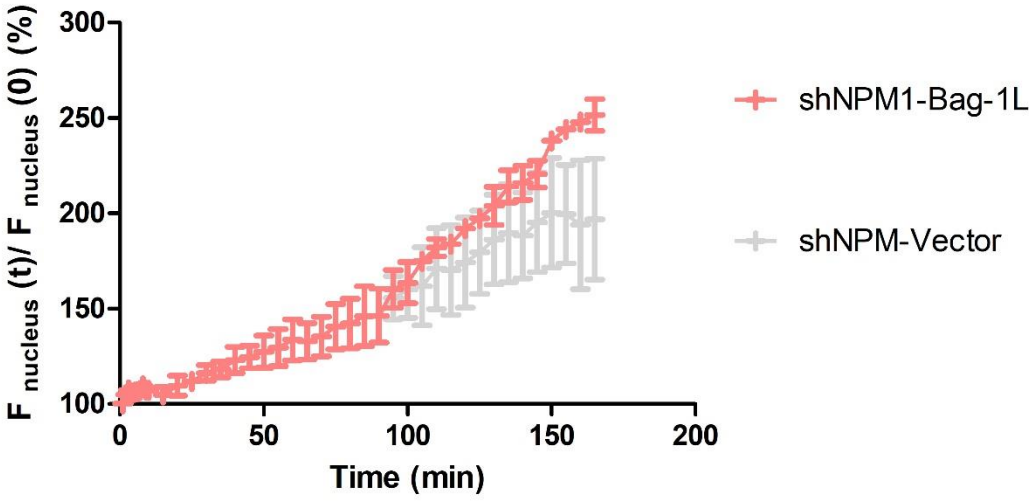

B

Figure 3.12: Bag-1L overexpression in NPM1 knockdown cells partially rescues AR nuclear translocation defect.

(A) A Western blot showing overexpression of Bag-1L in NPM1 KD LNCaP cells. Whole cell lysates from NPM1 KD-vector or NPM1 KD-Bag-1L were resolved on 10% SDS-PAGE and proteins detected with an anti-Bag-1 antibody. Histone H2A expression was determined with an anti-histone H2A-specific antibody

as internal reference for equal protein loading. (**B)** NPM1 KD-vector and NPM1 KD-Bag-1L cells were transiently transfected with CFP-AR-YFP and cultured in starvation medium for 48 h. Cells were then treated with DHT (10^{-8} M) and nuclear translocation of the AR into the nucleus was measured with Andor Revolution® XD spinning disk laser scanning microscope. The images were then quantified using imageJ software. (n = 3). Legend: Red curve – NPM1 knockdown+Bag-1L cells, Gray curve - Bag-1L knockout + empty vector cells (n = 3). These microscopy experiments were carried out with the help of Linxiao Yang.

3.7.4 NPM1 knockdown inhibits androgen-mediated prostate cancer cell proliferation

Androgen acting through the AR drives the proliferation of prostate cancer cells and having established that the knockdown of NPM1 impairs AR nuclear translocation, further investigation was carried out to compare the overall effect of the knockdown on androgen dependent proliferation between the control sh and shNPM1 cells. Here, equal number of cells from both shNPM1 and control cells were seeded in hormone deprived medium and starved for 72 h to deplete the basal hormone level in the cell. DHT or solvent was then administered repeatedly every 48 h and cells were counted at the following time points: 0, 1, 3, 5 and 7 days of growth. Day 0 cell count was the number of cell count at the end of 72 h starvation. The fold increase was obtained by normalizing cell count for each day to that of day 0. The results below showed a marginal increase in cell growth in the absence of androgen. On the other hand, in the presence of DHT, control cells showed about 5 fold higher proliferation rate at day 7 compared to the knockdown cells, indicating that NPM1 is important for androgen-mediated cell proliferation.

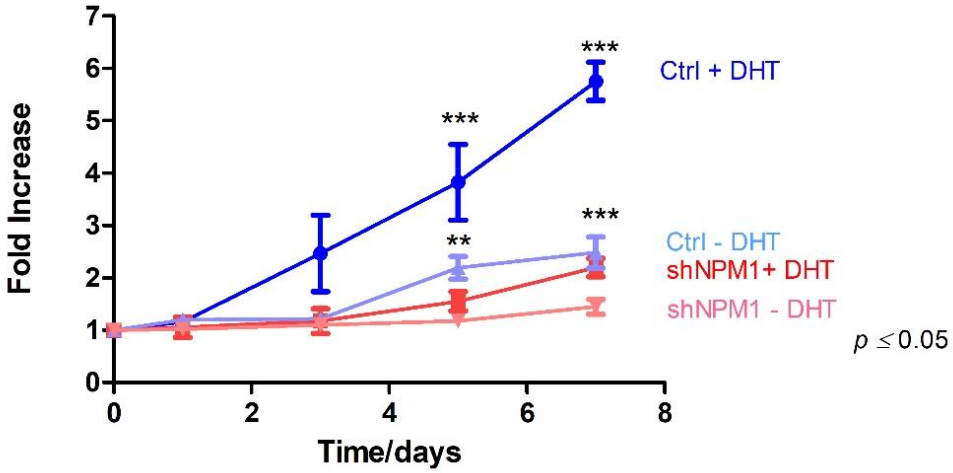

Figure 3.13: NPM1 knockdown impairs androgen dependent proliferation in LNCaP cells.

A total of 10^5 cells from both NPM1 knockdown and control were seeded in 6-well plates in duplicates in RPMI 1640 cell culture medium supplemented with 10% FCS and 1% L-glutamine. After 24 h, the cells were washed twice with 1x PBS and medium replaced with phenol red-free RPMI medium supplemented with 3% CCS and L-glutamine (starvation medium) and starved for 72 h. Thereafter, a batch of cells was counted and recorded as day 0 cell count. The remaining cells were then treated with DHT (10^{-8} M) or solvent (ethanol). DHT or solvent was added to the cells after every 48 h. Cells were counted on 0, 1, 3, 5 and 7 days. Fold increase in proliferation of cells was determined by normalizing each count from the indicated time points with the cell count from day 0. Legend: Light blue curve – control cell without DHT, Strong blue curve - control cells with DHT, Light red curve – ShNPM1 cells without DHT, Strong red curve – ShNPM1 cells with DHT. Graphs represent the mean of three independent experiments, ± standard error of mean (SEM). *p* - values were calculated using a standard t-test, *p ≤ 0.05.

3.7.5 Bag-1L knockout impairs androgen dependent prostate cancer cell proliferation in LNCaP cells

Due to the impaired AR translocation kinetics observed also in the Bag-1L KO cells compared with control cells, cell proliferation experiment similar to the one carried out in section 3.7.4 was carried out to investigate the effect of Bag-1L knockout on androgen-dependent cell proliferation. From **figure 3.14**, it could be shown that even though there was no significant difference in rate of proliferation between the control and Bag-1L KO cells in the absence of DHT, the proliferation rate in the Bag-1L KO cells was significantly

less (about 3 fold) compared to the control in the presence of DHT. This results agree with studies carried out by Cato et al., 2017 which show that Bag-1L knockout impairs cell proliferation in LNCaP prostate cancer cells.

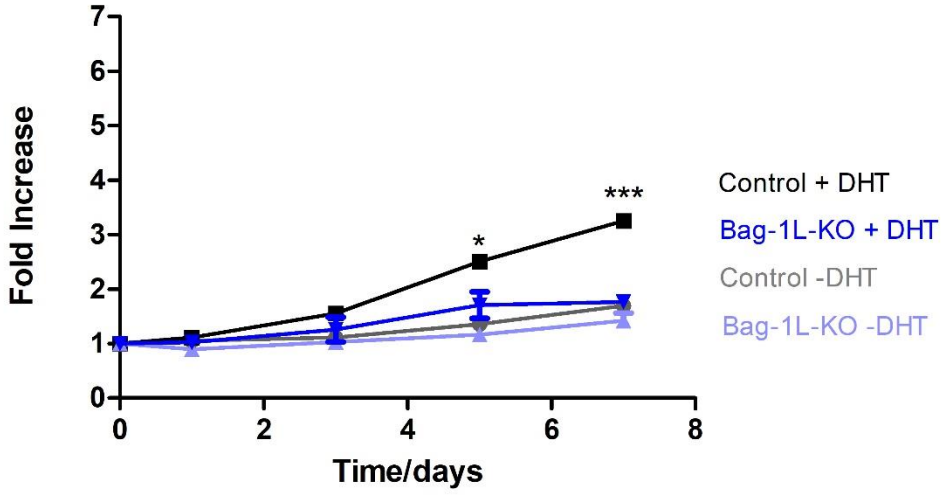

Figure 3.14: Bag-1L knockout impairs androgen dependent proliferation in LNCaP cells.

A total of 10^5 cells from both control and Bag-1L KO were seeded in each well of 6-well plates in duplicates in RPMI supplemented with 10% FCS and 1% L-glutamine as previously described. The rest of the experiments were carried out in a similar way as in **figure 3.13.** Graphs represent the mean of three independent experiments, ± standard error of mean (SEM). *p* - values were calculated using a standard t test, *p ≤ 0.05. Legend; Grey curve – Control sh (-DHT), Black curve – Control sh (+DHT), Light blue curve - Bag-1L knockout (-DHT) and Strong blue curve – Bag-1L knockout (+DHT).

3.7.6 Bag-1L overexpression partially rescues androgen-dependent proliferation defect in NPM1 knockdown LNCaP cells

Having shown that the knockdown of NPM1 leads to a reduction in Bag-1 expression, the question was asked whether overexpression of Bag-1L in the NMP1 KD cells would rescue the androgen-dependent growth defect in the NPM1 KD cells. This investigation was carried out in a similar way as in section 3.7.4 by seeding equal number of cells for NPM1 KD-vector and NPM1 KD-Bag-1L in hormone deprived medium and subsequently carrying out proliferation experiment as previously described. The results in **figure 3.15**

shows significant cell proliferation rate in the NPM1 KD-Bag-1L compared to the NPM1 KD-vector cells in the presence of DHT at days 5 to 7 (**Figure 3.15**). On the other hand, in the absence of DHT, there was no difference in proliferation rate between the NPM KD-Bag-1L and NPM1 KD-vector cells indicating that both NPM1 and Bag-1L function to enhance androgen-dependent cell proliferation.

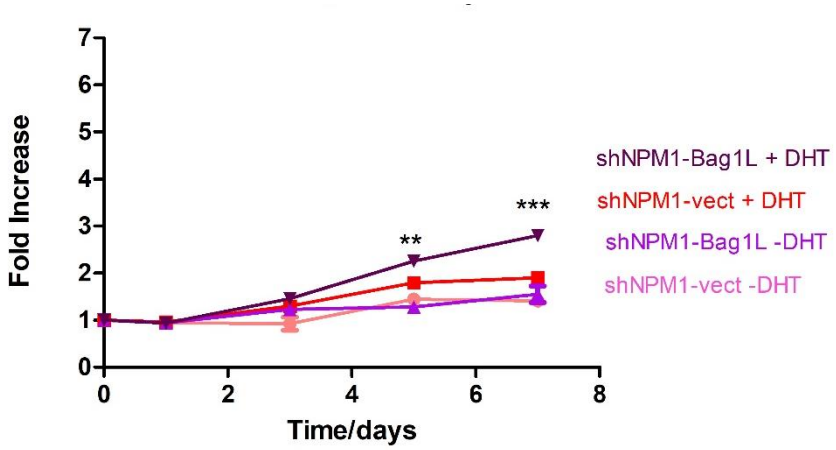

Figure 3.15: Bag-1L overexpression enhances androgen-dependent proliferation in NPM1 knockdown LNCaP cells.

Equal number cells from both NPM1 KD-vector and NPM1 KD-Bag-1L were seeded in duplicates in RPMI 1640 culture medium supplemented with 10% FCS and 1% L-glutamine. After 24 h, the cells were washed twice with PBS 1X and medium replaced with phenol red-free RPMI supplemented with 3% CCS and L-glutamine (starvation medium). Cells were then starved for 72 h. The cell count at the end of 72 h was recorded as day 0 cell count. The remaining cells were either treated with DHT (10^{-8} M) or solvent (ethanol). DHT or solvent was repeated every 48 h. Cells were counted on day 1, 3, 5 and day 7. Graphs are from means values of three independent experiments, ± standard error of mean (SEM). *p* - values were calculated using a standard t test, $*p \leq 0.05$. Legend: weak red – NPM1 KD-vector (-DHT), bright red – NPM1 KD-vector (+DHT), weak violet - NPM1 KD-Bag-1L (-DHT) and strong violet – NPM1 KD-Bag-1L (+DHT).

3.8 Androgen-mediated gene expression

3.8.1 NPM1 knockdown and Bag-1L knockout alter androgen-mediated gene expression in LNCaP cells

To investigate whether NPM1 and Bag-1L regulate common pathway(s) leading to androgen- dependent LNCaP cell proliferation, genome-wide transcriptomic analyses on NPM1 KD cell and that of Bag-1L knockout were carried out and compared as shown below:

LNCaP control sh and shNPM1 were seeded in triplicates in starvation medium for 72 h to remove residual hormone and treated with either DHT or solvent (ethanol) for 16 h. Total RNAs extracted from the cells for RNAsequencing analyses fell under these two experimental conditions:

1. Solvent treated NPM1 knockdown and control cells (difference in basal expression),
2. DHT treated NPM1 knockdown and control cells (difference in hormone induced expression).

The main goals of the sequencing and analyses were:

1. to identify androgen-regulated genes that are differentially expressed following NPM1 KD,
2. to identify androgen-regulated genes that are differentially expressed following Bag-1L KO (RNAseq carried out by Cato et al., 2017)
3. to investigate whether there is a commonality in the pattern of regulation of gene expression by androgen in the two cell lines that will identify common androgen-dependent cellular processes shared by NPM1 and Bag-1L.

The RNA-Seq libraries were sequenced and the data processed through a visualization pipeline for RNA-seq (also known as VIPER: https://bitbucket.org/cfce/viper). The data were then analysed using Limma (a package for differential expression analysis of data arising from microarray experiments) and DESEQ2 Bioconductor tools to obtain the differential expression analysis based on fold change (log_2[Fold Change] ≥ 0.58) or Log_2[1.5] = ~0.58 difference between DHT treated and solvent treated cells. Therefore,

the Genes of Interest (GOI) were distinguished by a fold change difference greater or equal to 0.58. For example, Log_2[shNPM1 Gene A] - Log_2[shControl Gene A] ≥ │0.58│. Differentially expressed genes were represented as Matrices. Coluor-coded genes of interest (GOI) were based on *p*-adjusted values (*p*adj ≤ 0.05) for the groups. In **figure 3.16A**, the gray zone represents genes that were not significantly different in NPM1 KD versus control. The red represents GOI that were significantly different and were uniquely expressed in NPM1 KD under DHT conditon and the blue represents GOI that were significantly different and were uniquely expressed in the control under DHT conditon. The violet represents significant GOI that were differentially expressed in both NPM1 knockdown and control cells.

Cato et al., 2017 had already carried out RNAseq sequencing experiments on Bag-1L KO that was analyzed previously with ChIPseq data [(Cato et al., 2017) GEO depository accession number GSE89939]. The RNAseq data on Bag-1L KO versus control from Cato and colleagues' work was re-analyzed using the same conditions used for NPM1 KD analysis and also represented as Matrix (**Figure 3.16B**). The coluor-coded GOI were also based on *p*-adj values (*p*adj ≤ 0.05) of the groups. Similarly, the gray zone represents genes that were not significantly different in the Bag-1L KO compared with control under DHT treatment. The yellow represents GOI that were uniquely significantly expressed in Bag-1L KO under DHT conditon. The blue represents GOI that were uniquely expressed in the control under DHT conditon and the green represents GOI that were differentially expressed in both Bag-1L KO and control cells.

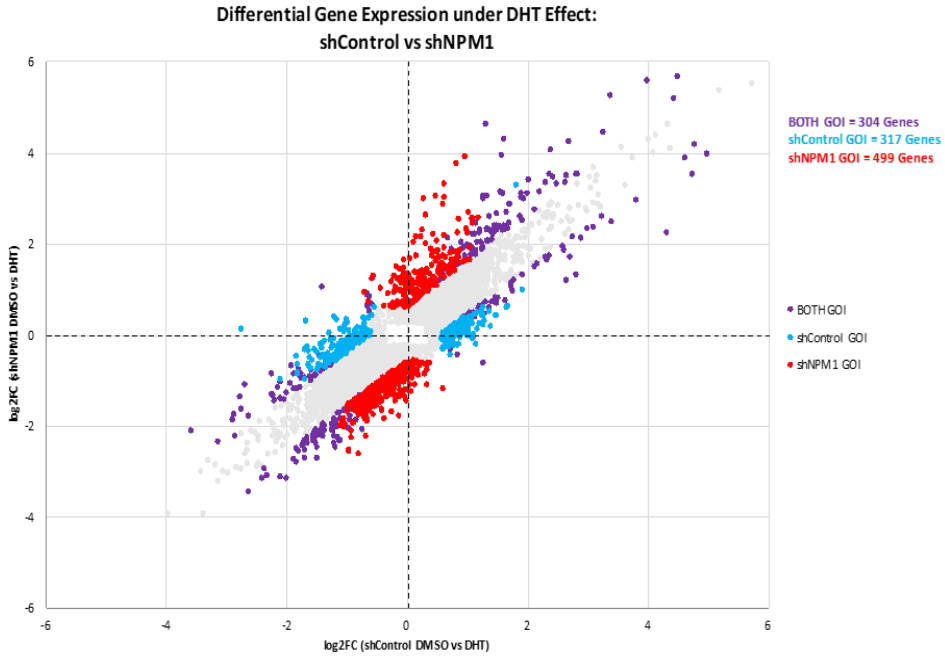
Differential Gene Expression under DHT Effect:
shControl vs shNPM1
BOTH GOI = 304 Genes
shControl GOI = 317 Genes
shNPM1 GOI = 499 Genes
BOTH GOI
shControl GOI
shNPM1 GOI
log2FC (shNPM1 DMSO vs DHT)
log2FC (shControl DMSO vs DHT)

A

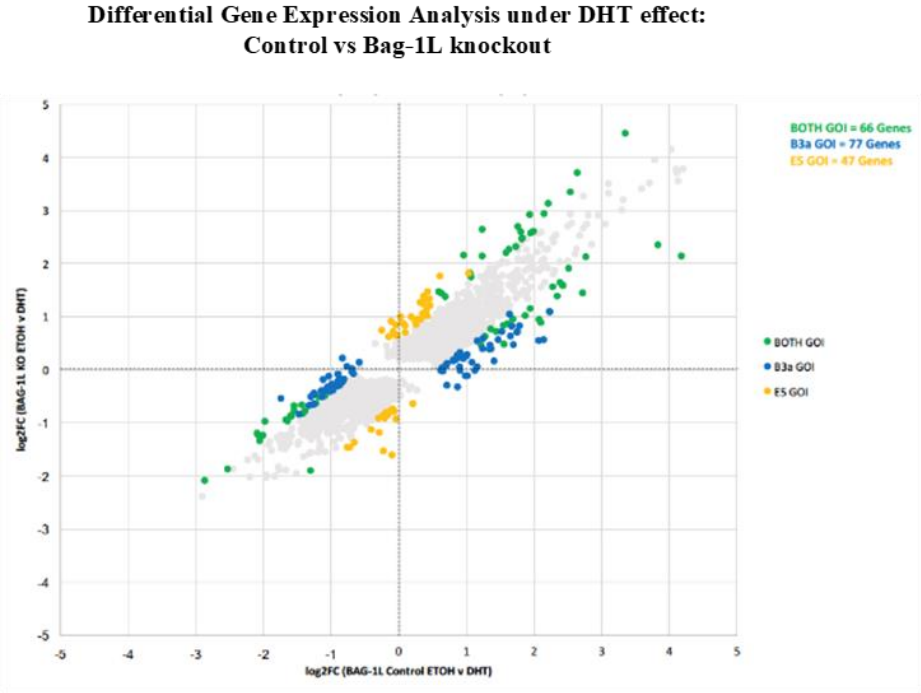
Differential Gene Expression Analysis under DHT effect:
Control vs Bag-1L knockout
BOTH GOI = 66 Genes
B3a GOI = 77 Genes
ES GOI = 47 Genes
BOTH GOI
B3a GOI
ES GOI
log2FC (BAG-1L KO ETOH v DHT)
log2FC (BAG-1L Control ETOH v DHT)

B

Figure 3.16: NPM1 knockdown and Bag-1L knockout lead to misregulation of androgen-mediated gene expression.

(A) Scatter plot comparing the genome-wide gene expression differences between solvent vs DHT treated NPM1 KD cells and solvent vs DHT treated control cells (16 h). Genes of interest (GOI) were sorted based on adjusted *p*-value (*p*-adj ≤ 0.05) into three colour-coded groups: **Violet**: represents genes that were differentially expressed in both NPM1 KD and control conditions, **Blue**: represents genes that were uniquely expressed in the Control sh and **Red**: represents genes that were uniquely expressed in only NPM1 KD condition. The axes were labelled: Control - solvent vs DHT Genes = X-coordinates and shNPM1 - solvent vs DHT Genes = Y-coordinates. **(B)** A similar scatter plot comparing the genome-wide gene expression differences between solvent treated and DHT treated Bag-1L knockout (E5) and Control (B3a) cells. Genes were sorted based on adjusted *p*-value (*p*-adj ≤ 0.05) into three colour-coded files: green: both conditions, blue: only Control condition and yellow: only Bag-1L KO condition. A total of 190 Genes of interest (GOI) were then distinguished by the Log_2 Fold Change (FCD) greater than 0.58. Differentially expressed genes were plotted as scatter plot. The axes were labelled: Control- Ethanol vs DHT Genes = X-coordinates and Bag-1LKO- Ethanol vs DHT Genes = Y-coordinates. This RNA sequencing experiment and analyses were carried out with the help of Jaice Rottenberg and Irene Lee.

3.8.2 GSEA HALLMARK analyses of uniquely expressed NPM1 knockdown and Bag-1L knockout genes show no overlap

Having obtained the genes of interest (GOI) from the RNAseq data from NPM1 KD versus control and Bag-1L KO versus control, pathway enrichment analyses were carried out to determine first of all, the HALLMARK gene signatures that characterized the uniquely expressed androgen regulated genes. Hallmark gene sets are coherently expressed gene signatures derived by aggregating many Molecular Signatures Database (MSigDB) gene sets to represent well-defined biological states or processes. Hallmark gene sets were defined and curated by the Broad Institute using a right-tailed Fisher's exact test (Subramanian et al., 2005). Analysis done using the HALLMARK function of the GSEA established that genes that were uniquely expressed in response to NPM1 KD as shown in **Figure 3.17A** were Estrogen responsive genes (both early and late), genes associated with tumour suppressor p53 pathways, Hypoxia, K-ras signaling as well as NF-κB signaling among others. On the other hand, genes that were uniquely expressed in the Bag-1L KO were associated with only androgen response as shown in **Figure 3.17B.** As could be seen in **Figures 3.17A and B,** there was no common processes or pathways

between the uniquely expressed genes of NPM1 KD and Bag-1L KO. Next, HALLMARK genes enrichment analysis was further carried out on the GOI that were differentially expressed in both control sh vs NPM1 KD and control vs Bag-1L KO.

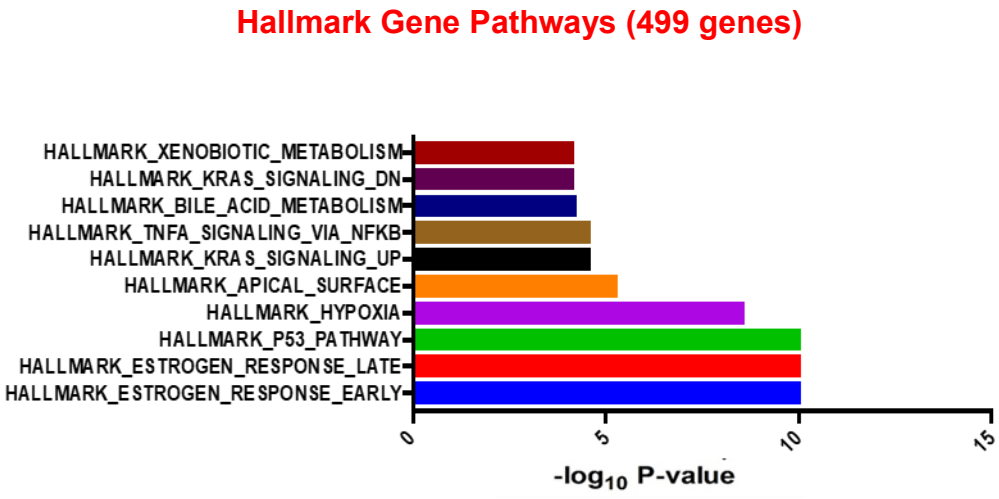

A

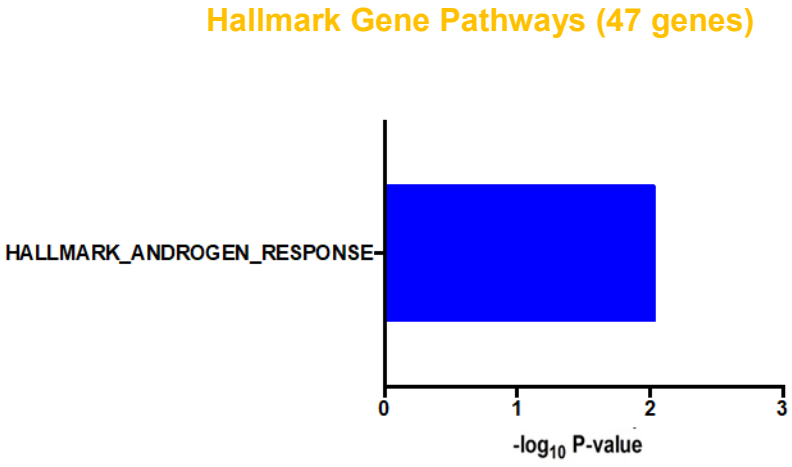

B

Figure 3.17: HALLMARK GSEA with uniquely expressed genes in NPM1 KD and Bag-1L KO showed no common pathway

(A) The figure shows pathways obtained by a HALLMARK GSEA terms analysis of 499 uniquely misregulated shNPM1 red colour-coded GOI from shNPM1 versus control (FDR < 10%). (**B)** The figure shows pathway obtained by a HALLMARK GSEA analysis of the 47 uniquely yellow colour-coded GOI from Bag-1L KO versus control under DHT conditions (FDR < 10%). These analyses were carried out with the help of Jaice Rottenberg and Irene Lee.

3.8.3 HALLMARK gene sets from differentially expressed NPM1 knockdown and Bag-1L knockout show overlapping processes

Having found no common biological pathway between the gene sets from uniquely expressed genes of NPM1 KD and Bag-1L KO, this study proceeded to investigate whether there are pathways enriched in the violet colour-coded GOI NPM1 KD versus control and green colour-coded Bag-1L KO versus control GOI. It could be shown that the analyzed enrichments in HALLMARK gene signatures using the violet colour-coded genes (**Figure 3.18A)** and the green colour-coded genes (**Figure 3.18B)** revealed a number of overlapping processes, including androgen responsive gene sets, inflammatory, estrogen responsive genes and well as UV response genes. Further identification of the genes revealed 25 genes as the overlapping gene set (**Figure 3.18C)**.

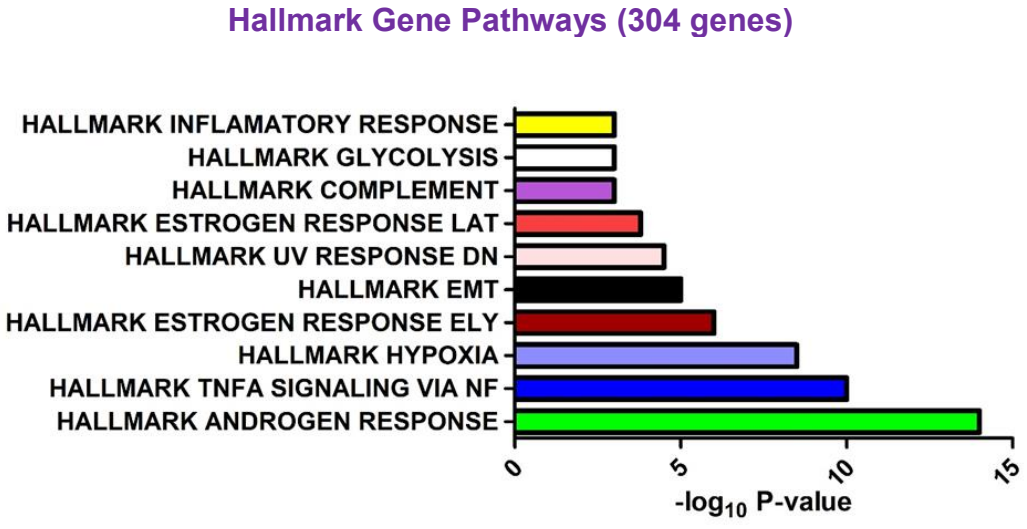

A

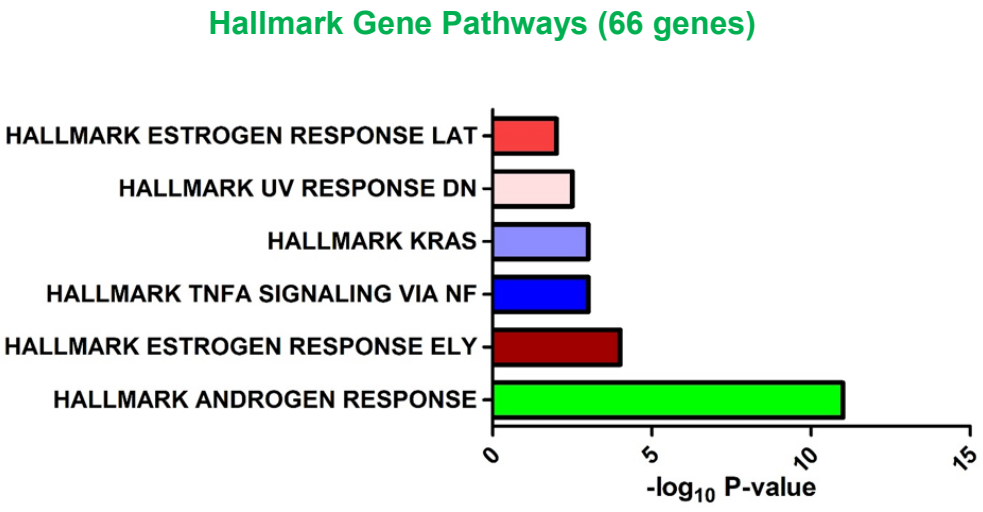

B

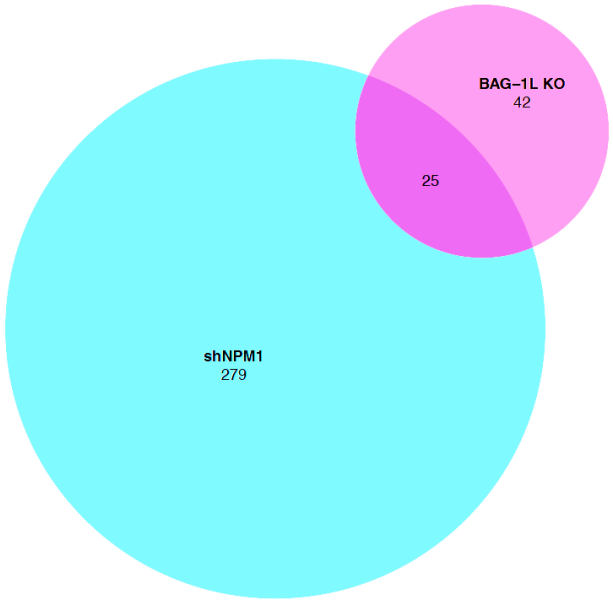

C

Figure 3.18: NPM1 knockdown and Bag-1L knockout lead to enrichment in gene sets associated with androgen response pathways, inflammation and estrogen response pathways.

(A) The figure shows pathways obtained by a HALLMARK GSEA terms analysis of 304 genes violet colour-coded GOI which were differentially expressed in shNPM1 and control under DHT conditions (FDR < 10%). (**B)** The figure shows pathways obtained by a HALLMARK GSEA terms analysis of 66 green colour-coded

GOI expressed differentially in Bag-1LKO and control under DHT conditions (FDR < 10%). (**C)** Venn diagram showing the overlapping genes of interest in the differentially expressed androgen target genes from the Control sh vs shNPM1 (violet colour-coded total number 304) and control vs Bag-1LKO (green colour-coded total number 66). The overlap consisted of 25 genes. These analyses were carried out with the help of Jaice Rottenberg and Irene Lee.

3.8.4 Signaling pathways regulated in common by both NPM1 and Bag-1L in LNCaP cells

Due to the fewer number of genes obtained as overlapping genes (25 genes), it was somewhat difficult to run pathway analysis on them. However, because of the partial rescue of androgen dependent cell proliferation observed (**figure 3.15)** when Bag-1L was overexpressed in NPM1 KD cell, data mining was therefore carried out to identify genes within this set (**table 3.0**) which regulate prostate cancer cell proliferation. Five genes within the list have already been reported to regulate prostate cancer cell proliferation. These are as follows:

BMPR1B inhibits growth and proliferation of prostate tumor cells through up-regulation of cyclin-dependent kinase inhibitor, CDKI (Brubaker et al., 2004; Ye et al., 2007).

CAMK2N1 contributes to human prostate cancer cell growth and survival through AR-dependent signalling. Plays a tumour suppressive role and serves as a crucial determinant of resistance of prostate cancer to endocrine therapies (Wang et al., 2014).

DOUX1: its enzyme activity promotes protein kinase B/AKT signalling in prostate cancer cells. DUOX1 is important in mediating epithelial cell migration and induction of various wound response genes. Actions of DUOX1 are largely mediated by H_2O_2-dependent regulation of redox-dependent cell signalling pathways (Pettigrew et al., 2012).

RUNX1**:** an androgen (and Enhancer of zeste homolog 2 (EZH2)) regulated gene, has differential roles in AR-dependent and -independent prostate cancer. Loss of *RUNX1* impairs AR-dependent transcription and cell growth (Takayama et al., 2015).

***SAT1* or *SSAT*:** rate-limiting enzyme of polyamine catabolic pathway and a key factor in producing a high level of ROS in the prostatic tissue. There is direct evidence linking SAT1 and ROS with increase in tumor development in the prostate (Basu et al., 2009; Mehraein-Ghomi et al., 2010; Huang et al., 2015).

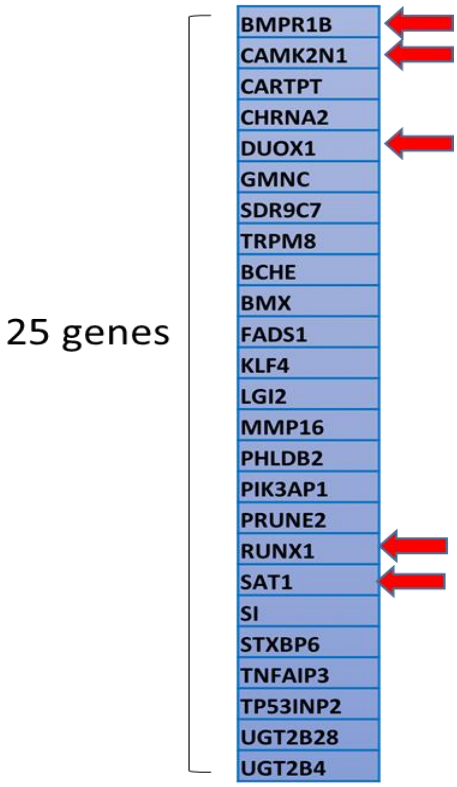

Table 3.0: Androgen responsive genes regulated by both NPM1 and Bag-1L.

A list of all overlapping genes of interest obtained by comparing NPM1 knockdown violet colour-coded data set and Bag-1L knockout green colour-coded data set. Highlighted are five genes which have been reported to regulate prostate cancer cell proliferation.

3.8.5 NPM1 knockdown and Bag-1L impairs the expression of *SAT1* and *DUOX1* genes

The study at this stage asked whether two or more genes exist that function together in a single signaling pathway to enhance androgen-mediated cell proliferation. A closer inspection revealed that two of the five genes Spermidine/Spermine N1-acetyl transferase (*SAT1)* and Dual Oxidase 1 (*DUOX1)* genes might be related in a pathway leading to proliferation in prostate cancer. SAT1 is a rate limiting enzyme responsible for androgen dependent oxidation of polyamines to produce putrescine and hydrogen peroxide (H_2O_2) (Basu et al., 2009) and DUOX1 is also a key enzyme whose function is to transfer electrons to molecular oxygen which combines with H_2O to yield H_2O_2 (Pettigrew et al.,

2012). It has been shown that hydrogen peroxide (H_2O_2) plays a central role in prostate cancer cells proliferation by preventing apoptosis and sustaining androgen-dependent cell proliferation (Polytarchou et al., 2005, 2009; Basu et al., 2009). Hydrogen peroxide functions as an intracellular second messenger (Sauer et al., 2001) in stimulating the activation of AKT (protein kinase B) and ERK 1/2 kinases (extracellular signal-regulated kinase), the two major constituents of the most potent survival and proliferative pathways in the cells (Burdon, 1995).

Using qRT-PCR, it was confirmed that the expression of *SAT1* and *DUOX1* were significantly reduced in both NPM1 KD (f**igures 3.18 A** – **B**) and Bag-1L KO (**Figures 3.18 C** – **D)** compared to their respective controls in the presence of DHT.

However, as both the knockdown of NPM1 and the knockout of Bag-1L resulted in impaired expression of the overlapping genes, the study further investigated whether the overexpression of Bag-1L in NPM1 KD cells would rescue the androgen mediated expression of these genes.

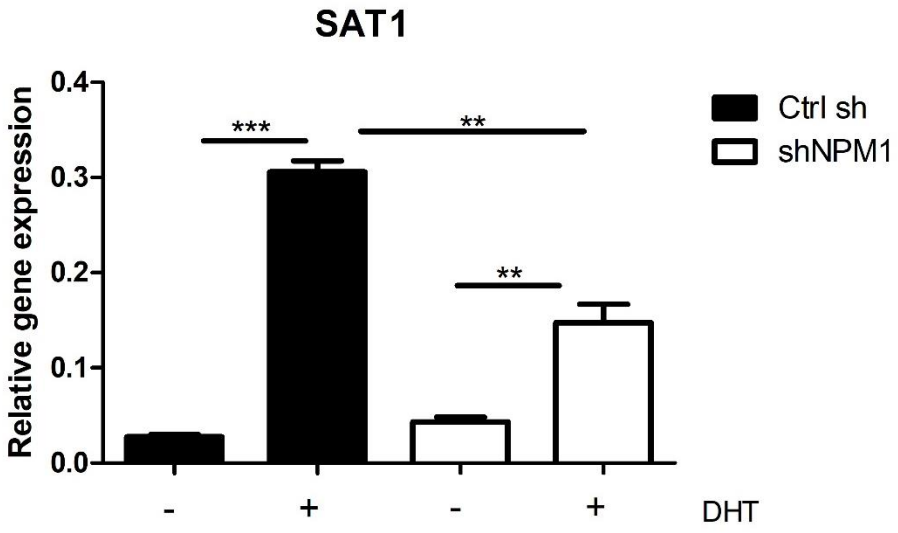

A

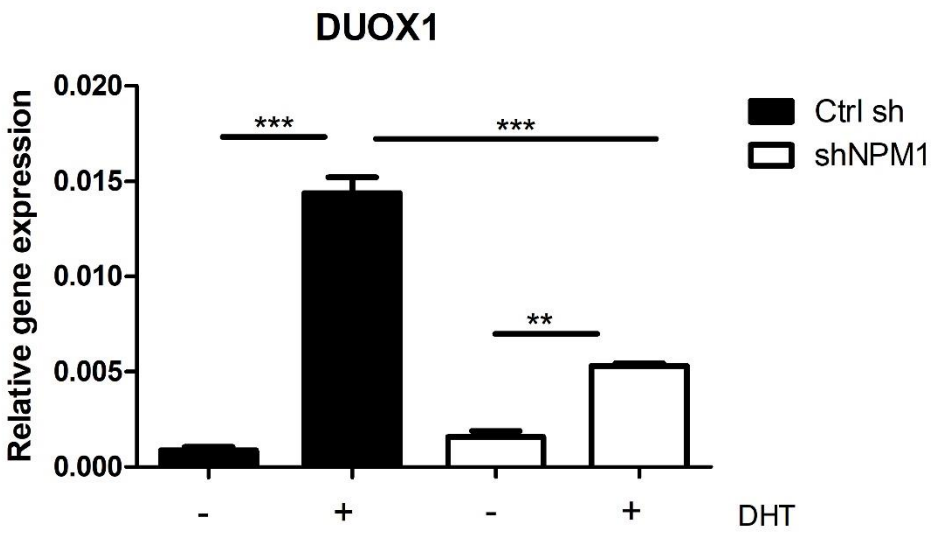
DUOX1
Relative gene expression
0.020
0.015
0.010
0.005
0.000
***
***
**
Ctrl sh
shNPM1
-
+
-
+
DHT

B

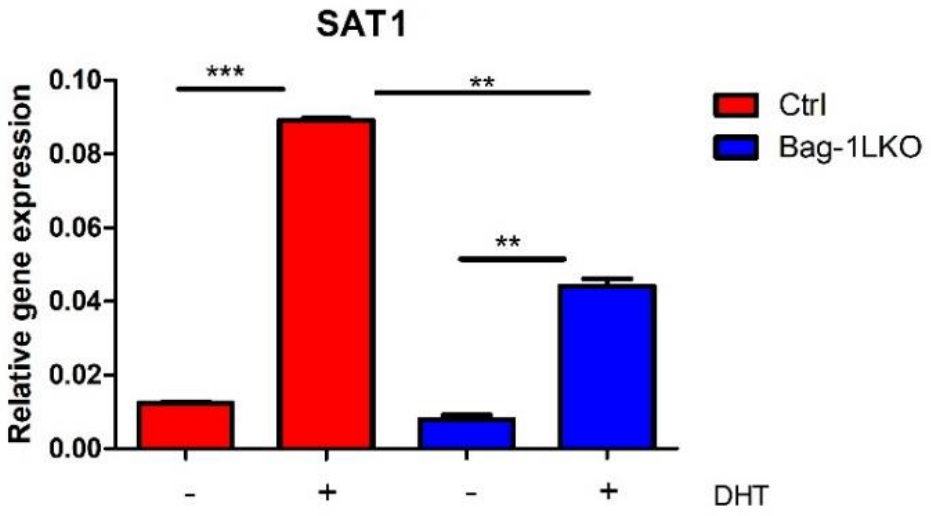
SAT1
Relative gene expression
0.10
0.08
0.06
0.04
0.02
0.00
***
**
**
Ctrl
Bag-1LKO
-
+
-
+
DHT

C

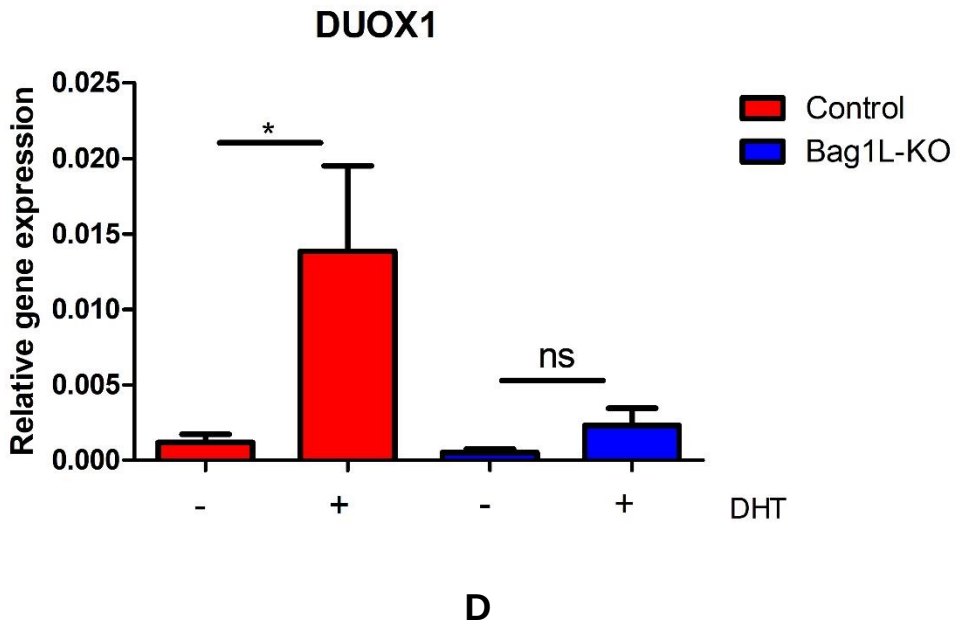

Figure 3.19: NPM1 knockdown and Bag-1L knockout impair androgen-mediated expression of *SAT1* and *DUOX1* genes.

NPM1 knockdown and control cells, as well as Bag-1L knockout and control cells, were first starved for 72 h and treated with either DHT (10^{-8}M) or solvent (ethanol) for 16 h and thereafter RNA extracted from the cells and 1 µg each reverse transcribed into cDNA for qRT-PCR. The data represent the mean of three independent experiments, each in duplicate ± standard error of mean (error bars). *p* values were calculated using a standard t test,* $p \leq 0.05$.

3.8.6 Bag-1L overexpression in NPM1 knockdown cells rescues impaired androgen-mediated expression of overlapping target genes

Having shown that the knockdown of NPM1 and Bag-1L KO results in impaired expression of overlapping genes, further investigation was carried out to ascertain whether overexpression of Bag-1L in the NMP1 KD cells rescues the expression of *SAT1* and *DUOX1* genes in the NPM1 KD cells. Gene expression analysis of *SAT1* and *DUOX1* genes were therefore carried out in NPM1 KD-vector and NPM1 KD-Bag-1L cells using qRT-PCR in the absence and presence of DHT. The results in **figures 3.19 A and B** show that Bag-1L overexpression (**figure 3.13A**) in NPM1 knockdown cells rescued the expression of *SAT1* and *DUOX1* in the presence of DHT compared with the vector control

which suggest that Bag-1L overexpression might have contributed to the partial rescued cell proliferation in **figure 3.15,** though further experiments would be needed to strengthen this conclusion.

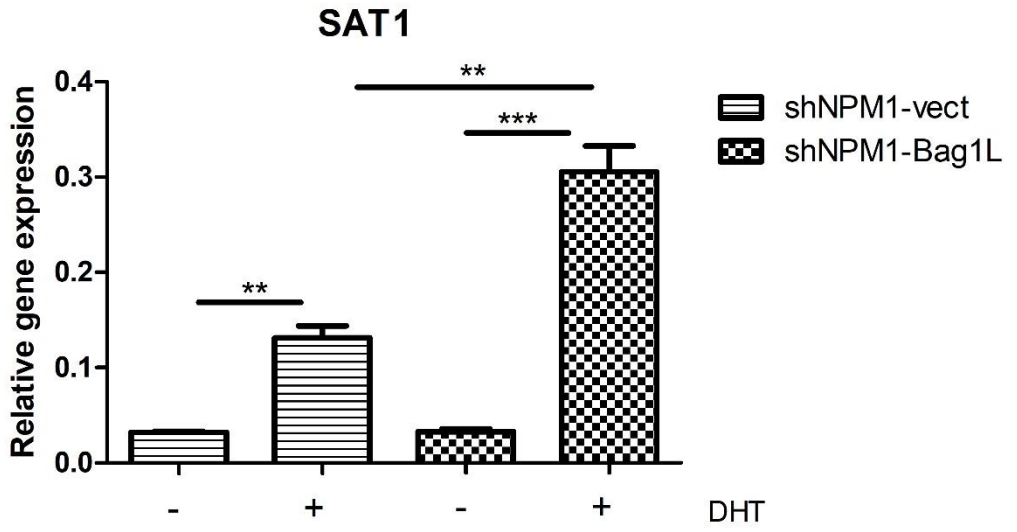

A

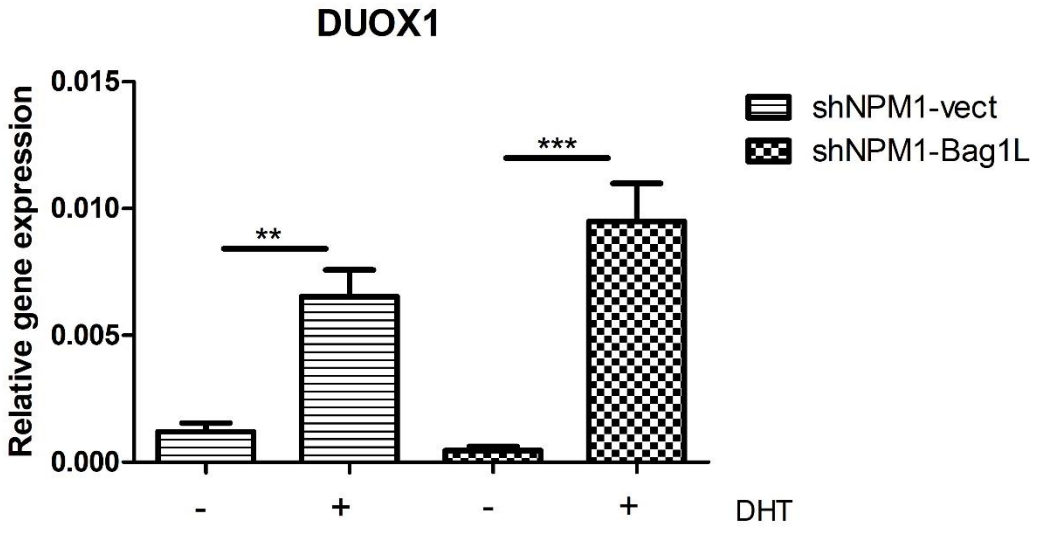

B

Figure 3.20: Bag-1L overexpression in NPM1 knockdown cells significantly rescued impaired androgen-mediated expression of *SAT1* and *DUOX1* genes.

(A and **B)** NPM1 KD-vector and NPM1 KD-Bag-1L LNCaP cells were seeded in phenol red-free RPMI 1640 cell culture medium and starved for 72 h and treated with either DHT (10^{-8}M) or solvent (ethanol) for 16 h and thereafter total RNA extracted from the cells and 1 µg each reverse transcribed into cDNA for qRT-PCR quantification of *SAT1* and *DUOX1* relative gene expression. The data represent the mean of three independent experiments, each in duplicate ± standard error of mean (error bars). *p* values were calculated using a standard t test,* $p \leq 0.05$.

4.0 Discussion

An important clinical management strategy of advanced prostate cancer (PCa) hinges on the use of androgen deprivation therapy (ADT) (Sharifi et al., 2005), which exploits the cancer's dependence on androgen signaling for cell proliferation (Huggins and Hodges, 1941). ADT is effective but for a short period (Dutt and Gao, 2009). Given time, virtually all patients progress to a disease state known as castration-resistant PCa (CRPC), a state that is characterized by persistent activation of androgen signaling; the hallmark of the lethal stage of the disease (Scher et al., 2004; Dutt and Gao, 2009; Knudsen and Scher, 2009). Androgen signaling plays a critical role in every stage of the disease, and it is mediated by the androgen receptor; the transcription factor which mediate androgen signaling (AR) (Gregory et al., 2001; Shafi et al., 2013). The correct folding of nascent AR into mature form, its transcriptional functions, as well as its role in prostate cell growth and proliferation are governed by a concerted action of several molecular chaperones; most of which reside in the cytoplasm, although some are localized in the nucleus of target cells (Cato et al., 2014). While studies about the regulation of AR action by the cytoplasmic chaperones is much advanced, not much is known about AR action regulation by the nuclear chaperones. Two nuclear chaperones: Bag-1L and NPM1, that interact with the AR and whose levels have been shown to correlate positively with the progression of prostate cancer were investigated in this work to ascertain whether they function together in promoting PCa cell proliferation.

In vitro interaction studies carried out in this work to ascertain whether Bag-1L, NPM1 and AR interact showed that NPM1 interacts with the NH_2-terminus of Bag-1L and with the AR. Furthermore, to determine whether Bag-1L and NPM1 function together with the AR to promote prostate cancer proliferation, a stable NPM1 knockdown (NPM1 KD) was generated in LNCaP prostate cancer cell line and used to carry out further investigations. It was shown in this work that NPM1 KD significantly reduced androgen dependent proliferation in LNCaP cells and also, further genome-wide transcriptomics studies carried out with the NPM1 KD cells under androgen-deprived and androgen treated conditions showed marked misregulation of expression of androgen target genes compared to the control. Comparison carried out between NPM1 KD RNAseq data and Bag-1L knockout

RNAseq data (carried out under similar conditions and published by Cato et al., 2017) showed a number of shared biological pathways. Overexpression of Bag-1L in the NPM1 knockdown cells partially rescued the impaired androgen mediated gene expression, as well as, androgen dependent prostate cancer cell proliferation in the NPM1 KD cells.

4.1 Bag-1L interacts with NPM1 and the AR

In vitro interaction studies carried out in this work showed that only Bag-1L within the family of Bag-1 proteins interacts with NPM1. At least four isoforms of Bag-1 protein can arise from alternative initiation of translation within a common mRNA: Bag-1S, Bag-1, Bag-1M and Bag-1L (Packham et al., 1997; Liu et al., 1998). These isoforms all contain an Hsp70-binding BAG domain near the COOH-terminus as well as the upstream ubiquitin-like (UBL) domain, but they differ in the lengths of their NH_2-terminal regions. Using truncated versions of Bag-1L, it was shown in this study that only the NH_2-terminus of Bag-1L interacts with NPM1. The NH_2-terminus of Bag-1L contains among other regulatory sequences the NLS (Froesch et al., 1998; Knee et al., 2001) and it is only Bag-1L that has been reported to be localized in the nucleus. Immunofluorescence assay carried out in this work to investigate co-localization between Bag-1 and NPM1 showed that the nuclear Bag-1 isoform co-localizes with NPM1 in the nuclei of LNCaP cells, suggesting that not only do these 2 proteins interacts *in vitro* but, most likely, also do *in vivo*. However, the immunofluorescence assay did not show any co-localization of NPM1 with Bag-1 in the cytoplasm, which somehow confirms the *in vitro* interaction studies that NPM1 interacts with only Bag-1L, the nuclear isoform of Bag-1 proteins.

The *in vitro* interaction between Bag-1L and NPM1 also pulled-down the androgen receptor in the same Western blot, which is a confirmation that Bag-1L interacts with AR (Takayama et al., 1995; Knee et al., 2001; Shatkina et al., 2003; Jehle et al., 2014) and also NPM1 interacts with AR (Léotoing et al., 2008; Stelloo et al., 2018). It is however not clear whether Bag-1L together with NPM1 might participate in the regulation of androgen receptor in a ternary complex and further studies would be needed to establish that. Bag-1L interaction with the AR, and their domain of interaction have already been determined (Knee et al., 2001; Shatkina et al., 2003; Jehle et al., 2014). Furthermore, this study

showed that the interaction between Bag-1L and NPM1 requires the domain of Bag-1L containing the NLS. This is in conformity with the report that NPM1 has affinity for NLS containing proteins (Szebeni et al., 1995). It was therefore not surprising that the domain of the AR that was reported to interact with NPM1 contained its NLS, i.e., the DBD / hinge region of AR (Léotoing et al., 2008). However, what these interactions mean to androgen signaling is further discussed.

4.2 NPM1 regulates Bag-1 protein levels

As this study found out that NPM1 interacts with the NLS containing domain of Bag-1L and from published report, also with AR (Léotoing et al., 2008; Stelloo et al., 2018), it further explored whether modulating NPM1 protein levels may affect the nuclear localization of either Bag-1L or AR or both. First of all, it was shown in this work that silencing NPM1 via transduction of shRNA against NPM1 reduced the total Bag-1 protein signal in immunofluorescence assay. This observation was confirmed using Western blotting. The reduced total Bag-1 protein level in the NPM1 knockdown cells was further uncovered in this study to be due to reduced Bag-1 mRNA. Coincidentally, NPM1 has been reported in another study to interact with the protein, FOXM1, and that, it regulates the action of this protein by regulating the mRNA level of the protein (Bhat et al., 2011). The reduced Bag-1 mRNA by NPM1 knockdown was shown to be caused by reduced stability of Bag-1 mRNA. Even though NPM1 binds both DNA and RNA (Wang et al., 1994) not much is known currently about how its absence may affect mRNA stability of proteins with which it interacts.

However, NPM1 interacts with APE1, a proteins with endonuclease activity reported to be important in RNA quality control mechanisms. Furthermore, it has been reported that NPM1 action is necessary to regulate the endonuclease activity of APE1 (Kim et al., 2010).Thus, most probably, the absence of NPM1 possibly might have enhanced the endonuclease action of APE1 thereby affecting the half-lives of specific transcripts.

4.3 NPM1 knockdown impairs AR nuclear translocation rate

This study could show that knockdown of NPM1 does not affect either the mRNA or protein level of the AR but drastically reduces its nuclear translocation rate. The impaired AR nuclear translocation rate could be due to the reduced level of Bag-1 proteins caused by the knockdown of NPM1 or the knockdown of NPM1 directly on AR or both. Cytoplasmic Bag-1 isoforms have been reported to play a role in glucocorticoid receptor nuclear trafficking (Schneikert et al., 1999). Although no such report has been published on the AR, the effect of reduced Bag-1 proteins on the AR nuclear trafficking might be similar to that reported for the GR. This is because the AR is a member of class 1 nuclear receptors which shares similar characteristics and is regulated somewhat similarly as other members in this class (other members includes progesterone receptor and estrogen receptors). As Bag-1 has been documented to form a complex with the AR as a co-chaperone of HSP70 in the cytoplasm (Cato et al., 2014), reduced total Bag-1 protein could affect the function of the complex and a consequence on AR nuclear trafficking. To investigate whether or not the consequential reduction of Bag-1 proteins in the NPM1 KD cells contributed to the impaired AR nuclear translocation, overexpression of the Bag-1 isoform which interacts with NPM1 (Bag-1L) in the NPM1 knockdown cells partially rescued the AR nuclear translocation defect which was observed in the NPM1 knockdown cells. This may suggest that the reduced Bag-1 proteins (including Bag-1L) might have played a role in the impaired AR translocation rate in the NPM1 KD cells. However, in this connection it must be pointed out that NPM1 has a high affinity for AR–DBD/hinge region which contains the NLS, and since it shuttles between the nucleus and cytoplasm (Borer et al., 1989; Yun et al., 2003; Haelens et al., 2007), it could regulate AR nuclear trafficking and cellular sub-localization directly. Alternatively, the involvement of other regulatory factors affected by the knockdown of NPM1 cannot be ruled out, which may suggest an indirect action of NPM1 on the nuclear translocation of the AR.

4.4 NPM1 promotes androgen-mediated gene expression

Further investigation carried out in this work to ascertain the consequence of silencing the expression of NPM1 on global androgen-mediated gene expression using RNA-

sequencing technology showed that the knockdown of NPM1 leads to wide-spread misregulation of androgen target genes expression indicating that NPM1 is important for transcriptional functions of the AR. It must be noted that this finding is in agreement with what has been reported earlier on by Léotoing et al., 2008. Using a single androgen regulated gene, kallikrein 3 (Prostate specific antigen, PSA), these authors could show that NPM1 KD impairs PSA expression. Intriguingly, this gene did not show up as one of the significantly misregulated genes in this work. This could be due to the fact that the threshold for the cut-off for the selection of this gene in the RNAseq was too stringent for its differential expression to be identified. Nevertheless, it must be noted that more than 400 androgen target genes were significantly downregulated and more than 300 genes were upregulated underscoring the importance of NPM1 in androgen driven transcription.

4.5 Bag-1L overexpression in NPM1 knockdown cells partially rescues impaired androgen dependent proliferation and gene expression

As it has been shown in this work that knockdown of NPM1 leads to reduced expression of Bag-1 proteins, including Bag-1L and impaired AR action and also, Bag-1L knockout has been shown in this work to impair androgen dependent cell proliferation, which is in agreement with earlier reports (Cato et al., 2017), it was argued that the reduced Bag-1L in the NPM1 KD cells might have contributed to the defective AR action. Indeed overexpression of Bag-1L in the NPM1 KD cells could rescue the defects in AR action identified in this work for the NPM1 KD cells. These include a rescue of the defective cytoplasmic-nuclear translocation of the receptor, a rescue of the defective AR-mediated regulation of transcription of some of the target genes and androgen dependent cell proliferation. The overexpression of Bag-1L in the NPM1 KD cells rescued androgen-mediated cell proliferation by almost 50%, implying that key androgen-dependent processes regulated by NPM1 to effect proliferation may also be regulated by Bag-1L as well. Therefore, the analyzed RNAseq data carried out on the NPM1 KD cells was compared with Bag-1L knockout RNAseq data (carried out by Cato et al., 2017) to identify common genes and pathway(s) regulated by the 2 proteins.

4.6 Bag1L and NPM1 regulate the same genes in H_2O_2 production pathways

The common genes shared between NPM1 and Bag-1L in AR regulation were identified to be 25 in number. A closer look at the functions of these genes revealed that a number of them have been reported to regulate androgen-dependent cell proliferation. A common pathway for the regulation of cell proliferation was identified to be oxidative stress (Basu et al., 2009; Mehraein-Ghomi et al., 2010; Pettigrew et al., 2012). The RNAseq carried out in this study showed that knockdown of NPM1 significantly impaired androgen-mediated expression of Spermidine/Spermine N1-acetyl transferase (*SAT1)* and Dual Oxidase 1 (*DUOX1)* genes. A similar pattern of expression was also observed in the Bag-1L knockout cells. The NPM1 and Bag-1L regulation of the androgen-mediated expression of *SAT1* and *DUOX1* were validated using quantitative RT-PCR and a further overexpression of Bag-1L in NPM1 knockdown cells was shown in this work to rescue the impaired androgen-mediated expression of these genes in the NPM1 KD cells. This identifies *SAT1* and *DUOX1* as common androgen-regulated genes that are positively regulated by both Bag-1L and NPM1.

SAT1 is a rate limiting enzyme responsible for androgen dependent oxidation of polyamines to produce putrescine and hydrogen peroxide (H_2O_2) (Basu et al., 2009). By far the spermine level in prostate cells has been reported to be the highest among most of the cell lines studied (Thomas and Thomas, 2003) and because of this high levels in human prostate and prostate cancer cells, this pathway seems all the more important in prostate cancer cells. DUOX1 is also a key enzyme whose function is to transfer electrons to molecular oxygen which combines with H_2O to yield H_2O_2. DUOX1 dependent hydrogen peroxide production has been reported to be the most dominant pathway of hydrogen peroxide production in another prostate cancer cell line, PC3 (Pettigrew et al., 2012). Even though further work is required to support the commensurate protein levels and the resultant amount of H_2O_2 produced by the recorded fold increases in mRNA expression of *SAT1* and *DUOX1*, one might be tempted to argue that the rescue of *SAT1* and *DUOX1* expression by Bag-1L overexpression in the NPM1 knockdown cells might have possibly played a key role in the rescued androgen dependent cell proliferation observed, though further work is needed to show that these 2 genes, indeed, were responsible for the rescued cell proliferation.

4.7 ROS mediated mitogenesis represents potential signaling convergence between NPM1 and Bag-1L actions in prostate cancer cells

So far, it has been shown in this work that both NPM1 and Bag-1L regulate the 2 genes responsible for production of Reactive Oxygen Species (ROS) in PCa cells. Furthermore, it has been shown that overexpression of Bag-1L in NPM1 KD cells rescued the expression of the 2 genes. ROS (e.g. includes peroxides, superoxide, hydroxyl radical, and singlet oxygen) that were once thought to be only detrimental to cell viability, have now gained recognition as stimulants for survival and proliferation of normal and malignant cells (McCord, 1995; Martin and Barrett, 2002). A series of publications in the last several years have shown that at least one ROS, hydrogen peroxide (H_2O_2), plays a central role in prostate cancer cells proliferation by preventing apoptosis and sustaining androgen-dependent proliferation (Lim et al., 2005; Polytarchou et al., 2005, 2009; Kumar et al., 2008; Basu et al., 2009; Mustafi et al., 2009). By functioning as an intracellular second messenger (Sauer et al., 2001), H_2O_2 can stimulate the activation of Akt (protein kinase B) and ERK 1/2 kinases (extracellular signal-regulated kinase); the two major constituents of the most potent survival pathways in the cell (Burdon, 1995).

Interestingly, NPM1 has been shown to be required for ERK1/2 phosphorylation leading to increased proliferation and migration capacities in LNCaP PCa cell line (Loubeau et al., 2014). However, whether the expression of *SAT1* and *DUOX1* for H_2O_2 production is an intermediary step ensured by NPM1 for the phosphorylation of ERK1/2 requires further clarification.

In addition, ROS has been demonstrated to regulate the expression and activation of AKT/PKB in prostate cancer cells (Kumar et al., 2008). Interestingly, apart from H_2O_2 dependent activation of AKT / PKB, further evidence by other studies show that Bag-1 also can interact with activated AKT to phosphorylate BAD (Bcl-2 / Bcl-XL-antagonist, causing cell death), a pro-apoptotic member of the Bcl-2 family, leading to inhibition of apoptosis and enhanced cells survival (Frebel and Wiese, 2006). Therefore, whether the rescue of SAT1 and DUOX1 expression by Bag-1L or direct action of Bag-1L in AKT dependent phosphorylation of BAD or both contributed to the outcome of the rescued cell proliferation will require further studies to fully clarify the mechanism.

4.8 Conclusion

To conclude, this work has demonstrated that NPM1 and Bag-1L first of all, play important roles in androgen receptor nuclear translocation and secondly, regulate the expression of androgen target genes required for oxidative stress generation in prostate cancer cells.

References

Abràmoff, M.D., Magalhães, P.J., and Ram, S.J. (2004). Image Processing with ImageJ Second Edition. Biophotonics Int. *11*: 36–42.

Ahn, J.Y., Liu, X., Cheng, D., Peng, J., Chan, P.K., Wade, P.A., et al. (2005). Nucleophosmin/B23, a nuclear PI(3,4,5)P3 receptor, mediates the antiapoptotic actions of NGF by inhibiting CAD. Mol. Cell *18*: 435–445.

Anfinsen, C.B. (1973). Principles that Govern the Folding of Protein Chains. Science (80-.). *181*: 223–230.

Antonarakis, E.S., Lu, C., Wang, H., Luber, B., Nakazawa, M., Roeser, J.C., et al. (2014). AR-V7 and Resistance to Enzalutamide and Abiraterone in Prostate Cancer. N. Engl. J. Med. *371*: 1028–1038.

Arnan, C., Saperas, N., Prieto, C., Chiva, M., and Ausió, J. (2003). Interaction of nucleoplasmin with core histones. J. Biol. Chem. *278*: 31319–31324.

Arndt, V., Daniel, C., Nastainczyk, W., Alberti, S., and Höhfeld, J. (2005). BAG-2 acts as an inhibitor of the chaperone-associated ubiquitin ligase CHIP. Mol. Biol. Cell *16*: 5891–900.

Avvakumov, N., Nourani, A., and Côté, J. (2011). Histone Chaperones: Modulators of Chromatin Marks. Mol. Cell *41*: 502–514.

Azad, A.A., Zoubeidi, A., Gleave, M.E., and Chi, K.N. (2015). Targeting heat shock proteins in metastatic castration-resistant prostate cancer. Nat. Rev. Urol. *12*: 26–36.

Basu, H.S., Thompson, T.A., Church, D.R., Clower, C.C., Mehraein-ghomi, F., Amlong, C.A., et al. (2009). A small molecule polyamine oxidase inhibitor blocks androgen-induced oxidative stress and delays prostate cancer progression in the transgenic adenocarcinoma of the mouse prostate model. Cancer Res. *69*: 7689–7695.

Belotserkovskaya, R., Oh, S., Bondarenko, V.A., Orphanides, G., Studitsky, V.M., and Reinberg, D. (2003). FACT facilitates transcription-dependent nucleosome alteration. Science (80-.). *301*: 1090–1093.

Berndsen, C.E., Tsubota, T., Lindner, S.E., Lee, S., Holton, J.M., Kaufman, P.D., et al. (2008). Molecular functions of the histone acetyltransferase chaperone complex Rtt109-Vps75. Nat. Struct. Mol. Biol. *15*: 948–956.

Bhat, U.G., Jagadeeswaran, R., Halasi, M., and Gartel, A.L. (2011). Nucleophosmin interacts with FOXM1 and modulates the level and localization of FOXM1 in human cancer cells. J. Biol. Chem. *286*: 41425–41433.

Bishr, M., and Saad, F. (2013). Overview of the latest treatments for castration-resistant prostate cancer. Nat. Rev. Urol. *10*: 522–528.

Bocker, T., Bittinger, A., Wieland, W., Buettner, R., Fauser, G., Hofstaedter, F., et al. (1995). In vitro and ex vivo expression of nucleolar proteins B23 and p120 in benign and malignant epithelial lesions of the prostate. Mod Pathol *8*: 226–231.

Borer, R.A., Lehner, C.F., Eppenberger, H.M., and Nigg, E.A. (1989). Major nucleolar proteins shuttle between nucleus and cytoplasm. Cell *56*: 379–390.

Briknarová, K., Takayama, S., Brive, L., Havert, M.L., Knee, D.A., Velasco, J., et al. (2001). Structural analysis of BAG-1 cochaperone and its interactions with Hsc70 heat shock protein. Nat. Struct. Biol. *8*: 349–352.

Brubaker, K.D., Corey, E., Brown, L.G., and Vessella, R.L. (2004). Bone morphogenetic protein signaling in prostate cancer cell lines. J. Cell. Biochem. *91*: 151–160.

Burdon, R.H. (1995). Superoxide and hydrogen peroxide in relation to mammalian cell proliferation. Free Radic. Biol. Med. *18*: 775–794.

Burgess, R.J., and Zhang, Z. (2013). Histone chaperones in nucleosome assembly and human disease. Nat. Struct. Mol. Biol. *20*: 14–22.

Cato, L., Neeb, A., Brown, M., and Cato, A.C.B. (2014). Control of steroid receptor dynamics and function by genomic actions of the cochaperones p23 and Bag-1L. Nucl. Recept. Signal. *12*: e005.

Cato, L., Neeb, A., Sharp, A., Buzón, V., Ficarro, S.B., Yang, L., et al. (2017). Development of bag-1L as a therapeutic target in androgen receptor-dependent prostate

cancer. Elife *6*: 1–27.

Chan, P.K., Aldrich, M., and Busch, H. (1985). Alterations in immunolocalization of the phosphoprotein B23 in HeLa cells during serum starvation. Exp. Cell Res. *161*: 101–110.

Chang, C., Saltzman, A., Yeh, S., Young, W., Keller, E., Lee, H.J., et al. (1995). Androgen receptor: an overview. Crit. Rev. Eukaryot. Gene Expr. *5*: 97–125.

Chen, J., Xiong, J., Liu, H., Chernenko, G., and Tang, S.-C. (2002). Distinct BAG-1 isoforms have different anti-apoptotic functions in BAG-1-transfected C33A human cervical carcinoma cell line. Oncogene *21*: 7050–7059.

Chen, Z.H., Zhu, M., Yang, J., Liang, H., He, J., He, S., et al. (2014). PTEN Interacts with Histone H1 and controls chromatin condensation. Cell Rep. *8*: 2003–2014.

Claessens, F., Helsen, C., Prekovic, S., Broeck, T. Van Den, Spans, L., Poppel, H. Van, et al. (2014). Emerging mechanisms of enzalutamide resistance in prostate cancer. Nat. Rev. Urol. *11*: 712–716.

Clemo, N.K., Collard, T.J., Southern, S.L., Edwards, K.D., Moorghen, M., Packham, G., et al. (2008). BAG-1 is up-regulated in colorectal tumour progression and promotes colorectal tumour cell survival through increased NF-κB activity. Carcinogenesis *29*: 849–857.

Colombo, E., Martinelli, P., Zamponi, R., Shing, D.C., Bonetti, P., Luzi, L., et al. (2006). Delocalization and destabilization of the Arf tumor suppressor by the leukemia-associated NPM mutant. Cancer Res. *66*: 3044–3050.

Costa, C.R. Da, Villadiego, J., Sancho, R., Fontana, X., Packham, G., Nateri, A.S., et al. (2010). Bag1-L Is a Phosphorylation-Dependent Coactivator of c-Jun during Neuronal Apoptosis. Mol. Cell. Biol. *30*: 3842–3852.

Cutress, R.I., Townsend, P. a, Sharp, A., Maison, A., Wood, L., Lee, R., et al. (2003). The nuclear BAG-1 isoform, BAG-1L, enhances oestrogen-dependent transcription. Oncogene *22*: 4973–82.

Dalenc, F., Drouet, J., Ader, I., Delmas, C., Rochaix, P., Favre, G., et al. (2002). Increased

expression of a COOH-truncated nucleophosmin resulting from alternative splicing is associated with cellular resistance to ionizing radiation in HeLa cells. Int. J. Cancer *100*: 662–668.

Demand, J., Alberti, S., Patterson, C., and Höhfeld, J. (2001). Cooperation of a ubiquitin domain protein and an E3 ubiquitin ligase during chaperone/proteasome coupling. Curr. Biol. *11*: 1569–1577.

Destouches, D., Sader, M., Terry, S., Marchand, C., Maillé, P., Soyeux, P., et al. (2016). Implication of NPM1 phosphorylation and preclinical evaluation of the nucleoprotein antagonist N6L in prostate cancer. Oncotarget *7*: 69397–69411.

Devireddy, L.R., Kumar, K.U., Pater, M.M., and Pater, A. (2000). BAG-1, a novel Bcl-2-interacting protein, activates expression of human JC virus. J. Gen. Virol. *81*: 351–357.

Dhar, S.K., and Clair, D.K. St. (2009). Nucleophosmin blocks mitochondrial localization of p53 and apoptosis. J. Biol. Chem. *284*: 16409–16418.

Dingwall, C., Dilworth, S.M., Black, S.J., Kearsey, S.E., Cox, L.S., and Laskey, R. a (1987). Nucleoplasmin cDNA sequence reveals polyglutamic acid tracts and a cluster of sequences homologous to putative nuclear localization signals. EMBO J. *6*: 69–74.

Doukhanina, E. V., Chen, S., Zalm, E. van der, Godzik, A., Reed, J., and Dickman, M.B. (2006). Identification and functional characterization of the BAG protein family in Arabidopsis thaliana. J. Biol. Chem. *281*: 18793–801.

Dumbar, T.S., Gentry, G. a, and Olson, M.O. (1989). Interaction of nucleolar phosphoprotein B23 with nucleic acids. Biochemistry *28*: 9495–9501.

Dutt, S.S., and Gao, A.C. (2009). Molecular mechanisms of castration-resistant prostate cancer progression. Future Oncol. *5*: 1403–13.

Elbi, C., Walker, D. a, Romero, G., Sullivan, W.P., Toft, D.O., Hager, G.L., et al. (2004). Molecular chaperones function as steroid receptor nuclear mobility factors. Proc. Natl. Acad. Sci. U. S. A. *101*: 2876–2881.

Evans, R. (1988). The steroid and thyroid hormone receptor superfamily. Science (80-.).

240: 889–895.

Fang, Y., Fliss, A.E., Robins, D.M., and Caplan, A.J. (1996). Hsp90 regulates androgen receptor hormone binding affinity in vivo. J. Biol. Chem. *271*: 28697–28702.

Fizazi, K., Scher, H.I., Molina, A., Logothetis, C.J., Chi, K.N., Jones, R.J., et al. (2012). Abiraterone acetate for treatment of metastatic castration-resistant prostate cancer: Final overall survival analysis of the COU-AA-301 randomised, double-blind, placebo-controlled phase 3 study. Lancet Oncol. *13*: 983–992.

Francini, E., Petrioli, R., and Roviello, G. (2014). No clear evidence of a clinical benefit of a sequential therapy regimen with abiraterone acetate and enzalutamide. Expert Rev. Anticancer Ther. *14*: 1135–1140.

Frebel, K., and Wiese, S. (2006). Signalling molecules essential for neuronal survival and differentiation. Biochem. Soc. Trans. *34*: 1287–1290.

Frehlick, L.J., Eirín-López, J.M., and Ausió, J. (2007). New insights into the nucleophosmin/nucleoplasmin family of nuclear chaperones. BioEssays *29*: 49–59.

Froesch, B.A., Takayama, S., and Reed, J.C. (1998). BAG-1L protein enhances androgen receptor function. J. Biol. Chem. *273*: 11660–11666.

Götz, R., Wiese, S., Takayama, S., Camarero, G.C., Rossoll, W., Schweizer, U., et al. (2005). Bag1 is essential for differentiation and survival of hematopoietic and neuronal cells. Nat. Neurosci. *8*: 1169–1178.

Greenhough, J., Papadakis, E.S., Cutress, R.I., Townsend, P.A., Oreffo, R.O.C., and Tare, R.S. (2016). Regulation of osteoblast development by Bcl-2-associated athanogene-1 (BAG-1). Sci. Rep. *6*: 1–15.

Gregory, C.W., He, B., Johnson, R.T., Ford, O.H., Mohler, J.L., French, F.S., et al. (2001). A mechanism for androgen receptor-mediated prostate cancer recurrence after androgen deprivation therapy. Cancer Res. *61*: 4315–4319.

Grisendi, S., Bernardi, R., Rossi, M., Cheng, K., Khandker, L., Manova, K., et al. (2005). Role of nucleophosmin in embryonic development and tumorigenesis. Nature *437*: 147–

153.

Grisendi, S., Mecucci, C., Falini, B., and Pandolfi, P.P. (2006). Nucleophosmin and cancer. Nat. Rev. Cancer *6*: 493–505.

Guzey, M., Takayama, S., and Reed, J.C. (2000). BAG1L enhances trans-activation function of the vitamin D receptor. J. Biol. Chem. *275*: 40749–40756.

Haelens, A., Tanner, T., Denayer, S., Callewaert, L., and Claessens, F. (2007). The hinge region regulates DNA binding, nuclear translocation, and transactivation of the androgen receptor. Cancer Res. *67*: 4514–4523.

He, Y., Peng, S., Wang, J., Chen, H., Cong, X., Chen, A., et al. (2016). Ailanthone targets p23 to overcome MDV3100 resistance in castration-resistant prostate cancer. Nat. Commun. *7*: 1–14.

Hershko, A., Ciechanover, A., and Rose, I.A. (1979). Resolution of the ATP-dependent proteolytic system from reticulocytes: a component that interacts with ATP. Proc. Natl. Acad. Sci. *76*: 3107–3110.

Hingorani, K., Szebeni, a, and Olson, M.O. (2000). Mapping the functional domains of nucleolar protein B23. J. Biol. Chem. *275*: 24451–24457.

Hisaoka, M., Ueshima, S., Murano, K., Nagata, K., and Okuwaki, M. (2010). Regulation of nucleolar chromatin by B23/nucleophosmin jointly depends upon its RNA binding activity and transcription factor UBF. Mol. Cell. Biol. *30*: 4952–4964.

Höhfeld, J., and Jentsch, S. (1997). GrpE-like regulation of the Hsc70 chaperone by the anti-apoptotic protein BAG-1. EMBO J. *16*: 6209–6216.

Horoszewicz, J.S., Leong, S.S., Kawinski, E., Karr, J.P., Rosenthal, H., Chu, T.M., et al. (1983). LNCaP Model of Human Prostatic Carcinoma. Cancer Res. *43*: 1809–1818.

Huang, W., Alessandrini, A., Crews, C.M., and Erikson, R.L. (1993). Raf-1 forms a stable complex with Mek1 and activates Mek1 by serine phosphorylation. Proc. Natl. Acad. Sci. U. S. A. *90*: 10947–51.

Huang, W., Eickhoff, J.C., Ghomi, F.M., Church, D.R., and Basu, H.S. (2015). Expression

of Spermidine/Spermine N1-Acetyl Transferase (SSAT) in Human Prostate Tissues is Related to Prostate Cancer Progression and Metastasis. Prostate *75*: 1150–1159.

Huggins, C., and Hodges, C. V. (1941). Studies of prostatic cancer: The effect of castration, of estrogen and of androgen injection on serum phosphatase in metastatic carcinoma of the prostate. Arch. Surg. *43*: 209.

Ito, Y., Yoshida, H., Nakano, K., Takamura, Y., Miya, A., Kobayashi, K., et al. (2003). Bag-1 expression in thyroid neoplasm: its correlation with Bcl-2 expression and carcinoma dedifferentiation. Anticancer Res. *23*: 569–576.

Jäättelä, M. (1999). Heat shock proteins as cellular lifeguards. Ann. Med. *31*: 261–271.

Jego, G., Hazoumé, A., Seigneuric, R., and Garrido, C. (2013). Targeting heat shock proteins in cancer. Cancer Lett. *332*: 275–285.

Jehle, K., Cato, L., Neeb, A., Muhle-Goll, C., Jung, N., Smith, E.W., et al. (2014). Coregulator control of androgen receptor action by a novel nuclear receptor-binding motif. J. Biol. Chem. *289*: 8839–51.

Kang, Y.J., Olson, M.O., Jones, C., and Busch, H. (1975). Nucleolar Phosphoproteins of Normal Rat Liver and Novikoff Hepatoma Ascites Cells. Cancer Res. *35*: 1470–1475.

Kim, W., King, D., and Lee, C.H. (2010). RNA-cleaving properties of human apurinic / apyrimidinic endonuclease 1 (APE1). Int J Biochem Mol Biol *1*: 12–25.

Kim, Y.S., Alarcon, S. V, Lee, S., Lee, M.-J., Giaccone, G., Neckers, L., et al. (2009). Update on Hsp90 inhibitors in clinical trial. Curr. Top. Med. Chem. *9*: 1479–1492.

Knee, D.A., Froesch, B.A., Nuber, U., Takayama, S., and Reed, J.C. (2001). Structure-function analysis of Bag1 proteins. Effects on androgen receptor transcriptional activity. J. Biol. Chem. *276*: 12718–12724.

Knudsen, K.E., and Scher, H.I. (2009). Starving the addiction: New opportunities for durable suppression of AR signaling in prostate cancer. Clin. Cancer Res. *15*: 4792–4798.

Koochekpour, S. (2010). Androgen receptor signaling and mutations in prostate cancer.

Asian J. Androl. *12*: 639–657.

Krajewska, M., Turner, B.C., Shabaik, A., Krajewski, S., and Reed, J.C. (2006). Expression of BAG-1 Protein Correlates With Aggressive Behavior of Prostate Cancers. Prostate *66*: 801–810.

Krajewski, S., Krajewska, M., Turner, B.C., Pratt, C., Howard, B., Zapata, J.M., et al. (1999). Prognostic significance of apoptosis regulators in breast cancer. Endocr. Relat. Cancer *6*: 29–40.

Kular, R.K., Yehiely, F., Kotlo, K.U., Cilensek, Z.M., Bedi, R., and Deiss, L.P. (2009). GAGE, an antiapoptotic protein binds and modulates the expression of nucleophosmin/B23 and interferon regulatory factor 1. J. Interf. Cytokine Res. *29*: 645–55.

Kullmann, M., Schneikert, J., Moll, J., Heck, S., Zeiner, M., Gehring, U., et al. (1998). RAP46 is a negative regulator of glucocorticoid receptor action and hormone-induced apoptosis. J. Biol. Chem. *273*: 14620–14625.

Kumar, B., Koul, S., Khandrika, L., Meacham, R.B., and Koul, H.K. (2008). Oxidative stress is inherent in prostate cancer cells and is required for aggressive phenotype. Cancer Res. *68*: 1777–1785.

Kumar, R., and Thompson, E.B. (1999). The structure of the nuclear hormone receptors. Steroids *64*: 310–319.

Kurki, S., Peltonen, K., and Laiho, M. (2004). Nucleophosmin, HDM2 and p53: Players in UV damage incited nucleolar stress response. Cell Cycle *3*: 976–979.

Lange, A., Mills, R.E., Lange, C.J., Stewart, M., Devine, S.E., and Corbett, A.H. (2007). Classical nuclear localization signals: Definition, function, and interaction with importin α. J. Biol. Chem. *282*: 5101–5105.

Laskey, R.A., Honda, B.M., Mills, A.D., and Finch, J.T. (1978). Nucleosomes are assembled by an acidic protein which binds histones and transfers them to DNA. Nature *275*: 416–420.

Lee, S.B., Xuan Nguyen, T.L., Choi, J.W., Lee, K.-H., Cho, S.-W., Liu, Z., et al. (2008). Nuclear Akt interacts with B23/NPM and protects it from proteolytic cleavage, enhancing cell survival. Proc. Natl. Acad. Sci. U. S. A. *105*: 16584–16589.

Lee, S.S., Crabb, S.J., Janghra, N., Carlberg, C., Williams, A.C., Cutress, R.I., et al. (2007). Subcellular localisation of BAG-1 and its regulation of vitamin D receptor-mediated transactivation and involucrin expression in oral keratinocytes: Implications for oral carcinogenesis. Exp. Cell Res. *313*: 3222–3238.

Leong, S.M., Tan, B.X., Ahmad, B.B., Yan, T., Chee, L.Y., Ang, S.T., et al. (2010). Mutant nucleophosmin deregulates cell death and myeloid differentiation through excessive caspase-6 and -8 inhibition. Blood *116*: 3286–3296.

Léotoing, L., Meunier, L., Manin, M., Mauduit, C., Decaussin, M., Verrijdt, G., et al. (2008). Influence of nucleophosmin/B23 on DNA binding and transcriptional activity of the androgen receptor in prostate cancer cell. Oncogene *27*: 2858–2867.

Lepor, H., Ross, A., and Walsh, P.C. (1982). The influence of hormonal therapy on survival of men with advanced prostatic cancer. J Urol *128*: 335–340.

Li, J., Zhang, X., Sejas, D.P., Bagby, G.C., and Pang, Q. (2004). Hypoxia-induced nucleophosmin protects cell death through inhibition of p53. J. Biol. Chem. *279*: 41275–41279.

Li, Y., Chan, S.C., Brand, L.J., Hwang, T.H., Silverstein, K.A.T., and Dehm, S.M. (2013). Androgen receptor splice variants mediate enzalutamide resistance in castration-resistant prostate cancer cell lines. Cancer Res. *73*: 483–489.

Lim, S.D., Sun, C., Lambeth, J.D., Marshall, F., Amin, M., Chung, L., et al. (2005). Increased Nox1 and hydrogen peroxide in prostate cancer. Prostate *62*: 200–207.

Lin, J., Hutchinson, L., Gaston, S.M., Raab, G., and Freeman, M.R. (2001). BAG-1 is a novel cytoplasmic binding partner of the membrane form of heparin-binding EGF-like growth factor. A unique role for proHB-EGF in cell survival regulation. J. Biol. Chem. *276*: 30127–30132.

Lindquist, S., and Craig, E. (1988). The Heat-Shock Proteins. Annu. Rev. Genet. *22*: 631–

677.

Liu, H.-Y., Wang, Z.-M., Bai, Y., Wang, M., Li, Y., Wei, S., et al. (2009). Different BAG-1 isoforms have distinct functions in modulating chemotherapeutic-induced apoptosis in breast cancer cells. Acta Pharmacol. Sin. *30*: 235–241.

Liu, R., Takayama, S., Zheng, Y., Froesch, B., Chen, G.Q., Zhang, X., et al. (1998). Interaction of BAG-1 with retinoic acid receptor and its inhibition of retinoic acid-induced apoptosis in cancer cells. J. Biol. Chem. *273*: 16985–16992.

Lonergan, P.E., and Tindall, D.J. (2011). Androgen receptor signaling in prostate cancer development and progression. J. Carcinog. *10*: 20.

Loubeau, G., Boudra, R., Maquaire, S., Lours-Calet, C., Beaudoin, C., Verrelle, P., et al. (2014). NPM1 silencing reduces tumour growth and MAPK signalling in prostate cancer cells. PLoS One *9*: e96293.

Love, M.I., Huber, W., and Anders, S. (2014). Moderated estimation of fold change and dispersion for RNA-seq data with DESeq2. Genome Biol. *15*: 1–21.

Lüders, J., Demand, J., and Höhfeld, J. (2000). The ubiquitin-related BAG-1 provides a link between the molecular chaperones Hsc70/Hsp70 and the proteasome. J. Biol. Chem. *275*: 4613–4617.

MacArthur, C. a, and Shackleford, G.M. (1997). Npm3: a novel, widely expressed gene encoding a protein related to the molecular chaperones nucleoplasmin and nucleophosmin. Genomics *42*: 137–40.

Maki, H.E., Saramaki, O.R., Shatkina, L., Martikainen, P.M., Tammela, T.L.J., Weerden, W.M. van, et al. (2007). Overexpression and gene amplification of BAG-IL in hormone-refractory prostate cancer. J. Pathol. *212*: 395–401.

Manchen, S.T., and Hubberstey, A. V. (2001). Human Scythe contains a functional nuclear localization sequence and remains in the nucleus during staurosporine-induced apoptosis. Biochem. Biophys. Res. Commun. *287*: 1075–1082.

Mangelsdorf, D.J., Thummel, C., Beato, M., Herrlich, P., Schütz, G., Umesono, K., et al.

(1995). The nuclear receptor superfamily: the second decade. Cell *83*: 835–839.

Martin, K.R., and Barrett, J.C. (2002). Reactive oxygen species as double-edged swords in cellular processes: Low-dose cell signaling versus high-dose toxicity. Hum. Exp. Toxicol. *21*: 71–75.

Matsumoto, T., Sakari, M., Okada, M., Yokoyama, A., Takahashi, S., Kouzmenko, A., et al. (2013). The androgen receptor in health and disease. Annu. Rev. Physiol. *75*: 201–24.

McCord, J.M. (1995). Superoxide radical: controversies, contradictions, and paradoxes. Proc Soc Exp Biol Med *209*: 112–117.

McLay, D.W., and Clarke, H.J. (2003). Remodelling the paternal chromatin at fertilization in mammals. Reproduction *125*: 625–633.

Mehraein-Ghomi, F., Basu, H.S., Church, D.R., Hoffmann, F.M., and Wilding, G. (2010). Androgen receptor requires JunD as a coactivator to switch on an oxidative stress generation pathway in prostate cancer cells. Cancer Res. *70*: 4560–4568.

Mendillo, M.L., Santagata, S., Koeva, M., Bell, G.W., Hu, R., Tamimi, R.M., et al. (2012). HSF1 drives a transcriptional program distinct from heat shock to support highly malignant human cancers. Cell *150*: 549–562.

Mitrea, D.M., Grace, C.R., Buljan, M., Yun, M.-K., Pytel, N.J., Satumba, J., et al. (2014). Structural polymorphism in the N-terminal oligomerization domain of NPM1. Proc. Natl. Acad. Sci. U. S. A. *111*: 4466–71.

Morris, S., Kirstein, M., Valentine, M., Dittmer, K., Shapiro, D., Saltman, D., et al. (1994). Fusion of a kinase gene, ALK, to a nucleolar protein gene, NPM, in non-Hodgkin's lymphoma. Science (80-.). *263*: 1281–1284.

Mostaghel, E.A., Marck, B.T., Plymate, S.R., Vessella, R.L., Balk, S., Matsumoto, A.M., et al. (2011). Resistance to CYP17A1 inhibition with abiraterone in castration-resistant prostate cancer: Induction of steroidogenesis and androgen receptor splice variants. Clin. Cancer Res. *17*: 5913–5925.

Mustafi, S.B., Chakraborty, P.K., Dey, R.S., and Raha, S. (2009). Heat stress upregulates chaperone heat shock protein 70 and antioxidant manganese superoxide dismutase through reactive oxygen species (ROS), p38MAPK, and Akt. Cell Stress Chaperones *14*: 579–589.

Neckers, L., and Workman, P. (2012). Hsp90 molecular chaperone inhibitors: Are we there yet? Clin. Cancer Res. *18*: 64–76.

Nishimura, Y., Ohkubo, T., Furuichi, Y., and Umekawa, H. (2002). Tryptophans 286 and 288 in the C-terminal region of protein B23.1 are important for its nucleolar localization. Biosci. Biotechnol. Biochem. *66*: 2239–42.

Nozawa, Y., Belzen, N. Van, Made, A.C.J.J. Van der, Dinjens, W.N.M.M., and Bosman, F.T. (1996). Expression of nucleophosmin/B23 in normal and neoplastic colorectal mucosa. J. Pathol. *178*: 48–52.

Okuda, M. (2002). The role of nucleophosmin in centrosome duplication. Oncogene *21*: 6170–6174.

Okuwaki, M. (2008). The structure and functions of NPM1/Nucleophsmin/B23, a multifunctional nucleolar acidic protein. J. Biochem. *143*: 441–448.

Okuwaki, M., Matsumoto, K., Tsujimoto, M., and Nagata, K. (2001). Function of nucleophosmin/B23, a nucleolar acidic protein, as a histone chaperone. FEBS Lett. *506*: 272–276.

Okuwaki, M., Tsujimoto, M., and Nagata, K. (2002). The RNA Binding Activity of a Ribosome Biogenesis Factor, Nucleophosmin/B23, Is Modulated by Phosphorylation with a Cell Cycle-dependent Kinase and by Association with Its Subtype. Mol. Biol. Cell *13*: 2016–2030.

Packham, G., Brimmell, M., and Cleveland, J.L. (1997). Mammalian cells express two differently localized Bag-1 isoforms generated by alternative translation initiation. Biochem. J. *328 (Pt 3*: 807–13.

Pettigrew, C.A., Clerkin, J.S., and Cotter, T.G. (2012). DUOX enzyme activity promotes AKT signalling in prostate cancer cells. Anticancer Res. *32*: 5175–5182.

Polytarchou, C., Hatziapostolou, M., and Papadimitriou, E. (2005). Hydrogen peroxide stimulates proliferation and migration of human prostate cancer cells through activation of activator protein-1 and up-regulation of the heparin affin regulatory peptide gene. J. Biol. Chem. *280*: 40428–40435.

Polytarchou, C., Hatziapostolou, M., Poimenidi, E., Mikelis, C., Papadopoulou, A., Parthymou, A., et al. (2009). Nitric oxide stimulates migration of human endothelial and prostate cancer cells through up-regulation of pleiotrophin expression and its receptor protein tyrosine phosphatase beta/zeta. Int. J. Cancer *124*: 1785–1793.

Prestayko, A.W., Olson, M.O.J., and Busch, H. (1974). Phosphorylation of proteins of ribosomes and nucleolar preribosomal particles from Novikoff hepatoma ascites cells. FEBS Lett. *44*: 131–5.

Prinos, P., Lacoste, M.C., Wong, J., Bonneau, A.M., and Georges, E. (2011). Mutation of cysteine 21 inhibits nucleophosmin/B23 oligomerization and chaperone activity. Int. J. Biochem. Mol. Biol. *2*: 24–30.

Querol, C.L., Lavery, D.N., and Bevan, C.L. (2013). Mini-review: Foldosome regulation of androgen receptor action in prostate cancer. Mol. Cell. Endocrinol. *369*: 52–62.

Raimondi, S.C., Dube, I.D., Valentine, M.B., Mirro, J.J., Watt, H.J., Larson, R.A., et al. (1989). Clinicopathologic manifestations and breakpoints of the t(3;5) in patients with acute nonlymphocytic leukemia. Leukemia *3*: 42–47.

Redner, R.L., Rush, E. a, Faas, S., Rudert, W. a, and Corey, S.J. (1996). The t(5;17) variant of acute promyelocytic leukemia expresses a nucleophosmin-retinoic acid receptor fusion. Blood *87*: 882–6.

Reed, J.C. (1994). Mini-Review: Cellular Mechanisms of Disease Series; Bcl-2 and the Regulation of Programmed Cell Death. J. Cell Biol. *124*: 1–6.

Robinson-Rechavi, M., Escriva, H., and Laudet, V. (2003). The nuclear receptor superfamily. J. Cell Sci. *116*: 585–586.

Ryan, C.J., and Tindall, D.J. (2011). Androgen receptor rediscovered: The new biology and targeting the androgen receptor therapeutically. J. Clin. Oncol. *29*: 3651–3658.

Sabbah, M., Radanyi, C., Redeuilh, G., and Baulieu, E.E. (1996). The 90 kDa heat-shock protein (hsp90) modulates the binding of the oestrogen receptor to its cognate DNA. Biochem. J. *314 (Pt 1*: 205–13.

Sauer, H., Wartenberg, M., and Hescheler, J. (2001). Reactive oxygen species as intracellular messengers during cell growth and differentiation. Cell. Physiol. Biochem. *11*: 173–86.

Savkur, R.S., and Olson, M.O.J. (1998). Preferential cleavage in pre-ribosomal RNA by protein B23 endoribonuclease. Nucleic Acids Res. *26*: 4508–4515.

Scher, H.I., Buchanan, G., Gerald, W., Butler, L.M., and Tilley, W.D. (2004). Targeting the androgen receptor: Improving outcomes for castration-resistant prostate cancer. Endocr. Relat. Cancer *11*: 459–476.

Scher, H.I., Fizazi, K., Saad, F., Taplin, M.-E., Sternberg, C.N., Miller, K., et al. (2012). Increased survival with enzalutamide in prostate cancer after chemotherapy. N. Engl. J. Med. *367*: 1187–97.

Scher, H.I., and Sawyers, C.L. (2005). Biology of progressive, castration-resistant prostate cancer: Directed therapies targeting the androgen-receptor signaling axis. J. Clin. Oncol. *23*: 8253–8261.

Scherer, W.F. (1953). Studies on the Propagation in Vitro of Poliomyelitis Viruses. IV. Viral Multiplication in a Stable Strain of Human Malignant Epithelial Cells (Strain Hela) Derived From an Epidermoid Carcinoma of the Cervix. J. Exp. Med. *97*: 695–710.

Schmidt-Zachmann, M.S., Hügle-Dörr, B., and Franke, W.W. (1987). A constitutive nucleolar protein identified as a member of the nucleoplasmin family. EMBO J. *6*: 1881–90.

Schneikert, J., Hübner, S., Langer, G., Petri, T., Jäättelä, M., Reed, J., et al. (2000). Hsp70-RAP46 interaction in downregulation of DNA binding by glucocorticoid receptor. EMBO J. *19*: 6508–6516.

Schneikert, J., Hübner, S., Martin, E., and Cato, A.C.B. (1999). A nuclear action of the eukaryotic cochaperone RAP46 in downregulation of glucocorticoid receptor activity. J.

Cell Biol. *146*: 929–940.

Shafi, A.A., Yen, A.E., and Weigel, N.L. (2013). Androgen receptors in hormone-dependent and castration-resistant prostate cancer. Pharmacol Ther *140*: 223–238.

Shandilya, J., Swaminathan, V., Gadad, S.S., Choudhari, R., Kodaganur, G.S., and Kundu, T.K. (2009). Acetylated NPM1 Localizes in the Nucleoplasm and Regulates Transcriptional Activation of Genes Implicated in Oral Cancer Manifestation. Mol. Cell. Biol. *29*: 5115–5127.

Sharifi, N., Gulley, J.L., and Dahut, W.L. (2005). Androgen deprivation therapy for prostate cancer. JAMA *294*: 238–244.

Shatkina, L., Mink, S., Rogatsch, H., Klocker, H., Langer, G., Nestl, A., et al. (2003). The cochaperone Bag-1L enhances androgen receptor action via interaction with the NH2-terminal region of the receptor. Mol. Cell. Biol. *23*: 7189–97.

Shields, L.B., Gerçel-Taylor, C., Yashar, C.M., Wan, T.C., Katsanis, W.A., Spinnato, J.A., et al. (1997). Induction of immune responses to ovarian tumor antigens by multiparity. J. Soc. Gynecol. Investig. *4*: 298–304.

Siegel, R. (2017). Cáncer Statistics. CA Cancer J Clin. *67*: 7–30.

Sondermann, H., Ho, A.K., Listenberger, L.L., Siegers, K., Moarefi, I., Wente, S.R., et al. (2002). Prediction of novel Bag-1 homologs based on structure/function analysis identifies Snl1p as an Hsp70 co-chaperone in Saccharomyces cerevisiae. J. Biol. Chem. *277*: 33220–33227.

Sondermann, H., Scheufler, C., Schneider, C., Hohfeld, J., Hartl, F.U., and Moarefi, I. (2001). Structure of a Bag/Hsc70 complex: Convergent functional evolution of Hsp70 nucleotide exchange factors. Science (80-.). *291*: 1553–1557.

Sprenger, C.C.T., and Plymate, S.R. (2014). The link between androgen receptor splice variants and castration-resistant prostate cancer. Horm. Cancer *5*: 207–17.

Sramkoski, R.M., Pretlow, T.G., Giaconia, J.M., Pretlow, T.P., Schwartz, S., Sy, M.-S., et al. (1999). A new human prostate carcinoma cell line, 22Rv1. Vitr. Cell. Dev. Biol. - Anim.

35: 403–409.

Stelloo, S., Nevedomskaya, E., Kim, Y., Hoekman, L., Bleijerveld, O.B., Mirza, T., et al. (2018). Endogenous androgen receptor proteomic profiling reveals genomic subcomplex involved in prostate tumorigenesis. Oncogene *37*: 313–322.

Subong, E.N., Shue, M.J., Epstein, J.I., Briggman, J. V, Chan, P.K., and Partin, A.W. (1999). Monoclonal antibody to prostate cancer nuclear matrix protein (PRO:4-216) recognizes nucleophosmin/B23. Prostate *39*: 298–304.

Subramanian, A., Tamayo, P., Mootha, V.K., Mukherjee, S., Ebert, B.L., Gillette, M.A., et al. (2005). Gene set enrichment analysis: A knowledge-based approach for interpreting genome-wide expression profiles. Proc. Natl. Acad. Sci. *102*: 15545–15550.

Sun, S., Sprenger, C.C.T., Vessella, R.L., Haugk, K., Soriano, K., Mostaghel, E.A., et al. (2010). Castration resistance in human prostate cancer is conferred by a frequently occurring androgen receptor splice variant. J. Clin. Invest. *120*: 2715–30.

Swaminathan, V., Kishore, A.H., Febitha, K.K., and Kundu, T.K. (2005). Human histone chaperone nucleophosmin enhances acetylation-dependent chromatin transcription. Mol. Cell. Biol. *25*: 7534–45.

Szebeni, a, and Olson, M.O. (1999). Nucleolar protein B23 has molecular chaperone activities. Protein Sci. *8*: 905–912.

Szebeni, A., Herrera, J.E., and Olson, M.O. (1995). Interaction of nucleolar protein B23 with peptides related to nuclear localization signals. Biochemistry *34*: 8037–8042.

Takahashi, N., Sasaki, R., Takahashi, J., Takayama, S., Reed, J.C., and Andoh, T. (2001). BAG-1M, an isoform of Bcl-2-interacting protein BAG-1, enhances gene expression driven by CMV promoter. Biochem. Biophys. Res. Commun. *286*: 807–814.

Takayama, K., Suzuki, T., Tsutsumi, S., Fujimura, T., Urano, T., Takahashi, S., et al. (2015). RUNX1, an androgen- and EZH2-regulated gene, has differential roles in AR-dependent and -independent prostate cancer. Oncotarget *6*: 2263–76.

Takayama, S., Bimston, D.N., Matsuzawa, S.I., Freeman, B.C., Aime-Sempe, C., Xie, Z.,

et al. (1997). BAG-1 modulates the chaperone activity of Hsp70/Hsc70. EMBO J. *16*: 4887–4896.

Takayama, S., Krajewski, S., Krajewska, M., Kitada, S., Zapata, J.M., Kochel, K., et al. (1998). Expression and location of Hsp70/Hsc-binding anti-apoptotic protein BAG- 1 and its variants in normal tissues and tumor cell lines. Cancer Res. *58*: 3116–3131.

Takayama, S., Sato, T., Krajewski, S., Kochel, K., Irie, S., Milian, J.A., et al. (1995). Cloning and functional analysis of BAG-1: A novel Bcl-2-binding protein with anti-cell death activity. Cell *80*: 279–284.

Tanaka, M., Sasaki, H., Kino, I., Sugimura, T., and Terada, M. (1992). Genes Preferentially Expressed in Embryo Stomach are Predominantly Expressed in Gastric Cancer. Cancer Res. *52*: 3372–3377.

Tang, S.C. (2002). BAG-1, an anti-apoptotic tumour marker. IUBMB Life *53*: 99–105.

Tang, S.C., Shaheta, N., Chernenko, G., Khalifa, M., and Wang, X. (1999). Expression of BAG-1 in invasive breast carcinomas. J. Clin. Oncol. *17*: 1710–1719.

Tarapore, P., Okuda, M., and Fukasawa, K. (2002). A mammalian in vitro centriole duplication system: evidence for involvement of CDK2/cyclin E and nucleophosmin/B23 in centrosome duplication. Cell Cycle *1*: 75–81.

Thomas, T., and Thomas, T.J. (2003). Polyamine metabolism and cancer. J. Cell. Mol. Med. *7*: 113–126.

Thompson, T.C. (1990). Growth factors and oncogenes in prostate cancer. Cancer Cells *2*: 345–54.

Torre, L.A., Bray, F., Siegel, R.L., Ferlay, J., Lortet-tieulent, J., and Jemal, A. (2015). Global Cancer Statistics, 2012. CA Cancer J Clin. *65*: 87–108.

Tsui, K.-H., Cheng, A.-J., Chang, P. ei-L., Pan, T.-L., and Yung, B.Y.-M. (2004). Association of nucleophosmin/B23 mRNA expression with clinical outcome in patients with bladder carcinoma. Urology *64*: 839–44.

Wang, D., Baumann, A., Szebeni, A., and Olson, M.O.J.J. (1994). The nucleic acid

binding activity of nucleolar protein B23.1 resides in its carboxyl-terminal end. J. Biol. Chem. *269*: 30994–30998.

Wang, D., Umekawa, H., and Olson, M.O. (1993). Expression and subcellular locations of two forms of nucleolar protein B23 in rat tissues and cells. Cell. Mol. Biol. Res. *39*: 33–42.

Wang, H.G., Rapp, U.R., and Reed, J.C. (1996a). Bcl-2 targets the protein kinase Raf-1 to mitochondria. Cell *87*: 629–638.

Wang, H.G., Takayama, S., Rapp, U.R., and Reed, J.C. (1996b). Bcl-2 interacting protein, BAG-1, binds to and activates the kinase Raf-1. Proc. Natl. Acad. Sci. U. S. A. *93*: 7063–7068.

Wang, T., Guo, S., Liu, Z., Wu, L., Li, M., Yang, J., et al. (2014). CAMK2N1 inhibits prostate cancer progression through androgen receptor-dependent signaling. Oncotarget *5*: 10293–10306.

Wang, W., Budhu, A., Forgues, M., and Wang, X.W. (2005). Temporal and spatial control of nucleophosmin by the Ran-Crm1 complex in centrosome duplication. Nat. Cell Biol. *7*: 823–830.

Westin, P., Stattin, P., Damber, J.E., and Bergh, A. (1995). Castration therapy rapidly induces apoptosis in a minority and decreases cell proliferation in a majority of human prostatic tumors. Am. J. Pathol. *146*: 1368–75.

Witcher, M., Yang, X., Pater, A., and Tang, S.C. (2001). Bag-1 p50 isoform interacts with the vitamin D receptor and its cellular overexpression inhibits the vitamin D pathway. Exp. Cell Res. *265*: 167–173.

Wu, M.H., Chang, J.H., Chou, C.C., and Yung, B.Y.M. (2002a). Involvement of nucleophosmin/B23 in the response of HeLa cells to UV irradiation. Int. J. Cancer *97*: 297–305.

Wu, M.H., Chang, J.H., and Yung, B.Y.M. (2002b). Resistance to UV-induced cell-killing in nucleophosmin/B23 over-expressed NIH3T3 fibroblasts: enhancement of DNA repair and up-regulation of PCNA in association with nucleophosmin/B23 over-expression.

Carcinogenesis *23*: 93–9100.

Yamauchi, H., Adachi, M., Sakata, K. ichi, Hareyama, M., Satoh, M., Himi, T., et al. (2001). Nuclear BAG-1 localization and the risk of recurrence after radiation therapy in laryngeal carcinomas. Cancer Lett. *165*: 103–110.

Yang, L., Shang, L., and Nienhaus, G.U. (2013). Mechanistic aspects of fluorescent gold nanocluster internalization by live HeLa cells. Nanoscale *5*: 1537.

Yang, X., Chernenko, G., Hao, Y., Ding, Z., Pater, M.M., Pater, a, et al. (1998). Human BAG-1/RAP46 protein is generated as four isoforms by alternative translation initiation and overexpressed in cancer cells. Oncogene *17*: 981–9.

Yang, X., Hao, Y., Ferenczy, A., Tang, S.C., and Pater, A. (1999). Overexpression of anti-apoptotic gene BAG-1 in human cervical cancer. Exp. Cell Res. *247*: 200–207.

Ye, L., Lewis-Russell, J.M., Kyanaston, H.G., and Jiang, W.G. (2007). Bone morphogenetic proteins and their receptor signaling in prostate cancer. Histol. Histopathol. *22*: 1129–47.

Yoneda-Kato, N., Look, A.T., Kirstein, M.N., Valentine, M.B., Raimondi, S.C., Cohen, K.J., et al. (1996). The t(3;5)(q25.1;q34) of myelodysplastic syndrome and acute myeloid leukemia produces a novel fusion gene, NPM-MLF1. Oncogene *12*: 265–75.

Yu, Y., Maggi, L.B., Brady, S.N., Apicelli, A.J., Dai, M.-S., Lu, H., et al. (2006). Nucleophosmin Is Essential for Ribosomal Protein L5 Nuclear Export. Mol. Cell. Biol. *26*: 3798–3809.

Yun, J.P., Chew, E.C., Liew, C.T., Chan, J.Y.H., Jin, M.L., Ding, M.X., et al. (2003). Nucleophosmin/B23 Is a Proliferate Shuttle Protein Associated with Nuclear Matrix. J. Cell. Biochem. *90*: 1140–1148.

Zeiner, M., Gebauer, M., and Gehring, U. (1997). Mammalian protein RAP46: An interaction partner and modulator of 70 kDa heat shock proteins. EMBO J. *16*: 5483–5490.

Zeiner, M., Niyaz, Y., and Gehring, U. (1999). The hsp70-associating protein Hap46 binds

to DNA and stimulates transcription. Proc Natl Acad Sci U S A *96*: 10194–10199.

Zhang, M.J., Ding, Y.L., Xu, C.W., Yang, Y., Lian, W.X., Zhan, Y.Q., et al. (2012). Erythroid differentiation-associated gene interacts with NPM1 (nucleophosmin/B23) and increases its protein stability, resisting cell apoptosis. FEBS J. *279*: 2848–2862.

ACKNOWLEDGEMENT

My profound gratitude goes to my supervisor Prof. Dr. Andrew Cato for his exceptional supervision, encouragements and mentorship he provided throughout my studies. I thank him so much for the excellent friendship we built together and I'm very sorry for putting him through difficulties during those troubled times. In all honesty, he was an excellent supervisor, mentor and a friend. Thank you Andy!

I would like to also thank my Thesis Advisory Committee (TAC) members, PD. Dr. Christine Blattner and PD. Dr. Carsten Weiss for supporting me throughout this study period. They supported this work with lots of critical contributions which shaped the direction of the work. I'm really grateful for that. In addition, Dr. Blattner, was always there to support me with recommendation letters to prolong my scholarship year after year. I'm exceedingly grateful to her for her support!

I am extremely grateful to Prof. Dr. Jörg Kämper for his invaluable input and accepting the onus task of being my second corrector. Thank you for the invaluable help, Sir!

This acknowledgment would not be complete without mentioning that Dr. Mohammed Salama, a former PhD student in Cato Lab, generated the NPM1 knockdown clones that I used for the work in this PhD thesis. It was a great service to me. Thank you Mohammed!

I am extremely grateful to Dr. Antje Neeb and Dr. Katja Jehle for allowing me to use some of their data in this thesis.

I must also mention that I am really grateful to the group of Prof. Dr. Gerd Ulrich Nienhaus and especially, Linxiao Yang with whom I had a very fruitful collaboration.

I am also very grateful to Dr. Laura Cato, Dr. Irene Lee and Jaice Rottenberg in the group of Prof. Myles Brown, Dana–Farber Cancer Institute, Harvard Medical School, for a great collaboration. I am really grateful to you for the help!

I am also very grateful to Nane Kuznik, Jutta Stöber, Rebecca Seeger, Yang Feng and past members of Cato Lab for providing invaluable technical support for the success of this work. Thanks very much Cato group!

I am extremely grateful to Dr. Leonel Munoz for assisting me with lots of technical supports throughout the course of this study. Thank you ‘Senior PostDoc’ LEO!

I must add that I’m very grateful to Prof. Dr. Nicholas S. Foulkes, the Dean of BIFTM Graduate School, KIT, for his constant encouragements. I’m really thankful for his support! In addition, I’m also very grateful for support given me by Dr. Larissa Kaufmann.

I honestly owe Mr. Hartmut Speck and Mr. Döring Florian at the International Office, KIT, lots of gratitude for helping me to have smooth life in Germany. I’m really grateful!

My utmost thanks also goes to my Landlord and Landlady Alex Catoir and Juliane Freiesleben-Catoir for hosting me in their home for more than 3 years! I’m really grateful to them for providing me with a home in Germany!

My sincere gratitude also goes to various local and foreign collaborators whose assistance have been of tremendous value along the way.

I would like to thank all other persons that because of time and space, I could not single them out who were instrumental in making this work a success.

Finally, my deepest gratitude goes to my wife Akose and my son, Kobby, for their patience throughout my studies abroad.